Genome-wide survey and molecular characterization of vacuolar-ATPase subunit genes in the yellow fever mosquito *Aedes aegypti* (Diptera: Culicidae)

by

Basak Coskun

B.S., Ege University, 2012

A THESIS

submitted in partial fulfillment of the requirements for the degree

MASTER OF SCIENCE

Department of Entomology
College of Agriculture

KANSAS STATE UNIVERSITY
Manhattan, Kansas

2017

Approved by:

Co-Major Professor
Kun Yan Zhu

Approved by:

Co-Major Professor
Kristopher Silver

Copyright

© Basak Coskun 2017.

Abstract

The yellow fever mosquito, *Aedes aegypti*, is a significant vector of several viral diseases, including Zika, dengue fever, yellow fever, and chikungunya. Since vaccines are not currently available for these viruses, control of the disease vectors by using insecticides is the most common practice for preventing disease. As a result, *Ae. aegypti* has developed resistance against many of the most commonly used insecticides, including organophosphates and pyrethroids. The rise in resistance in vector mosquitoes requires the search for new control strategies, such as RNA interference (RNAi), to manage mosquito populations. Vacuolar H^+-ATPase (V-ATPase), a multi-subunit enzyme involved in many cellular processes, including membrane energization, acidification of organelles, and entry of dengue virus into the cytoplasm, is a potential target for RNAi, though little is known about its genetic structure or expression patterns in *Ae. aegypti*.

In this study, I performed genome-wide surveys to identify the genes encoding different subunits of the V-ATPase protein complex, partially characterized the molecular properties and expression patterns of selected V-ATPase subunit genes, and tested the feasibility of using oral-based delivery of nanoparticles formed from double-stranded RNA (dsRNA) and chitosan to suppress the expression of selected V-ATPase subunit genes in *Ae. aegypti*. My genome-wide surveys revealed that *Ae. aegypti* V-ATPase consists of 13 different subunits (A, B, C, D, E, F, G, H, a, c, c", d, e) encoded by 14 genes. Analysis of exon-intron arrangements for each gene demonstrated that each V-ATPase subunit gene has between one (subunit c) and 12 (subunit C) exons, with most genes (11) having 3 to 6 exons. Subsequent phylogenetic analysis of the deduced amino acid sequences of each subunit showed that V-ATPase subunits A, B, C, F, G, H, and a exhibited high levels of conservation among all the examined species, but subunits D, E, c, c", d, and e showed high conservation only among dipteran species.

Analysis of the expression profiles in different tissues and developmental stages of three specific V-ATPase subunits (A, D, and H) showed that whereas the expression of these genes varied between tissues and developmental stages, the patterns of expression of subunits A, D, and H were very similar. The highest mRNA expression level was observed in Malpighian tubules in fourth-instar larvae. Interestingly, expression of subunits A, D, or H in different tissues of adults was highest in male hindgut versus Malpighian tubules in females. Feeding mosquito larvae with chitosan nanoparticles made with dsRNA complementary to subunits A, D, or H resulted in significant suppression of mRNA transcript levels of each of these subunits. Peak suppression of V-ATPase A, D, or H transcripts occurred on the fifth day, where the gene transcript level was suppressed by 66.0, 27.3, or 70.4%, respectively, as compared with those of the control. Additionally, feeding of dsRNA/chitosan nanoparticles targeting subunit D caused mortality starting on day 3, with cumulative larval mortality reaching 14.8% on the sixth day. These results suggest that oral delivery of dsRNA/chitosan nanoparticles can substantially suppress target gene expression in *Ae. aegypti* larvae. However, increasing RNAi efficiency in targeting V-ATPase subunit genes in mosquito larvae appears to be necessary in order to obtain higher larval mortality using oral delivery of dsRNA/chitosan nanoparticles.

Table of Contents

List of Figures

List of Tables

Acknowledgements

I would like to thank all those who provided invaluable support in so many ways during my thesis process.

First, I would like to express my appreciation to Dr. Kun Yan Zhu and Dr. Kristopher Silver, for their guidance, feedback, and advising on this research. Especially, I thank them for aiding me when I needed help in laboratory experiments. Without their valuable assistance, this work would not have been completed. Second, I am grateful to the other members of my supervisory committee, Dr. Yoonseong Park and Dr. David Margolies for their extraordinary support and suggestions in this thesis process. Third, I would like to thank the Turkish Government for sponsoring me throughout my graduate study. This project would have been impossible without the support of the Ministry of National Education of Turkey. Finally, I will never forget the help of my friends Moustapha Soumaila Issa, Anastasia Cooper, Siyi Wang, Jianxiu Yao, and several others.

Specimens used in this research are deposited as voucher number 250 in the KSU Museum of Entomological and Prairie Arthropod Research.

Dedication

To my parents

Rahime and Ahmet,

my wonderful husband

Burak,

and my precious daughter

Zeynep

for their unfailing love, support, affection, and encouragement.

Chapter 1 - Literature Review

1.1. Vacuolar H^+-ATPase

The vacuolar H^+-ATPase, also called V-ATPase, is one of the most important ancient enzymes that has significant, diverse functions in eukaryotic organisms (Nelson et al., 2000). This enzyme acidifies various intracellular compartments and transports protons across the plasma membrane in various cell types (Cotter et al., 2015; Nishi and Forgac, 2002). Acidification of endocytic compartments is necessary for entry of envelope viruses, including dengue (Perreira et al., 2015) and chikungunya viruses (Gay et al., 2012).

1.1.1. A brief history

Many researchers, working on many different organisms in many different laboratories, contributed directly to the discovery and characterization of V-ATPase. The first evidence of V-ATPase activity in animal cells was found in chromaffin granules of the bovine adrenal medulla (Kirshner, 1962). Chromaffin granules are storage vesicles that contain high levels of catecholamines, and it was observed that catecholamine uptake into these vesicles was dependent on both Mg^{2+} and ATP (Kirshner, 1962; Taugner, 1971). Further investigation showed that catecholamine uptake was also highly sensitive to membrane disruption and metabolic uncouplers, leading to the conclusion that this unknown ATPase was membrane bound and likely involved in the transport of protons across the membrane (Bashford et al., 1975). Subsequent isolation of this membrane-bound ATPase revealed that it was different from the already known mitochondrial ATPase (Cidon and Nelson, 1983). Following this discovery, similar V-ATPases were identified in other organisms including plants, such as red beet (Walker and Leigh, 1981) and yeast (Kakinuma et al., 1981), and that these ATPases were associated not only with plant

vacuoles, but also with clathrin-coated vesicles and endosomal membranes of lysosomes (Nelson, 1992; Stevens and Forgac, 1997).

1.1.2. Function of V-ATPase

V-ATPases are highly conserved proton pumps that are found in all eukaryotic organisms and are involved in many different cellular processes such as coupled transport and protein degradation (Cotter et al., 2015). These enzymes are located at the plasma membrane of many cell types such as midgut cells of insects (Cipriano et al., 2008), and are involved in pH homeostasis and membrane energization (Beyenbach and Wieczorek, 2006; Nishi and Forgac, 2002).

V-ATPases are also found within the membranes of many organelles. They acidify intracellular compartments such as early and late endosomes, lysosomes, Golgi-derived vesicles, or secretory vesicles in every eukaryotic cell (Forgac, 2007; Kane, 2006). Intracellular V-ATPases process and degrade the macromolecules in secretory and digestive compartments. For instance, they operate coupled transport of tiny molecules such as neurotransmitters and ATP in the entry of pathogenic agents, including envelope viruses and bacterial toxins (Cipriano et al., 2008).

V-ATPases have significant roles in endocytosis and vesicular traffic. The pHs of the intracellular compartments (4.5-7.0) in endocytic pathways are more acidic than extracellular pH (~7.4) (Maxson and Grinstein, 2014). Low pH allows for the uncoupling of internalized ligand-receptor complexes and recycling of these unoccupied receptors back to the cell surface (Forgac, 2007). In addition, acidification of endosomes is required for the formation of endosomal carrier vesicles that carry ligands from early to late endosomes (Nishi and Forgac, 2002). Lysosomes are

one of the most significant organelles in cells, and they are involved in protein degradation through endocytic pathways (Saftig and Klumperman, 2009). The degradative enzymes contained within lysosomes are activated at low pH level and degrade internalized macromolecules (Forgac, 2007).

1.1.3. Structure of V-ATPase

Structural examination of V-ATPases in animals, plants, and fungi revealed a multi-subunit complex (Moriyama and Nelson, 1987) that can be subdivided into two functional domains that are named V_1 and V_0 (Forgac, 1998). The V_1 domain is a peripheral complex of 600-650 kDa located on the cytoplasmic side of the membrane. Consisting of eight different subunits (A, B, C, D, E, F, G, H), the V_1 domain is responsible for ATP hydrolysis (Drory and Nelson, 2006). In contrast, the V_0 domain is a membrane-embedded complex of 260 kDa responsible for the transposition of protons from the cytoplasm to the organelle/vesicle lumen or extracellular space (Forgac, 2007). The V_0 domain is composed of at least four different subunits (a, d, c, e) in organisms ranging from yeast to insects and mammals (Forgac, 1998). These two large multi-subunit complexes, V_1 and V_0, associate to form a functional proton pump.

Early studies showed that the V_1 domain detaches from the V_0 domain in response to glucose deprivation in yeast cells and at the apical plasma membrane of tobacco hornworm (Kane, 1995; Kane et al., 2012; Sumner et al., 1995). These studies showed that V-ATPase activity can be regulated by a process called reversible disassembly. It has been identified in eukaryotes in yeast, insects, and mammals (Huss et al., 2011). Since this mechanism is found in many different organisms, this indicates that reversible dissociation of the V-ATPase is an evolutionarily conserved mechanism.

Dissociation of the V_1 and V_0 domains was first demonstrated in the midgut of tobacco hornworm as an *in vivo* control mechanism that regulates energy usage (Sumner et al., 1995), and other studies showed that the activity of V-ATPase is regulated by reversible dissociation of the V_1 and V_0 domains in a variety of cells (Beyenbach and Piermarini, 2009; Beyenbach and Wieczorek, 2006; Dames et al., 2006). The peripheral V_1 domain and the membrane-embedded V_0 domain dissociate during molting or starvation in tobacco hornworm in order to save the energy (Beyenbach and Wieczorek, 2006; Sumner et al., 1995). The dissociation of the V_1 and V_0 complexes occurs as a result of changes in the ATP/ADP ratio in cells (Huss and Wieczorek, 2007). The mechanism of dissociation is still uncertain; however, Voss et al. (2007) showed that dephosphorylation of subunit C in the V_1 complex causes dissociation of the V_1 and V_0 domains in the midgut of tobacco hornworm. To date, the mechanisms that control the activity of V-ATPase have not been fully elucidated.

1.1.4. RNAi-based silencing of V-ATPase genes

RNA interference (RNAi) was first discovered in nematodes (*Caenorhabditis elegans*) where it was demonstrated that exogenous dsRNA could suppress expression of mRNA transcripts (Fire et al., 1998). After its discovery, it has been extensively used to analyze the function, regulation, and interaction of genes and their products at cellular and organismal levels in many different organisms (Agrawal et al., 2003). RNAi is a posttranscriptional technique to silence specific genes by administering double-stranded RNA (dsRNA) or small interfering RNA (siRNA) that is complementary to the gene of interest.

RNAi-mediated gene silencing starts with the delivery of dsRNA into insects. Long dsRNA (generally less than 1000 bp) is taken up and recognized by the host cell and is processed

into siRNAs (21-23 bp) (Hamilton and Baulcombe, 1999; Hammond et al., 2000) by the enzyme, Dicer. Each siRNA is separated into two single-stranded RNAs (ssRNAs); the passenger strand and the guide strand. The passenger strand is degraded while the guide strand binds to an argonaute multi-domain protein and generates the RNA-induced silencing complex (RISC). siRNAs have complementary base pairs to messenger RNAs (mRNA). When siRNAs bind to their complementary mRNA, the mRNA is degraded, preventing translation of the mRNA into protein (Siomi and Siomi, 2009).

To date, RNAi has been widely used to understand the function and regulation of genes in many organisms, including insects (Scott et al., 2013). It also has potential novel applications for insect pest management (Zhu, 2013), allowing researchers to knockdown genes which have essential biological or physiological functions for developing novel and sustainable pest management strategies (Burand and Hunter, 2013; Huvenne and Smagghe, 2010).

Davies et al. (1996) reported that the first animal knockout of a V-ATPase subunit (subunit B) was identified in *Drosophila* and that caused a larval lethal phenotype. Baum et al. (2007) demonstrated that feeding with dsRNA against V-ATPase subunit A suppressed the targeted mRNA in western corn rootworm (*Diabrotica virgifera virgifera*). When western corn rootworm was reared on transgenic corn plants that express V-ATPase A dsRNA, the transcript level of subuit A was reduced, and feeding damage on transgenic plants was much less compared to control. Thereafter, RNAi has been extensively used to elucidate the function of V-ATPase genes in various insect species including *Aedes aegypti* (Coy et al., 2012), *Peregrinus maidis* (Yao et al., 2013), *Bemisia tabaci* (Thakur et al., 2014), *Helicoverpa armigera* (Jin et al., 2015; Mao et al., 2015), and *Aethina tumida* (Powell et al., 2017).

Adult female *Ae. aegypti* mosquitoes were fed with sucrose meals including dsRNA targeting V-ATPase A. They observed 2.4 to 2.5-fold reduction in transcript level of subunit A (Coy et al., 2012). Yao et al. (2013) also showed that feeding and injection of dsRNA against the V-ATPase subunit D reduced the mRNA transcript level of subunit D and caused phenotypic changes such as curly and short wings in planthopper (*P. maidis*). Transgenic tobacco plants that express dsRNA complementary to V-ATPase A suppressed the transcript level of subunit A by 62% and caused mortality in whiteflies (*B. tabaci*) (Thakur et al., 2014). Injection of V-ATPase subunit A dsRNA into *A. tumida* caused phenotypic changes and significant reductions of 31-54% of V-ATPase A transcripts, whereas 48 h of feeding the same dsRNA did not affect mRNA levels despite causing 50% larval mortality (Powell et al., 2017). Given the vital role of V-ATPases in these other organisms, I examined the expression of selected V-ATPase subunit genes (*V-ATPase A, V-ATPase D,* and *V-ATPase H*) in *Ae. aegypti* and evaluated both the importance of these subunits to mosquito survival and the potential of these targets for mosquito control using RNAi.

1.2. Yellow fever mosquito (*Aedes aegypti*)

1.2.1. Significance of *Aedes aegypti*

Aedes aegypti belongs to the subfamily of Culicinae in the family Culicidae. *Ae. aegypti* originated from Central Africa where it is found in greatest abundance (Christophers, 1960; Tabachnick, 1991). However, this mosquito species has spread globally due to global trade and shipping activities, and is now established in all tropical and subtropical and some temperate areas around the world (Powell and Tabachnick, 2013; WHO, 2016).

Ae. aegypti is critically important as a carrier of human disease. *Ae. aegypti* has a very high vectorial capacity for yellow fever (Jentes et al., 2011), dengue fever (Simmons et al., 2012), chikungunya (Leparc-Goffart et al., 2014), and Zika (Musso and Gubler, 2016) viruses, and the number of people affected by these diseases has dramatically increased over the last 50 years (Weaver, 2014). A recent study indicates that over 390 million people are affected by dengue fever per year (Bhatt et al., 2013), while 3.9 billion people, in 128 countries, are at risk of infection with dengue virus (Brady et al., 2012). More recently, the World Health Organization declared Zika virus, which can be passed from a pregnant woman to her fetus and is associated with birth defects, as a public health emergency of international concern (WHO, 2016).

Whereas there is a safe and efficacious vaccine against yellow fever, control of transmission of Zika, dengue fever, and chikungunya is currently completely dependent on eliminating mosquito vectors. In these cases, insecticides are most commonly used to control the mosquito vectors, but widespread use of organophosphates and pyrethroids has resulted in the development of resistance to these chemicals in *Ae. aegypti* (Fox, 1961; Ranson et al., 2010). Therefore, it is imperative that novel methods and targets are developed to implement new management strategies for *Ae. aegypti* and controlling transmission of these viruses.

1.2.2. Biology of *Aedes aegypti*

Ae. aegypti has four developmental stages; egg, larvae, pupae, and adult (Christophers, 1960). The first three stages (egg, larvae, and pupae) are aquatic whereas the last stage (adult) is terrestrial. Each female mosquito lays 100 to 200 eggs at a time in a cluster on the water surface. After being laid, the eggs, which are white in color, harden and convert to a shiny black within minutes (Christophers, 1960; Schlaeger and Fuchs, 1974). The eggs can remain viable even

when dry for months, but hatch when they become flooded with water (Harwood and James, 1979).

After hatching, *Ae. aegypti* larvae grow through four instars, requiring five to ten days for completion of its larval stage, though variation of temperature and diets can increase or shorten this time period. The fourth-instar larvae of *Ae. aegypti* pupate when large enough. The completion of larval and pupal stages typically occurs within 12 days. Adults, male and female, survive approximately 20 to 30 days and feed on nectar. Female mosquitoes, however, require a blood meal in order to produce eggs.

1.3. V-ATPase studies in *Aedes aegypti*

V-ATPase studies in *Ae. aegypti* have focused on transportation of protons across the insect epithelia since it is thought to be energized by V-ATPase. Researches showed that V-ATPase is found in plasma membranes of insect epithelia to generate an electrochemical gradient across the membrane (Wieczorek et al., 1999). This membrane voltage has a role for nutrition uptake, fluid secretion and alkalizing the gut lumen (Harvey et al., 1998).

V-ATPases are expressed in all osmoregulatory organs including midgut and Malpighian tubules to provide the energy for transepithelial transport in adult and larval *Ae. aegypti* (Patrick et al., 2006). Malpighian tubules in the adult mosquito showed high expression of V-ATPase in the brush border membrane of principal cells but not in stellate cells (Beyenbach et al., 2009). The expression of A, B and C subunits of V-ATPase are increased in female adult *Ae. aegypti* after blood feeding, suggesting that V-ATPase might have an important role in the transport of ions, solutes and amino acids present in a blood meal (Sanders et al., 2003).

To date, there are several reports on silencing of V-ATPase in *Ae. aegypti* using RNAi techniques. Coy et al. (2012) demonstrated that oral delivery of dsRNA targeting V-ATPase A suppressed the transcript level of subunit A by 2.4 - 2.5 fold, but they did not observe phenotypic changes or mortality in adult female *Ae. aegypti*. However, other studies have shown that RNAi knockdown of several V-ATPase genes in different insect species cause mortality (Baum et al., 2007; Mao et al., 2015; Powell et al., 2017). Recently, *Ae. aegypti* V-ATPase was identified as a necessary host factor since dsRNA-mediated suppression of V-ATPase subunits (vATP-ac39, vATP-V0B, vATP-f, and vATP-16) reduced dengue virus titers up to 98%. They also showed that the function of V-ATPase enzymes as a whole complex is required for efficient dengue virus infection in *Ae. aegypti* (Kang et al., 2014).

1.4. Research goals and objectives

Although significant research has revealed details about the structure and biological function of V-ATPases in a few insect species, only a few studies have focused on understanding the role of V-ATPase subunits in *Ae. aegypti* and their potential for use as targets in mosquito control. Further, there is only limited knowledge about the roles of each subunit of V-ATPase or the function of the complete enzyme in insects. Accordingly, I propose to characterize molecular properties of three selected V-ATPase subunit genes (*V-ATPase A, V-ATPase D,* and *V-ATPase H*) in the mosquito, *Ae. aegypti,* and evaluate the significance of these genes to mosquito growth and development by using RNAi techniques to suppress their mRNA transcript levels.

The objectives of this study include:

1. To identify V-ATPase subunit genes using genome-wide analyses of mRNA sequences in *Ae. aegypti* and evaluate their evolutionary relationship with like subunits in other insect species.
2. To characterize the genetic structure of selected V-ATPase subunit genes and determine their relative expression in different tissues and developmental stages.
3. To reveal the importance of selected V-ATPase subunit genes for survival of mosquito larvae and evaluate these subunits as targets for insect vector control using RNAi.

This study is expected to generate new knowledge on the genetic structures of V-ATPase subunits in *Ae. aegypti*, which have not been well studied; improve our understanding of the biological importance of key V-ATPase subunit genes; and help researchers to develop RNAi-based strategies for managing mosquitoes and other insect pests by targeting various V-ATPase subunit genes.

References

Agrawal, N., Dasaradhi, P.V.N., Mohmmed, A., Malhotra, P., Bhatnagar, R.K., Mukherjee, S.K., 2003. RNA interference: biology, mechanism, and applications. Microbiol. Mol. Biol. Rev. 67, 657-685.

Bashford, C.L., Casey, R.P., Radda, G.K., Ritchie, G.A., 1975. The effect of uncouplers on catecholamine incorporation by vesicles of chromaffin granules. Biochem. J. 148, 153-155.

Baum, J.A., Bogaert, T., Clinton, W., Heck, G.R., Feldmann, P., Ilagan, O., Johnson, S., Plaetinck, G., Munyikwa, T., Pleau, M., Vaughn, T., Roberts, J., 2007. Control of coleopteran insect pests through RNA interference. Nat. Biotech. 25, 1322-1326.

Beyenbach, K.W., Baumgart, S., Lau, K., Piermarini, P.M., Zhang, S., 2009. Signaling to the apical membrane and to the paracellular pathway: changes in the cytosolic proteome of *Aedes* Malpighian tubules. J. Exp. Biol. 212, 329-340.

Beyenbach, K.W., Piermarini, P., 2009. Osmotic and ionic regulation in insects. In: Evans, D.H. (Eds.), Osmotic and Ionic Regulation: Cells and Animals. CRC Press, Boca Raton, FL, pp. 231-293.

Beyenbach, K.W., Wieczorek, H., 2006. The V-type H+ ATPase: molecular structure and function, physiological roles and regulation. J. Exp. Biol. 209, 577-589.

Bhatt, S., Gething, P.W., Brady, O.J., Messina, J.P., Farlow, A.W., Moyes, C.L., Drake, J.M., Brownstein, J.S., Hoen, A.G., Sankoh, O., Myers, M.F., George, D.B., Jaenisch, T., Wint, G.W., Simmons, C.P., Scott, T.W., Farrar, J.J., Hay, S.I., 2013. The global distribution and burden of dengue. Nature 496, 504-507.

Brady, O.J., Gething, P.W., Bhatt, S., Messina, J.P., Brownstein, J.S., Hoen, A.G., Moyes, C.L., Farlow, A.W., Scott, T.W., Hay, S.I., 2012. Refining the global spatial limits of dengue virus transmission by evidence-based consensus. PLoS Negl. Trop. Dis. 6, e1760.

Burand, J.P., Hunter, W.B., 2013. RNAi: future in insect management. J. Invertebr. Pathol. 112, S68-S74.

Christophers, S.R., 1960. *Aedes aegypti* (L.) The Yellow Fever Mosquito: Its Life History, Bionomics and Structure. Cambridge University Press, London.

Cidon, S., Nelson, N., 1983. A novel ATPase in the chromaffin granule membrane. J. Biol. Chem. 258, 2892-2898.

Cipriano, D.J., Wang, Y., Bond, S., Hinton, A., Jefferies, K.C., Qi, J., Forgac, M., 2008. Structure and regulation of the vacuolar ATPases. Biochim. Biophys. Acta. 1777, 599-604.

Cotter, K., Stransky, L., McGuire, C., Forgac, M., 2015. Recent insights into the structure, regulation and function of the V-ATPases. Trends Biochem. Sci. 40, 611-622.

Coy, M.R., Sanscrainte, N.D., Chalaire, K.C., Inberg, A., Maayan, I., Glick, E., Paldi, N., Becnel, J.J., 2012. Gene silencing in adult *Aedes aegypti* mosquitoes through oral delivery of double-stranded RNA. J. Appl. Entomol. 136, 741-748.

Dames, P., Zimmermann, B., Schmidt, R., Rein, J., Voss, M., Schewe, B., Walz, B., Baumann, O., 2006. cAMP regulates plasma membrane vacuolar-type H(+)-ATPase assembly and activity in blowfly salivary glands. Proc. Natl. Acad. Sci. USA. 103, 3926-3931.

Davies, S.A., Goodwin, S.F., Kelly, D.C., Wang, Z., Sozen, M.A., Kaiser, K., Dow, J.A.T., 1996. Analysis and inactivation of vha55, the gene encoding the vacuolar ATPase B-

subunit in *Drosophila melanogaster* reveals a larval lethal phenotype. J. Biol. Chem. 271, 30677-30684.

Drory, O., Nelson, N., 2006. Structural and functional features of yeast V-ATPase subunit C. Biochim. Biophys. Acta. 1757, 297-303.

Fire, A., Xu, S., Montgomery, M.K., Kostas, S.A., Driver, S.E., Mello, C.C., 1998. Potent and specific genetic interference by double-stranded RNA in *Caenorhabditis elegans*. Nature 391, 806-811.

Forgac, M., 2007. Vacuolar ATPases: rotary proton pumps in physiology and pathophysiology. Nat. Rev. Mol. Cell Biol. 8, 917-929.

Forgac, M., 1998. Structure, function and regulation of the vacuolar (H+)-ATPases. FEBS Lett. 440, 258-263.

Fox, I., 1961. Resistance of *Aedes aegypti* to certain chlorinated hydrocarbon and organophosphorus insecticides in Puerto Rico. Bull. World Health Organ. 24, 489-494.

Gay, B., Bernard, E., Solignat, M., Chazal, N., Devaux, C., Briant, L., 2012. pH-dependent entry of chikungunya virus into *Aedes albopictus* cells. Infect. Genet. Evol. 12, 1275-1281.

Hamilton, A.J., Baulcombe, D.C., 1999. A species of small antisense RNA in posttranscriptional gene silencing in plants. Science 286, 950-952.

Hammond, S.M., Bernstein, E., Beach, D., Hannon, G.J., 2000. An RNA-directed nuclease mediates post-transcriptional gene silencing in *Drosophila* cells. Nature 404, 293-296.

Harvey, W.R., Maddrell, S.H.P., Telfer, W.H., Wieczorek, H., 1998. H+ V-ATPases energize animal plasma membranes for secretion and absorption of ions and fluids. Am. Zool. 38, 426-441.

Harwood, R.F., James, M.T., 1979. Entomology in Human and Animal Health, seventh ed. MacMillan, New York.

Huss, M., Vitavska, O., Albertmelcher, A., Bockelmann, S., Nardmann, C., Tabke, K., Tiburcy, F., Wieczorek, H., 2011. Vacuolar H+-ATPases: intra- and intermolecular interactions. Eur. J. Cell Biol. 90, 688-695.

Huss, M., Wieczorek, H., 2007. Influence of ATP and ADP on dissociation of the V-ATPase into its V1 and V0 complexes. FEBS Lett. 581, 5566-5572.

Huvenne, H., Smagghe, G., 2010. Mechanisms of dsRNA uptake in insects and potential of RNAi for pest control: a review. J. Insect Physiol. 56, 227-235.

Jentes, E.S., Poumerol, G., Gershman, M.D., Hill, D.R., Lemarchand, J., Lewis, R.F., Staples, J.E., Tomori, O., Wilder-Smith, A., Monath, T.P., 2011. The revised global yellow fever risk map and recommendations for vaccination, 2010: consensus of the Informal WHO Working Group on Geographic Risk for Yellow Fever. Lancet Infect. Dis. 11, 622-632.

Jin, S., Singh, N.D., Li, L., Zhang, X., Daniell, H., 2015. Engineered chloroplast dsRNA silences *cytochrome p450 monooxygenase, V-ATPase* and *chitin synthase* genes in the insect gut and disrupts *Helicoverpa armigera* larval development and pupation. Plant Biotechnol. J. 13, 435-446.

Kakinuma, Y., Ohsumi, Y., Anraku, Y., 1981. Properties of H+-translocating adenosine triphosphatase in vacuolar membranes of *Saccharomyces cerevisiae*. J. Biol. Chem. 256, 10859-10863.

Kane, P.M., 2012. Targeting reversible disassembly as a mechanism of controlling V-ATPase activity. Curr. Protein Pept. Sci. 13, 117-123.

Kane, P.M., 2006. The where, when, and how of organelle acidification by the yeast vacuolar H+-ATPase. Microbiol. Mol. Biol. Rev. 70, 177-191.

Kane, P.M., 1995. Disassembly and reassembly of the yeast vacuolar H+-ATPase *in vivo*. J. Biol. Chem. 270, 17025-17032.

Kang, S., Shields, A.R., Jupatanakul, N., Dimopoulos, G., 2014. Suppressing dengue-2 infection by chemical inhibition of *Aedes aegypti* host factors. PLoS Negl. Trop. Dis. 8, e3084.

Kirshner, N., 1962. Uptake of catecholamines by a particulate fraction of the adrenal medulla. J. Biol. Chem. 237, 2311-2317.

Leparc-Goffart, I., Nougairede, A., Cassadou, S., Prat, C., de Lamballerie, X., 2014. Chikungunya in the Americas. The Lancet 383, 514.

Mao, J., Zhang, P., Liu, C., Zeng, F., 2015. Co-silence of the coatomer *β* and *v-ATPase A* genes by siRNA feeding reduces larval survival rate and weight gain of cotton bollworm, *Helicoverpa armigera*. Pestic. Biochem. Physiol. 118, 71-76.

Maxson, M.E., Grinstein, S., 2014. The vacuolar-type H+-ATPase at a glance - more than a proton pump. J. Cell. Sci. 127, 4987-4993.

Moriyama, Y., Nelson, N., 1987. The purified ATPase from chromaffin granule membranes is an anion-dependent proton pump. J. Biol. Chem. 262, 9175-9180.

Musso, D., Gubler, D.J., 2016. Zika virus. Clin. Microbiol. Rev. 29, 487-524.

Nelson, N., 1992. The vacuolar H(+)-ATPase — one of the most fundamental ion pumps in nature. J. Exp. Biol. 172, 19-27.

Nelson, N., Perzov, N., Cohen, A., Hagai, K., Padler, V., Nelson, H., 2000. The cellular biology of proton-motive force generation by V-ATPases. J. Exp. Biol. 203, 89-95.

Nishi, T., Forgac, M., 2002. The vacuolar (H+)-ATPases — nature's most versatile proton pumps. Nat. Rev. Mol. Cell Biol. 3, 94-103.

Patrick, M.L., Aimanova, K., Sanders, H.R., Gill, S.S., 2006. P-type Na+/K+-ATPase and V-type H+-ATPase expression patterns in the osmoregulatory organs of larval and adult mosquito *Aedes aegypti*. J. Exp. Biol. 209, 4638-4651.

Perreira, J.M., Aker, A.M., Savidis, G., Chin, C.R., McDougall, W.M., Portmann, J.M., Meraner, P., Smith, M.C., Rahman, M., Baker, R.E., Gauthier, A., Franti, M., Brass, A.L., 2015. RNASEK is a V-ATPase-associated factor required for endocytosis and the replication of rhinovirus, influenza A virus, and dengue virus. Cell Rep. 12, 850-863.

Powell, J.R., Tabachnick, W.J., 2013. History of domestication and spread of *Aedes aegypti* - a review. Mem. Inst. Oswaldo Cruz. 108, 11-17.

Powell, M.E., Bradish, H.M., Gatehouse, J.A., Fitches, E.C., 2017. Systemic RNAi in the small hive beetle *Aethina tumida* Murray (Coleoptera: Nitidulidae), a serious pest of the European honey bee *Apis mellifera*. Pest Manag. Sci. 73, 53-63.

Ranson, H., Burhani, J., Lumjuan, N., Black IV, W.C., 2010. Insecticide resistance in dengue vectors. TropIKA.net 1, 0-0.

Saftig, P., Klumperman, J., 2009. Lysosome biogenesis and lysosomal membrane proteins: trafficking meets function. Nat. Rev. Mol. Cell Biol. 10, 623-635.

Sanders, H.R., Evans, A.M., Ross, L.S., Gill, S.S., 2003. Blood meal induces global changes in midgut gene expression in the disease vector, *Aedes aegypti*. Insect Biochem. Mol. Biol. 33, 1105-1122.

Schlaeger, D.A., Fuchs, M.S., 1974. Effect of dopa-decarboxylase inhibition on *Aedes aegypti* eggs: evidence for sclerotization. J. Insect Physiol. 20, 349-357.

Scott, J.G., Michel, K., Bartholomay, L., Siegfried, B.D., Hunter, W.B., Smagghe, G., Zhu, K.Y., Douglas, A.E., 2013. Towards the elements of successful insect RNAi. J. Insect Physiol. 59, 1212-1221.

Simmons, C.P., Farrar, J.J., Nguyen, V.V., Wills, B., 2012. Dengue. N. Engl. J. Med. 366, 1423-1432.

Siomi, H., Siomi, M.C., 2009. On the road to reading the RNA-interference code. Nature 457, 396-404.

Stevens, T.H., Forgac, M., 1997. Structure, function and regulation of the vacuolar (H+)-ATPase. Annu. Rev. Cell Dev. Biol. 13, 779-808.

Sumner, J.P., Dow, J.A.T., Earley, F.G., Klein, U., Jäger, D., Wieczorek, H., 1995. Regulation of plasma membrane V-ATPase activity by dissociation of peripheral subunits. J. Biol. Chem. 270, 5649-5653.

Tabachnick, W.J., 1991. Evolutionary genetics and arthropod-borne disease: the yellow fever mosquito. Am. Entomol. 37, 14-26.

Taugner, G., 1971. The membrane of catecholamine storage vesicles of adrenal medulla catecholamine fluxes and ATPase activity. Naunyn-Schmiedebergs Arch. Pharmak. 270, 392-406.

Thakur, N., Upadhyay, S.K., Verma, P.C., Chandrashekar, K., Tuli, R., Singh, P.K., 2014. Enhanced whitefly resistance in transgenic tobacco plants expressing double stranded RNA of *v-ATPase A* gene. PLoS ONE 9, e87235.

Voss, M., Vitavska, O., Walz, B., Wieczorek, H., Baumann, O., 2007. Stimulus-induced phosphorylation of vacuolar H+-ATPase by protein kinase A. J. Biol. Chem. 282, 33735-33742.

Walker, R.R., Leigh, R.A., 1981. Characterization of a salt-stimulated ATPase activity associated with vacuoles isolated from storage roots of red beet (*Beta vulgaris L.*). Planta 153, 140-149.

Weaver, S.C., 2014. Arrival of chikungunya virus in the new world: prospects for spread and impact on public health. PLoS Negl. Trop. Dis. 8, e2921.

Wieczorek, H., Brown, D., Grinstein, S., Ehrenfeld, J., Harvey, W.R., 1999. Animal plasma membrane energization by proton-motive V-ATPases. Bioessays 21, 637-648.

World Health Organization, 2016. WHO statement on the first meeting of the International Health Regulations (2005) (IHR 2005) Emergency Committee on Zika virus and observed increase in neurological disorders and neonatal malformations. http://www.who.int/mediacentre/news/statements/2016/1st-emergency-committee-zika/en/ (accessed 03.03.17).

Yao, J., Rotenberg, D., Afsharifar, A., Barandoc-Alviar, K., Whitfield, A.E., 2013. Development of RNAi methods for *Peregrinus maidis*, the corn planthopper. PLoS ONE 8, e70243.

Zhu, K.Y., 2013. RNA interference: a powerful tool in entomological research and a novel approach for insect pest management. Insect Sci. 20, 1-3.

Chapter 2 - Genome-wide Survey and Phylogenetic Analyses of the Vacuolar H^+-ATPase Gene Family in the Yellow Fever Mosquito *Aedes aegypti* (Diptera: Culicidae)

Abstract

Vacuolar H^+-ATPases (V-ATPase) are multi-subunit enzymes that play significant roles in higher organisms, including using ATP to transport H^+ across biological membranes and generate electrochemical potentials. Animal knockouts of V-ATPase subunits cause lethality in insect larvae, showing that V-ATPase is an essential enzyme and potential target for insect control using RNAi. Since very little is known about V-ATPase subunits in *Aedes aegypti*, I performed a genome-wide survey to identify subunit genes and understand their phylogenetic relationship to those in other species. My genome-wide survey of V-ATPase genes demonstrated that this mosquito has 13 different subunits (A, B, C, D, E, F, G, H, a, c, c", d, e) encoded by 14 genes (two genes were identified for subunit a). Analysis of exon-intron arrangements for each gene revealed that each V-ATPase subunit gene has between one (subunit c) and 12 (subunit C) exons, with most genes (11) having 3 to 6 exons. Subsequent phylogenetic analysis of the deduced amino acid sequences of each subunit showed that V-ATPase subunits A, B, C, F, G, H, and a exhibited a high level of conservation among all the examined species, but subunits D, E, c, c", d, and e showed high conservation only among Dipteran species. Here, for the first time I have made a genome-wide survey of V-ATPase genes in *Ae. aegypti*. My results generally indicate that each subunit of V-ATPase is highly conserved among different insect species. However, the level of the conservation varies among the subunits even for the same insect species in the comparison.

Keywords: *Aedes aegypti*, exon-intron organization, genome-wide survey, phylogenetic analysis, V-ATPase

2.1. Introduction

Vacuolar H^+-ATPases (V-ATPase) are ATP-dependent proton pumps that function to acidify various intracellular compartments or transport protons from the cytoplasm to the extracellular space (Cotter et al., 2015; Marshansky et al., 2014; Nelson, 2013). In the plasma membrane, this enzyme uses ATP to transport protons outside of the cell and provides the energy for secondary active transporters that are vital for osmoregulation and the retention of ions, water, and nutrients (Bradley, 2008).

Acidification of endocytic compartments is important for dissociation of internalized ligand-receptor complexes and recycling of these unoccupied receptors back to the cell surface in endosomes, as well as protein degradation in lysosomes (Forgac, 2007). V-ATPases transport protons from the cytoplasm to the inside of the organelles including endosomes and lysosomes. In both organelles, internal pH and membrane potential are distinct from each other. Internal pH in endosomes is lower than lysosomes (Nelson, 2013). In endosomes, acidification is necessary for the entry of many envelope viruses and toxins into the cytoplasm (Gruenberg and van der Goot, 2006).

The V-ATPase is a multi-subunit complex that is composed of several subunits, which are assembled into two domains, the peripheral V_1 domain and the membrane embedded V_0 domain (Cipriano et al., 2008; Forgac, 2007; Marshansky and Futai, 2008). The peripheral V_1 domain is generally composed of eight different subunits (A, B, C, D, E, F, G, H), and is the domain responsible for ATP hydrolysis. A catalytic hexamer of six subunits (three A and three B) combine to perform the ATPase activity (Breton and Brown, 2013). In contrast, the membrane embedded V_0 domain consists of at least four subunits (a, c, d, e), and is responsible for proton transportation across the membrane (Forgac, 1998).

Aedes aegypti is the primary vector of dengue and yellow fevers and the object of intense investigation for novel methods of control. The publication of the *Ae. aegypti* genome by Nene et al. (2007) has provided an ideal tool to research the genes encoding V-ATPase subunits in this mosquito species. In this study, I performed a genome-wide, comprehensive analysis of V-ATPase genes in the yellow fever mosquito using several databases (NCBI, VectorBase, and Flybase). As a result of this research, I found that V-ATPase is composed of 13 different subunits in *Ae. aegypti*. In addition, my results showed that each subunit of V-ATPase is generally conserved among different insect species, but the level of the conservation varies among the subunits even between the same insect species in the comparison.

2.2. Materials and Methods

2.2.1. Database searches and sequence analysis

V-ATPase sequences were downloaded from three online databases: the National Center for Biotechnology Information database (NCBI) (https://www.ncbi.nlm.nih.gov/); VectorBase, a bioinformatics resource for invertebrate vectors of human pathogens (https://www.vectorbase.org/); and FlyBase, the *Drosophila* genes and genomes database (http://flybase.org/). *Drosophila* V-ATPase genes (Allan et al., 2005) were used as search queries in both the VectorBase and NCBI databases to identify *Ae. aegypti* genes.

In order to determine the correct names of genes, including up to date annotation, V-ATPase sequences were downloaded from VectorBase and used on the NCBI database as BLASTP or BLASTX queries. *Drosophila* V-ATPase sequences were used to identify *Ae. aegypti* sequences in VectorBase and NCBI, and the accession numbers for *Ae. aegypti* were obtained from NCBI.

2.2.2. Exon-intron organizations

The gene structure display server (http://gsds.cbi.pku.edu.cn/) (Hu et al., 2015) was used to determine the exon-intron organization of V-ATPase genes using coding and genomic sequences. For selected subunits of V-ATPase genes (*V-ATPase A, V-ATPase D,* and *V-ATPase H*), amino acid sequences were aligned with their genomic DNA sequences to obtain the exon-intron structure, and create the exon-intron maps for each selected gene.

2.2.3. Multiple alignments and phylogenetic analysis

The amino acid sequences of V-ATPase were confirmed by a homology search of other corresponding gene sequences, which are available on the GenBank database of the NCBI website (https://www.ncbi.nlm.nih.gov/). These sequences were blasted against other insect taxa by using the Basic Local Alignment Search Tool (BLAST) and protein BLAST (BLASTP) with standard parameters. The amino acid sequences of corresponding gene homologs from other insect species and their accession numbers were obtained from the NCBI database.

Multiple sequence alignments at the protein level were carried out using Clustal Omega software (http://www.ebi.ac.uk/Tools/msa/clustalo/) with default parameters. Alignments were then finalized to demonstrate conserved regions using BoxShade software (http://www.ch.embnet.org/software/BOX_form.html). Sequences from *Ae. aegypti* and other insect species that belong to Diptera, Coleoptera, Lepidoptera, Hemiptera and Hymenoptera were used for multiple alignment analyses.

Phylogenetic analyses were conducted using Muscle through the Molecular Evolutionary Genetic Analysis version 7 software (MEGA7) (http://www.megasoftware.net/) (Kumar et al., 2016). V-ATPase sequences from eight different insect species were included in the

phylogenetic trees. Phylogenetic trees were constructed using the maximum likelihood method (Le and Gascuel, 2008) with 1000 bootstrap replications to check for reliability of the results. Phylogenetic trees demonstrated the conservative relationship for selected V-ATPase subunits A, D, and H between *Ae. aegypti* and other holometabolous insects.

In this study, phylogenetic trees were constructed for each subunit of V-ATPase using these insect species: *Ae. aegypti, Drosophila melanogaster, Culex quinquefasciatus, Musca domestica, Bombyx mori, Tribolium castaneum, Apis mellifera,* and *Acyrthosiphon pisum*. The following accession numbers are in the order that they were mentioned in this paragraph:

V-ATPase subunit A: XP_001659520.1 (*Ae. aegypti*), NP_652004.2 (*D. melanogaster*), XP_001849275.1 (*C. quinquefasciatus*), XP_011291042.1 (*M. domestica*), NP_001091829.1 (*B. mori*), NP_001164361.1 (*T. castaneum*), XP_623495.1 (*A. mellifera*), NP_001119645.2 (*A. pisum*).

V-ATPase subunit D: XP_001660426.1 (*Ae. aegypti*), NP_651987.1 (*D. melanogaster*), XP_001865673.1 (*C. quinquefasciatus*), XP_005180029.1 (*M. domestica*), NP_001040286.1 (*B. mori*), XP_975872.1 (*T. castaneum*), XP_394769.2 (*A. mellifera*), NP_001119691.1 (*A. pisum*).

V-ATPase subunit H: XP_001652018.1 (*Ae. aegypti*), NP_523585.2 (*D. melanogaster*), XP_001844037.1 (*C. quinquefasciatus*), XP_005181998.1 (*M. domestica*), NP_001040488.1 (*B. mori*), NP_001280516.1 (*T. castaneum*), XP_003251675.1 (*A. mellifera*), XP_001949116.3 (*A. pisum*).

2.3. Results and Discussion

2.3.1. V-ATPase gene family in *Aedes aegypti*

Although very little information is available about different V-ATPase subunits in insects, we were able to identify genes for each V-ATPase subunit in *Ae. aegypti*. Previous studies demonstrated the genes encoding V-ATPase subunits in *Drosophila* (Allan et al., 2005). In my study, I used *Drosophila* V-ATPase genes as queries to identify the V-ATPase genes in the completed *Ae. aegypti* genome sequence (Nene et al., 2007).

Traditionally, all the genes encoding different V-ATPase subunits are characterized as the V-ATPase gene family because all these subunits form a V-ATPase protein complex. However, the concept of the family in this case is different from what is usually meant by gene family as different V-ATPase subunits are not necessarily evolutionarily related. According to my genome-wide survey, the *Ae. aegypti* V-ATPase has thirteen subunits (A, B, C, D, E, F, G, H, a, c, c", d, e) that corresponded to those identified previously in *Drosophila.* These subunits combine to form the two domains of the V-ATPase, the V_1 (peripheral domain) and V_0 (integral domain). The V_1 domain was composed of eight different subunits (A, B, C, D, E, F, G, H), whereas the V_0 domain consisted of five subunits (a, c, c'', d, e) in *Ae. aegypti* (Tables 2.1. and 2.2.). The V-ATPase multigene family was encoded by 33 genes in *D. melanogaster* and most of the V-ATPase subunits are encoded by more than two genes (Allan et al., 2005). In contrast, my results indicated that the V-ATPase gene family in *Ae. aegypti* was encoded by 14 genes and each subunit was encoded by single gene except for subunit a (encoded by 2; Table 2.1.).

2.3.2. Genomic distribution of V-ATPase genes

The genomic location of each V-ATPase subunit gene is difficult to identify in *Ae. aegypti*. The genes encoding the different subunits of the V-ATPase enzyme are spread throughout the genome. Only three genes *V-ATPase a*, *V-ATPase D*, and *V-ATPase H* were positively identified as being located on chromosome 1, 3, or 2, respectively. The chromosomal location of the other 13 genes remains unknown.

After identification of the V-ATPase genes in *Ae. aegypti*, their deduced amino acid sequences were blasted against the insect taxa to identify their homologs. As a result of the database search, I found that there was a close relationship of V-ATPase subunits among insects (Tables 2.3. and 2.4.). Specifically, the V-ATPase genes in *Ae. aegypti* have a very high amino acid sequence identity level to those of *C. quinquefasciatus* and *D. melanogaster*.

The identity levels of the deduced amino acid sequence for each selected subunit (A, D and H) among the dipteran species were extremely high. For example, subunit A in *Ae. aegypti* showed 97 and 94% identities to the orthologs of *C. quinquefasciatus* (Diptera: Culicidae) or *D. melanogaster* (Diptera: Drosophilidae), respectively. Similarly, subunit D in *Ae. aegypti* showed 97 and 89% identities to the orthologs of *C. quinquefasciatus* or *D. melanogaster*, respectively. Meanwhile, subunit H in *Ae. aegypti* showed 96 and 80% identities to the orthologs of *C. quinquefasciatus* or *D. melanogaster*, respectively. Interestingly, the two genes encoding subunit a, a part of the V_0 domain, showed only a 56% identitiy to each other when their deduced amino acid sequences were compared.

2.3.3. Exon-intron organizations

In *Ae. aegypti*, the V-ATPase enzyme was encoded by 14 genes which have various exon-intron organizations. The number of exons for each subunit gene ranged from one to 12, with the majority of genes having three to six exons (Table 2.1.). The gene encoding V-ATPase subunit C had 12 exons, the highest number of exons, whereas the gene encoding V-ATPase subunit c'' had only one exon. In this study, I chose three subunits (*V-ATPase A*, *V-ATPase D*, and *V-ATPase H*) for further analyses to diagram their exon-intron organizations. My results showed that the genes encoding V-ATPase subunit A or D had five exons whereas the gene for subunit H had six exons (Figures 2.1., 2.4., and 2.7.).

2.3.4. Phylogenetic analysis

Phylogenetic trees were constructed using the maximum likelihood method (Le and Gascuel, 2008) in order to examine the evolutionary relationship of V-ATPase subunits among different insect taxa. Phylogenetic analysis of the deduced amino acid sequences from different insect species and orders including Diptera, Coleoptera, Lepidoptera, Hemiptera and Hymenoptera showed that V-ATPase subunits from *Ae. aegypti* were closely related to those from *C. quinquefasciatus* and *D. melanogaster*.

The analysis showed *Ae. aegypti* subunit A clustered with other dipteran insects, including *C. quinquefasciatus*, *D. melanogaster*, and *M. domestica*, with two distinct subgroups: Cyclorrhapha (*D. melanogaster* and *M. domestica*) and Orthorrhapha, (*C. quinquefasciatus* and *Ae. aegypti*) (Figure 2.2.). The *Ae. aegypti* subunits D and H also clustered with other Dipterans, including *C. quinquefasciatus*, *D. melanogaster*, and *M. domestica* (Figures 2.5. and 2.8.). Furthermore, based on my phylogenetic analyses the molecular relativeness of *V-ATPase A* and

V-ATPase H genes exhibited a high levels of conservation among selected species. However, *V-ATPase D* gene only showed high conservation among dipteran species.

Multiple alignments of the deduced amino acid sequences of each of the three selected V-ATPase subunits (A, D and H) showed that the amino acid sequences of these subunits are highly conserved among different insect species (Figures 2.3., 2.6., and 2.9.). I observed only a few amino acid differences among the sequences of each selected subunit. In addition, multiple sequence alignments at the protein level and phylogenetic analyses were performed for the rest of the V-ATPase subunits in *Ae. aegypti* (Figures A.1.-A.20), and like subunits A, D, and H, these comparisons showed high similarity between the amino acid sequences of *Ae. aegypti* with those of the other insects included in the analysis.

In conclusion, for the first time I have made a genome-wide survey of V-ATPase genes in *Ae. aegypti*. The results generally demonstrated that each subunit of V-ATPase was highly conserved among different insect species. However, the level of the conservation varied among the subunits even for the same insect species in the comparison. For instance, the amino acid identity level of subunit A is 94% between *Ae. aegypti* and *D. melanogaster* whereas the amino acid identity level of subunit e is 66% between the two species.

References

Allan, A.K., Du, J., Davies, S.A., Dow, J.A.T., 2005. Genome-wide survey of V-ATPase genes in *Drosophila* reveals a conserved renal phenotype for lethal alleles. Physiol. Genomics 22, 128-138.

Bradley, T.J., 2008. Active transport in insect recta. J. Exp. Biol. 211, 835-836.

Breton, S., Brown, D., 2013. Regulation of luminal acidification by the V-ATPase. Physiol. 28, 318-329.

Cipriano, D.J., Wang, Y., Bond, S., Hinton, A., Jefferies, K.C., Qi, J., Forgac, M., 2008. Structure and regulation of the vacuolar ATPases. Biochim. Biophys. Acta 1777, 599-604.

Cotter, K., Stransky, L., McGuire, C., Forgac, M., 2015. Recent insights into the structure, regulation and function of the V-ATPases. Trends Biochem. Sci. 40, 611-622.

Forgac, M., 2007. Vacuolar ATPases: rotary proton pumps in physiology and pathophysiology. Nat. Rev. Mol. Cell Biol. 8, 917-929.

Forgac, M., 1998. Structure, function and regulation of the vacuolar (H+)-ATPases. FEBS Lett. 440, 258-263.

Gruenberg, J., van der Goot, F.G., 2006. Mechanisms of pathogen entry through the endosomal compartments. Nat. Rev. Mol. Cell Biol. 7, 495-504.

Hu, B., Jin, J., Guo, A., Zhang, H., Luo, J., Gao, G., 2015. GSDS 2.0: an upgraded gene feature visualization server. Bioinformatics 31, 1296-1297.

Kumar, S., Stecher, G., Tamura, K., 2016. MEGA7: molecular evolutionary genetics analysis version 7.0 for bigger datasets. Mol. Biol. Evol. 33, 1870-1874.

Le, S.Q., Gascuel, O., 2008. An improved general amino acid replacement matrix. Mol. Biol. Evol. 25, 1307-1320.

Marshansky, V., Futai, M., 2008. The V-type H+-ATPase in vesicular trafficking: targeting, regulation and function. Curr. Opin. Cell Biol. 20, 415-426.

Marshansky, V., Rubinstein, J.L., Grüber, G., 2014. Eukaryotic V-ATPase: novel structural findings and functional insights. Biochim. Biophys. Acta 1837, 857-879.

Nelson, N., 2013. Organellar Proton-ATPases, Springer science and Business Media, Texas.

Nene, V., Wortman, J.R., Lawson, D., Haas, B., Kodira, C., Tu, Z., Loftus, B., Xi, Z., Megy, K., Grabherr, M., Ren, Q., Zdobnov, E.M., Lobo, N.F., Campbell, K.S., Brown, S.E., Bonaldo, M.F., Zhu, J., Sinkins, S.P., Hogenkamp, D.G., Amedeo, P., Arensburger, P., Atkinson, P.W., Bidwell, S., Biedler, J., Birney, E., Bruggner, R.V., Costas, J., Coy, M.R., Crabtree, J., Crawford, M., deBruyn, B., DeCaprio, D., Eiglmeier, K., Eisenstadt, E., El-Dorry, H., Gelbart, W.M., Gomes, S.L., Hammond, M., Hannick, L.I., Hogan, J.R., Holmes, M.H., Jaffe, D., Johnston, J.S., Kennedy, R.C., Koo, H., Kravitz, S., Kriventseva, E.V., Kulp, D., LaButti, K., Lee, E., Li, S., Lovin, D.D., Mao, C., Mauceli, E., Menck, C.F.M., Miller, J.R., Montgomery, P., Mori, A., Nascimento, A.L., Naveira, H.F., Nusbaum, C., O'Leary, S., Orvis, J., Pertea, M., Quesneville, H., Reidenbach, K.R., Rogers, Y., Roth, C.W., Schneider, J.R., Schatz, M., Shumway, M., Stanke, M., Stinson, E.O., Tubio, J.M.C., VanZee, J.P., Verjovski-Almeida, S., Werner, D., White, O., Wyder, S., Zeng, Q., Zhao, Q., Zhao, Y., Hill, C.A., Raikhel, A.S., Soares, M.B., Knudson, D.L., Lee, N.H., Galagan, J., Salzberg, S.L., Paulsen, I.T., Dimopoulos, G., Collins, F.H., Birren, B., Fraser-Liggett, C., Severson, D.W., 2007. Genome sequence of *Aedes aegypti*, a major arbovirus vector. Science 316, 1718-1723.

Smith, A.N., Lovering, R.C., Futai, M., Takeda, J., Brown, D., Karet, F.E., 2003. Revised nomenclature for mammalian vacuolar-type H+-ATPase subunit genes. Mol. Cell 12, 801-803.

Table 2.1. V-ATPase gene family in *Aedes aegypti*.

Most V-ATPase genes shown here demonstrated high similarity (e $<10^{-10}$) to V-ATPase genes in *Drosophila*. BLAST was used to identify the genes in *Ae. aegypti*. Light blue cells represent the selected subunits of V-ATPase analyzed in this study.

	Subunit	Genes in *Ae. aegypti*	Exon number	Length	E-value	Genes in *D. melanogaster*
V_1 Domain	A	AAEL008787	6	3108	0	vha68-1 (CG12403)
						vha68-2 (CG3762)
						vha68-3 (CG5075)
	B	AAEL005798	3		0	vha55 (CG17369)
	C	AAEL005173	12	2088	1e-166	vha44 (CG8048)
	D	AAEL009808	5	1140	2e-160	vha36-1 (CG8186)
						vha36-2 (CG13167)
						vha36-3 (CG8310)
	E	AAEL012035	6	3027	3e-86	vha26 (CG1088)
	F	AAEL002464	5	567	7e-81	vha14-1 (CG8210)
					8e-27	vha14-2 (CG1076)
	G	AAEL007184	3	1251	4e-33	vha13 (CG6213)
	H	AAEL006516	6	2166	0	vhaSFD (CG17332)
V_0 Domain	a	AAEL003743	10	3201	0	vha100-1 (CG1709)
		AAEL014053	5	2743	0	vha100-2 (CG7679)
					5e-174	vha100-3 (CG30329)
					0	vha100-4 (CG7678)
					0	vha100-5 (CG12602)
	c	AAEL000291	3	2972	4e-90	vha16-1 (CG3161)
					1e-54	vha16-2 (CG32089)
					4e-63	vha16-3 (CG32090)
					2e-39	vha16-4 (CG9013)
					2e-38	vha16-5 (CG6737)
	c"	AAEL012113	1	636	9e-95	vhaPPA1-1 (CG7007)
					4e-57	vhaPPA1-2 (CG7026)
	e	AAEL010819	3	1105	2e-32	vhaM9.7-1 (CG1268)
					2e-31	vhaM9.7-2 (CG7625)
					7e-17	vhaM9.7-3 (CG11589)
					6e-10	vhaM9.7-4 (CG14909)
	d	AAEL011025	3	1680	0	vhaAC39-1 (CG2934)
					2e-117	vhaAC39-2 (CG4624)

Table 2.2. Accession numbers of the V-ATPase genes in *Ae. aegypti* by database.

	Subunits in *Ae. aegypti*	Database	
		NCBI	VectorBase
V_1 Domain	A	XP_001659520.1	AAEL008787
	B	XP_001651458.1	AAEL005798
	C	XP_001650489.1	AAEL005173
	D	XP_001660426.1	AAEL009808
	E	XP_001655825.1	AAEL012035
	F	XP_001655376.1	AAEL002464
	G	XP_001652605.1	AAEL007184
	H	XP_001652018.1	AAEL006516
V_0 Domain	a	XP_001657232.1	AAEL003743
		XP_001657344.1	AAEL014053
	c	XP_001654757.1	AAEL000291
	c"	XP_001662256.1	AAEL012113
	d	XP_001661299.1	AAEL011025

Table 2.3. Comparisons of the V-ATPase genes of the V1 domain in Ae. aegypti and other insects. Light blue cells represent the selected subunits of V-ATPase analyzed in this study.

Genes identified in *Ae. aegypti*	Most similar genes found in other insect species by BLASTP search				Proposed Function/Location (Smith et al., 2003)
	Species	Accession number	Amino acid identity (%)	E-value	
AaV-ATPaseA	*Drosophila melanogaster*	NP_652004.2	94	0.0	Catalytic ATP binding
	Culex quinquefasciatus	XP_001849275.1	97	0.0	
	Musca domestica	XP_011291042.1	93	0.0	
	Bombyx mori	NP_001091829.1	91	0.0	
	Tribolium castaneum	NP_001164361.1	28	1e-28	
	Apis mellifera	XP_623495.1	92	0.0	
	Acyrthosiphon pisum	NP_001119645.2	28	1e-27	
AaV-ATPaseB	*Drosophila melanogaster*	NP_476908.1	98	0.0	Non catalytic ATP binding
	Culex quinquefasciatus	XP_001845188.1	98	0.0	
	Musca domestica	XP_005181053.1	98	0.0	
	Bombyx mori	NP_001091828.1	96	0.0	
	Tribolium castaneum	NP_001164361.1	26	2e-28	
	Apis mellifera	XP_624112.1	96	0.0	
	Acyrthosiphon pisum	NP_001280473.1	98	7e-153	
AaV-ATPaseC	*Drosophila melanogaster*	NP_477266.1	85	7e-177	Peripheral stator
	Culex quinquefasciatus	XP_001843335.1	76	0.0	
	Musca domestica	XP_005174884.1	86	2e-177	
	Bombyx mori	NP_001040138.1	83	2e-169	
	Tribolium castaneum	XP_015836982.1	91	0.0	
	Apis mellifera	XP_006562159.1	81	1e-173	
	Acyrthosiphon pisum	XP_001946227.1	83	0.0	
AaV-ATPaseD	*Drosophila melanogaster*	NP_651987.1	89	1e-158	Central rotor
	Culex quinquefasciatus	XP_001865673.1	97	2e-172	
	Musca domestica	XP_005180029.1	90	5e-163	
	Bombyx mori	NP_001040286.1	86	2e-136	
	Tribolium castaneum	XP_975872.1	85	2e148	
	Apis mellifera	XP_394769.2	83	2e-141	
	Acyrthosiphon pisum	NP_001119691.1	81	1e-138	
AaV-ATPaseE	*Drosophila melanogaster*	NP_524237.1	74	1e-118	Peripheral stator
	Culex quinquefasciatus	XP_001849126.1	89	2e-149	
	Musca domestica	XP_005178098.1	77	1e-123	
	Bombyx mori	NP_001040451.1	75	2e-116	
	Tribolium castaneum	XP_970621.1	73	3e-118	
	Apis mellifera	XP_625098.1	75	2e-117	
	Acyrthosiphon pisum	NP_001155650.1	68	3e-99	
AaV-ATPaseF	*Drosophila melanogaster*	NP_476969.1	91	4e-80	Central rotor
	Culex quinquefasciatus	XP_001866561.1	98	8e-91	
	Musca domestica	XP_005179584.1	91	6e-82	
	Bombyx mori	NP_001040448.1	90	9e-79	
	Tribolium castaneum	XP_975016.1	89	5e-77	
	Apis mellifera	XP_624852.1	86	8e-74	
	Acyrthosiphon pisum	NP_001119690.1	84	2e-72	

AaV-ATPaseG	*Drosophila melanogaster*	NP_477437.1	75	7e-55	Peripheral stator
	Culex quinquefasciatus	XP_001864556.1	93	2e-73	
	Musca domestica	XP_005180412.1	77	1e-59	
	Bombyx mori	NP_001040287.1	78	2e-60	
	Tribolium castaneum	XP_973974.1	79	1e-59	
	Apis mellifera	XP_624346.1	76	2e-57	
	Acyrthosiphon pisum	NP_001119628.1	80	1e-60	
AaV-ATPaseH (SFD)	*Drosophila melanogaster*	NP_523585.2	80	0.0	Peripheral stator
	Culex quinquefasciatus	XP_001844037.1	96	0.0	
	Musca domestica	XP_005181998.1	83	0.0	
	Bombyx mori	NP_001040488.1	73	0.0	
	Tribolium castaneum	NP_001280516.1	74	0.0	
	Apis mellifera	XP_003251675.1	76	0.0	
	Acyrthosiphon pisum	XP_001949116.3	70	0.0	

Table 2.4. The comparison of V-ATPase genes of the V_0 domain in *Ae. aegypti* and other insects.

Genes identified in *A.aegypti*	Most similar genes found in other insect species by BLASTP search				Proposed Function/Location (Smith et al., 2003)
	Species	Accession number	Amino acid identity (%)	E-value	
AaV-ATPase-a	*Drosophila melanogaster*	NP_001163768.1	80	0.0	H+ translocation
	Culex quinquefasciatus	XP_001847258.1	89	0.0	
	Musca domestica	XP_005182099.1	82	0.0	
	Bombyx mori	XP_012550179.1	76	0.0	
	Tribolium castaneum	XP_008200809.1	78	0.0	
	Apis mellifera	XP_016769523.1	80	0.0	
	Acyrthosiphon pisum	XP_008183003.1	78	0.0	
AaV-ATPase-a	*Drosophila melanogaster*	NP_650722.1	74	0.0	H^+ translocation
	Culex quinquefasciatus	XP_001845000.1	85	0.0	
	Musca domestica	XP_005182534.1	76	0.0	
	Bombyx mori	XP_004931128.1	74	0.0	
	Tribolium castaneum	XP_968579.1	72	0.0	
	Apis mellifera	XP_016768513.1	70	0.0	
	Acyrthosiphon pisum	XP_016663159.1	68	0.0	
AaV-ATPase-c	*Drosophila melanogaster*	NP_476801.1	94	2e-101	H^+ translocation
	Culex quinquefasciatus	XP_001861266.1	95	7e-99	
	Musca domestica	XP_005184512.1	95	5e-98	
	Bombyx mori	NP_001091762.1	93	4e-100	
	Tribolium castaneum	NP_001161226.1	33	2e-15	
	Apis mellifera	NP_001011570.1	92	1e-97	
	Acyrthosiphon pisum	NP_001155531.1	94	1e-101	
AaV-ATPase-c''	*Drosophila melanogaster*	NP_652010.1	77	2e-101	H^+ translocation
	Culex quinquefasciatus	XP_001846404.1	96	5e-131	
	Musca domestica	XP_005178527.1	83	2e-108	
	Bombyx mori	NP_001040169.1	79	4e-98	
	Tribolium castaneum	NP_001161226.1	68	3e-82	
	Apis mellifera	XP_392599.1	83	1e-116	
	Acyrthosiphon pisum	NP_001155679.1	75	1e-105	
AaV-ATPase-d	*Drosophila melanogaster*	NP_570080.1	95	0.0	Nonintegral membrane component
	Culex quinquefasciatus	XP_001870744.1	99	0.0	
	Musca domestica	XP_005180381.2	95	0.0	
	Bombyx mori	NP_001040429.1	93	0.0	
	Tribolium castaneum	XP_974905.1	92	0.0	
	Apis mellifera	XP_393438.2	93	0.0	
	Acyrthosiphon pisum	NP_001191854.1	90	0.0	
AaV-ATPase-e	*Drosophila melanogaster*	NP_649327.2	64	1e-33	Membrane sector-associated
	Culex quinquefasciatus	XP_001863465.1	89	1e-58	
	Musca domestica	XP_005187210.1	65	3e-33	
	Bombyx mori	XP_004933731.1	65	3e-36	
	Tribolium castaneum	XP_971898.1	72	2e-39	
	Apis mellifera	XP_624787.1	73	2e-37	
	Acyrthosiphon pisum	XP_003242132.1	78	6e-41	

Figure 2.1. Exon-intron organization of the V-ATPase subunit A gene (*V-ATPase A*) in *Ae. aegypti.*

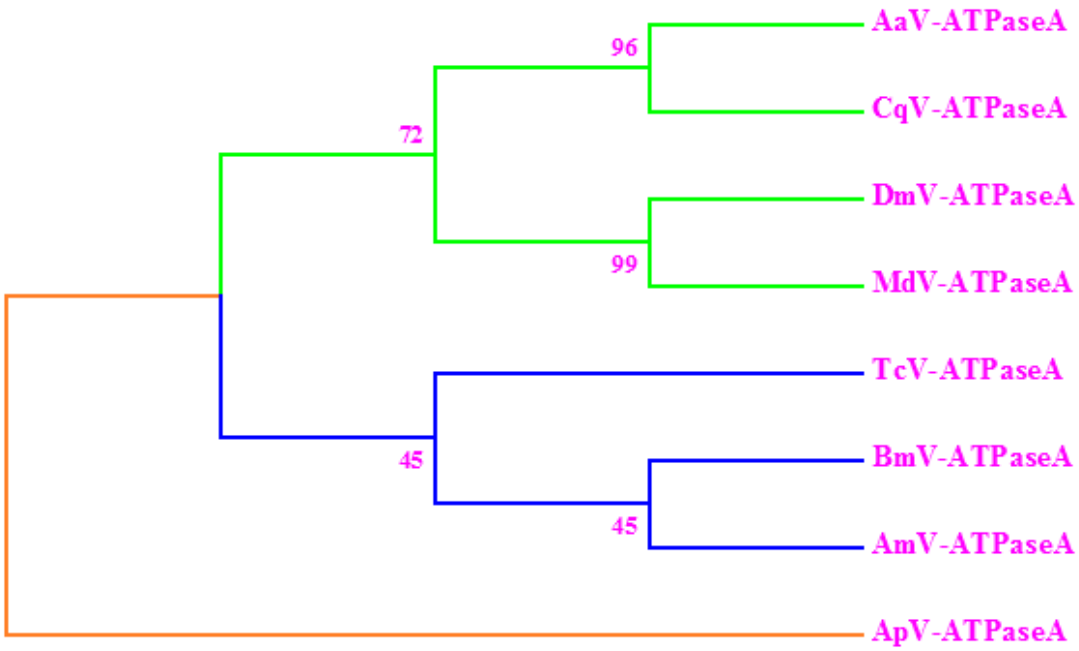

Figure 2.2. Phylogenetic relationship of the deduced amino acid sequences of *V-ATPase A* genes.

This rooted phylogenetic tree was constructed using the maximum likelihood method. Nodes indicate bootstrap values calculated with 1000 replications. The green branches represent the order Diptera, orange branch shows the outgroup, and blue branches represent other orders. The accession numbers for the sequences are as follows: AaV-ATPaseA (XP_001659520.1, *Aedes aegypti*); DmV-ATPaseA (NP_652004.2, *Drosophila melanogaster*); CqV-ATPaseA (XP_001849275.1, *Culex quinquefasciatus*); MdV-ATPaseA (XP_011291042.1, *Musca domestica*); BmV-ATPaseA (NP_001091829.1, *Bombyx mori*); TcV-ATPaseA (XP_976188.1; *Tribolium castaneum*); AmV-ATPaseA (XP_623495.1; *Apis mellifera*); ApV-ATPaseA (XP_008179407.1; *Acyrthosiphon pisum*).

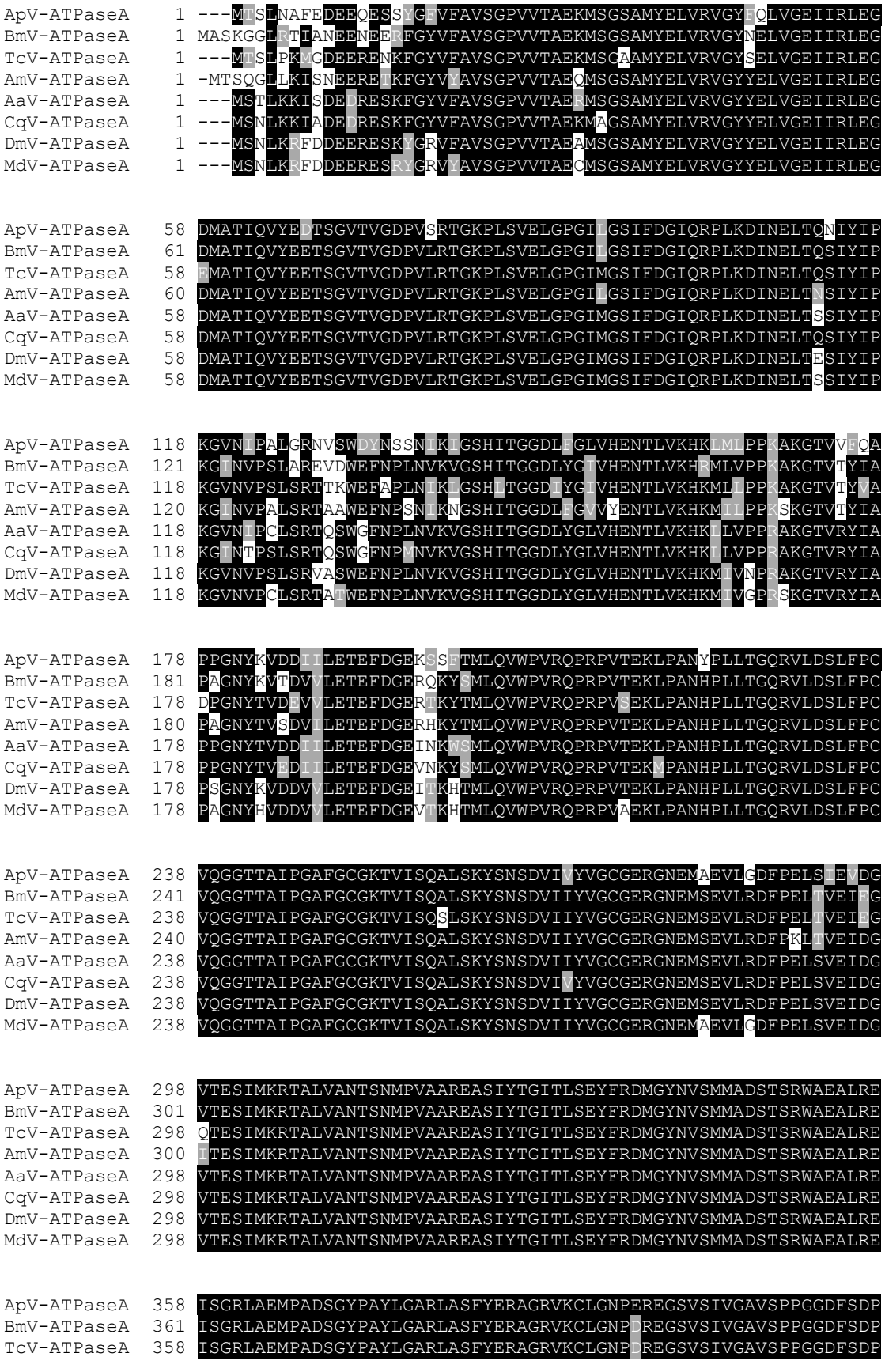
ApV-ATPaseA 1 ---MTSLNAFEDEEQESSYGFVFAVSGPVVTAEKMSGSAMYELVRVGYFQLVGEIIRLEG
BmV-ATPaseA 1 MASKGGLFTIANEENEERFGYVFAVSGPVVTAEKMSGSAMYELVRVGYNELVGEIIRLEG
TcV-ATPaseA 1 ---MTSLPKMGDEERENKFGYVFAVSGPVVTAEKMSGAAMYELVRVGYSELVGEIIRLEG
AmV-ATPaseA 1 -MTSQGLLKISNEERETKFGYVYAVSGPVVTAEQMSGSAMYELVRVGYYELVGEIIRLEG
AaV-ATPaseA 1 ---MSTLKKISDEDRESKFGYVFAVSGPVVTAERMSGSAMYELVRVGYYELVGEIIRLEG
CqV-ATPaseA 1 ---MSNLKKIADEDRESKFGYVFAVSGPVVTAEKMAGSAMYELVRVGYYELVGEIIRLEG
DmV-ATPaseA 1 ---MSNLKFFDDEERESKYGRVFAVSGPVVTAEAMSGSAMYELVRVGYYELVGEIIRLEG
MdV-ATPaseA 1 ---MSNLKFFDDEERESRYGRVYAVSGPVVTAECMSGSAMYELVRVGYYELVGEIIRLEG
ApV-ATPaseA 58 DMATIQVYEDTSGVTVGDPVSRTGKPLSVELGPGILGSIFDGIQRPLKDINELTQNIYIP
BmV-ATPaseA 61 DMATIQVYEETSGVTVGDPVLRTGKPLSVELGPGILGSIFDGIQRPLKDINELTQSIYIP
TcV-ATPaseA 58 EMATIQVYEETSGVTVGDPVLRTGKPLSVELGPGIMGSIFDGIQRPLKDINELTQSIYIP
AmV-ATPaseA 60 DMATIQVYEETSGVTVGDPVLRTGKPLSVELGPGILGSIFDGIQRPLKDINELTNSIYIP
AaV-ATPaseA 58 DMATIQVYEETSGVTVGDPVLRTGKPLSVELGPGIMGSIFDGIQRPLKDINELTSSIYIP
CqV-ATPaseA 58 DMATIQVYEETSGVTVGDPVLRTGKPLSVELGPGIMGSIFDGIQRPLKDINELTQSIYIP
DmV-ATPaseA 58 DMATIQVYEETSGVTVGDPVLRTGKPLSVELGPGIMGSIFDGIQRPLKDINELTESIYIP
MdV-ATPaseA 58 DMATIQVYEETSGVTVGDPVLRTGKPLSVELGPGIMGSIFDGIQRPLKDINELTSSIYIP
ApV-ATPaseA 118 KGVNIPALGRNVSWDYNSSNIKIGSHITGGDLFGLVHENTLVKHKLMLPPKAKGTVVFQA
BmV-ATPaseA 121 KGINVPSLAREVDWEFNPLNVKVGSHITGGDLYGIVHENTLVKHRMLVPPKAKGTVTYIA
TcV-ATPaseA 118 KGVNVPSLSRTTKWEFAPLNIKLGSHLTGGDIYGIVHENTLVKHKMLLPPKAKGTVTYVA
AmV-ATPaseA 120 KGINVPALSRTAAWEFNPSNIKNGSHITGGDLFGVVYENTLVKHKMILPPKSKGTVTYIA
AaV-ATPaseA 118 KGVNIPCLSRTQSWGFNPLNVKVGSHITGGDLYGLVHENTLVKHKLLVPPRAKGTVRYIA
CqV-ATPaseA 118 KGINTPSLSRTQSWGFNPMNVKVGSHITGGDLYGLVHENTLVKHKLLVPPRAKGTVRYIA
DmV-ATPaseA 118 KGVNVPSLSRVASWEFNPLNVKVGSHITGGDLYGLVHENTLVKHKMIVNPRAKGTVRYIA
MdV-ATPaseA 118 KGVNVPCLSRTATWEFNPLNVKVGSHITGGDLYGLVHENTLVKHKMTVGPRSKGTVRYIA
ApV-ATPaseA 178 PPGNYKVDDIILETEFDGEKSSFTMLQVWPVRQPRPVTEKLPANYPLLTGQRVLDSLFPC
BmV-ATPaseA 181 PAGNYKVTDVVLETEFDGERQKYSMLQVWPVRQPRPVTEKLPANHPLLTGQRVLDSLFPC
TcV-ATPaseA 178 DPGNYTVDHVVLETEFDGERIKYTMLQVWPVRQPRPVSEKLPANHPLLTGQRVLDSLFPC
AmV-ATPaseA 180 PAGNYTVSDVILETEFDGERHKYTMLQVWPVRQPRPVTEKLPANHPLLTGQRVLDSLFPC
AaV-ATPaseA 178 PPGNYTVDDIILETEFDGEINKWSMLQVWPVRQPRPVTEKLPANHPLLTGQRVLDSLFPC
CqV-ATPaseA 178 PPGNYTVEDIILETEFDGEVNKYSMLQVWPVRQPRPVTEKMPANHPLLTGQRVLDSLFPC
DmV-ATPaseA 178 PSGNYKVDDVVLETEFDGEITKHTMLQVWPVRQPRPVTEKLPANHPLLTGQRVLDSLFPC
MdV-ATPaseA 178 PAGNYHVDDVVLETEFDGEVIKHTMLQVWPVRQPRPVAEKLPANHPLLTGQRVLDSLFPC
ApV-ATPaseA 238 VQGGTTAIPGAFGCGKTVISQALSKYSNSDVIVYVGCGERGNEMAEVLGDFPELSIEVDG
BmV-ATPaseA 241 VQGGTTAIPGAFGCGKTVISQALSKYSNSDVIIYVGCGERGNEMSEVLRDFPELTVEIEG
TcV-ATPaseA 238 VQGGTTAIPGAFGCGKTVISQSLSKYSNSDVIIYVGCGERGNEMSEVLRDFPELTVEIEG
AmV-ATPaseA 240 VQGGTTAIPGAFGCGKTVISQALSKYSNSDVIIYVGCGERGNEMSEVLRDFPKLTVEIDG
AaV-ATPaseA 238 VQGGTTAIPGAFGCGKTVISQALSKYSNSDVIIYVGCGERGNEMSEVLRDFPELSVEIDG
CqV-ATPaseA 238 VQGGTTAIPGAFGCGKTVISQALSKYSNSDVIVYVGCGERGNEMSEVLRDFPELSVEIDG
DmV-ATPaseA 238 VQGGTTAIPGAFGCGKTVISQALSKYSNSDVIIYVGCGERGNEMSEVLRDFPELSVEIDG
MdV-ATPaseA 238 VQGGTTAIPGAFGCGKTVISQALSKYSNSDVIIYVGCGERGNEMAEVLGDFPELSVEIDG
ApV-ATPaseA 298 VTESIMKRTALVANTSNMPVAAREASIYTGITLSEYFRDMGYNVSMMADSTSRWAEALRE
BmV-ATPaseA 301 VTESIMKRTALVANTSNMPVAAREASIYTGITLSEYFRDMGYNVSMMADSTSRWAEALRE
TcV-ATPaseA 298 QTESIMKRTALVANTSNMPVAAREASIYTGITLSEYFRDMGYNVSMMADSTSRWAEALRE
AmV-ATPaseA 300 ITESIMKRTALVANTSNMPVAAREASIYTGITLSEYFRDMGYNVSMMADSTSRWAEALRE
AaV-ATPaseA 298 VTESIMKRTALVANTSNMPVAAREASIYTGITLSEYFRDMGYNVSMMADSTSRWAEALRE
CqV-ATPaseA 298 VTESIMKRTALVANTSNMPVAAREASIYTGITLSEYFRDMGYNVSMMADSTSRWAEALRE
DmV-ATPaseA 298 VTESIMKRTALVANTSNMPVAAREASIYTGITLSEYFRDMGYNVSMMADSTSRWAEALRE
MdV-ATPaseA 298 VTESIMKRTALVANTSNMPVAAREASIYTGITLSEYFRDMGYNVSMMADSTSRWAEALRE
ApV-ATPaseA 358 ISGRLAEMPADSGYPAYLGARLASFYERAGRVKCLGNPEREGSVSIVGAVSPPGGDFSDP
BmV-ATPaseA 361 ISGRLAEMPADSGYPAYLGARLASFYERAGRVKCLGNPDREGSVSIVGAVSPPGGDFSDP
TcV-ATPaseA 358 ISGRLAEMPADSGYPAYLGARLASFYERAGRVKCLGNPDREGSVSIVGAVSPPGGDFSDP

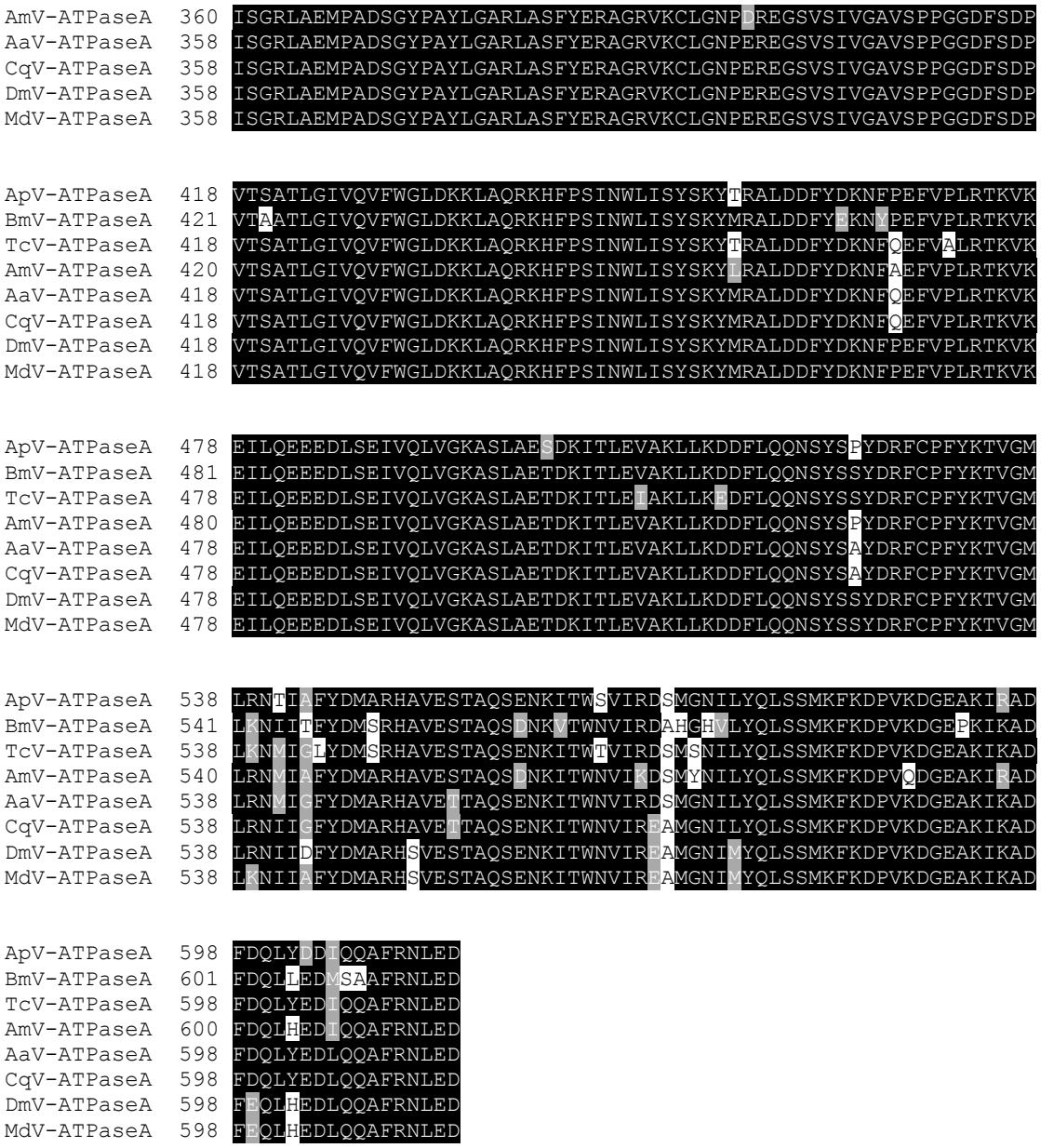

Figure 2.3. Multiple alignments of deduced amino acid sequences of V-ATPase subunit A (*Ae. aegypti, D. melanogaster, C. quinquefasciatus, M. domestica, B. mori, T. castaneum, A. mellifera, A. pisum*).

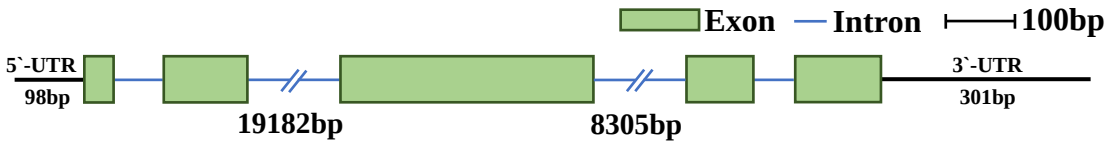

Figure 2.4. Exon-intron organization of the V-ATPase subunit D gene (*V-ATPase D*) in *Ae. aegypti.*

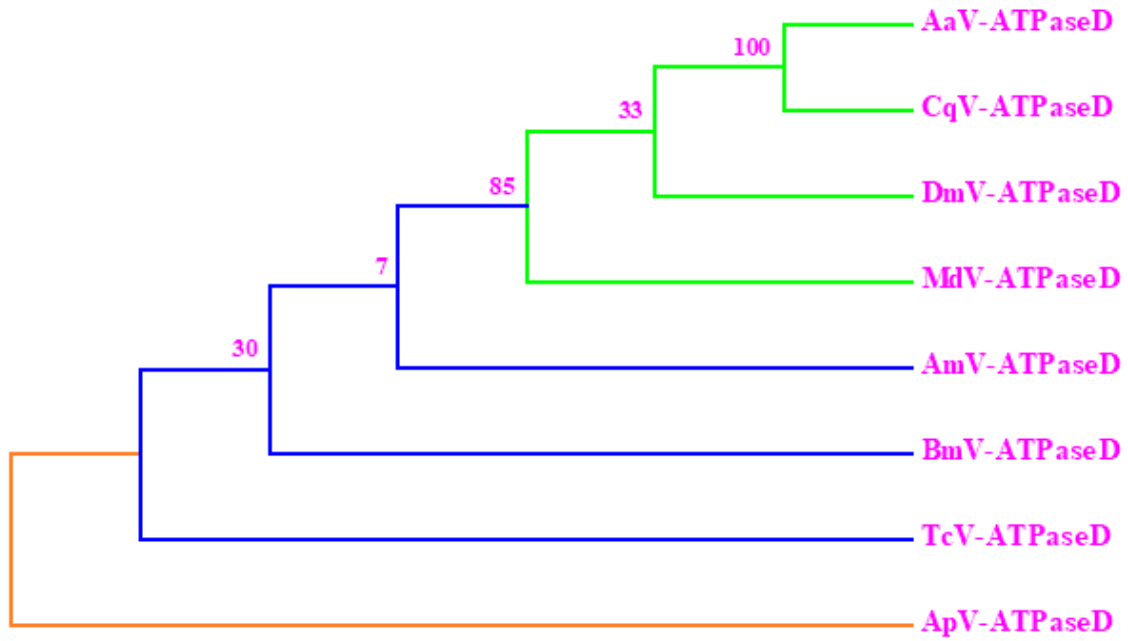

Figure 2.5. Phylogenetic relationship of the deduced amino acid sequences of *V-ATPase D* gene.

This rooted phylogenetic tree was constructed using the maximum likelihood method. Nodes indicate bootstrap values calculated with 1000 replications. The green branches represent the order Diptera, orange branch shows the outgroup, and blue branches represent other orders. The accession numbers for the sequences are as follows: AaV-ATPaseD (XP_001660426.1, *Aedes aegypti*); DmV-ATPaseD (NP_651987.1, *Drosophila melanogaster*); CqV-ATPaseD (XP_001865673.1, *Culex quinquefasciatus*); MdV-ATPaseD (XP_005180029.1, *Musca domestica*); BmV-ATPaseD (NP_001040286.1, *Bombyx mori*); TcV-ATPaseD (XP_975872.1; *Tribolium castaneum*); AmV-ATPaseD (XP_394769.2; *Apis mellifera*); ApV-ATPaseD (NP_001119691.1; *Acyrthosiphon pisum*).

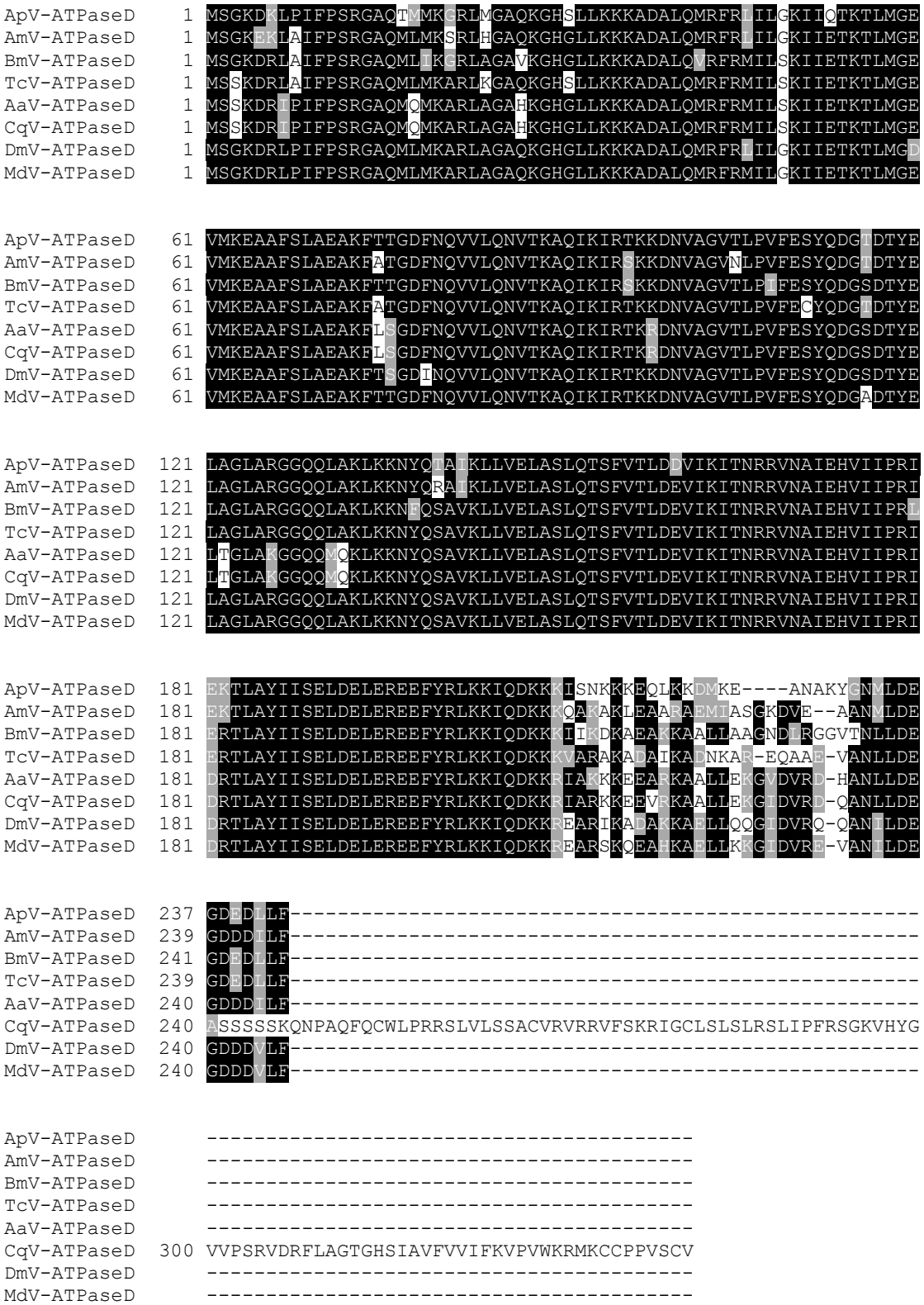

Figure 2.6. Multiple alignments of deduced amino acid sequences of V-ATPase subunit D (*Ae. aegypti, D. melanogaster, C. quinquefasciatus, M. domestica, B. mori, T. castaneum, A. mellifera, A. pisum*).

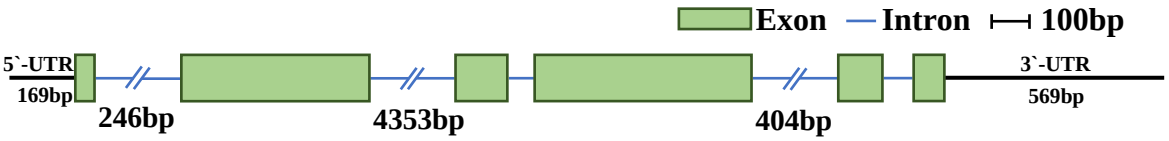

Figure 2.7. Exon-intron organization of the V-ATPase subunit H gene (*V-ATPase H*) in *Ae. aegypti.*

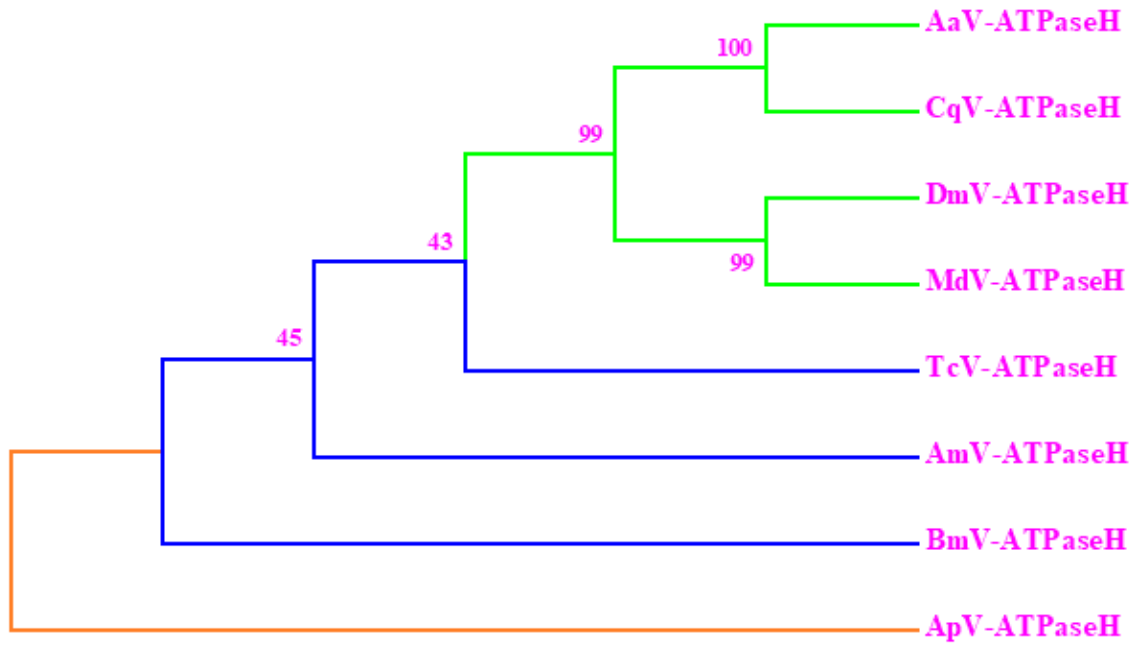

Figure 2.8. Phylogenetic relationship of the deduced amino acid sequences of *V-ATPase H* gene.

This rooted phylogenetic tree was constructed using the maximum likelihood method. Nodes indicate bootstrap values calculated with 1000 replications. The green branches represent the order Diptera, orange branch shows the outgroup, and blue branches represent other orders. The accession numbers for the sequences are as follows: AaV-ATPaseH (XP_001652018.1, *Aedes aegypti*); DmV-ATPaseH (NP_523585.2, *Drosophila melanogaster*); CqV-ATPaseH (XP_001844037.1, *Culex quinquefasciatus*); MdV-ATPaseH (XP_005181998.1, *Musca domestica*); BmV-ATPaseH (NP_001040488.1, *Bombyx mori*); TcV-ATPaseH (XP_966693.3; *Tribolium castaneum*); AmV-ATPaseH (XP_003251675.1; *Apis mellifera*); ApV-ATPaseH (XP_001949116.3; *Acyrthosiphon pisum*).

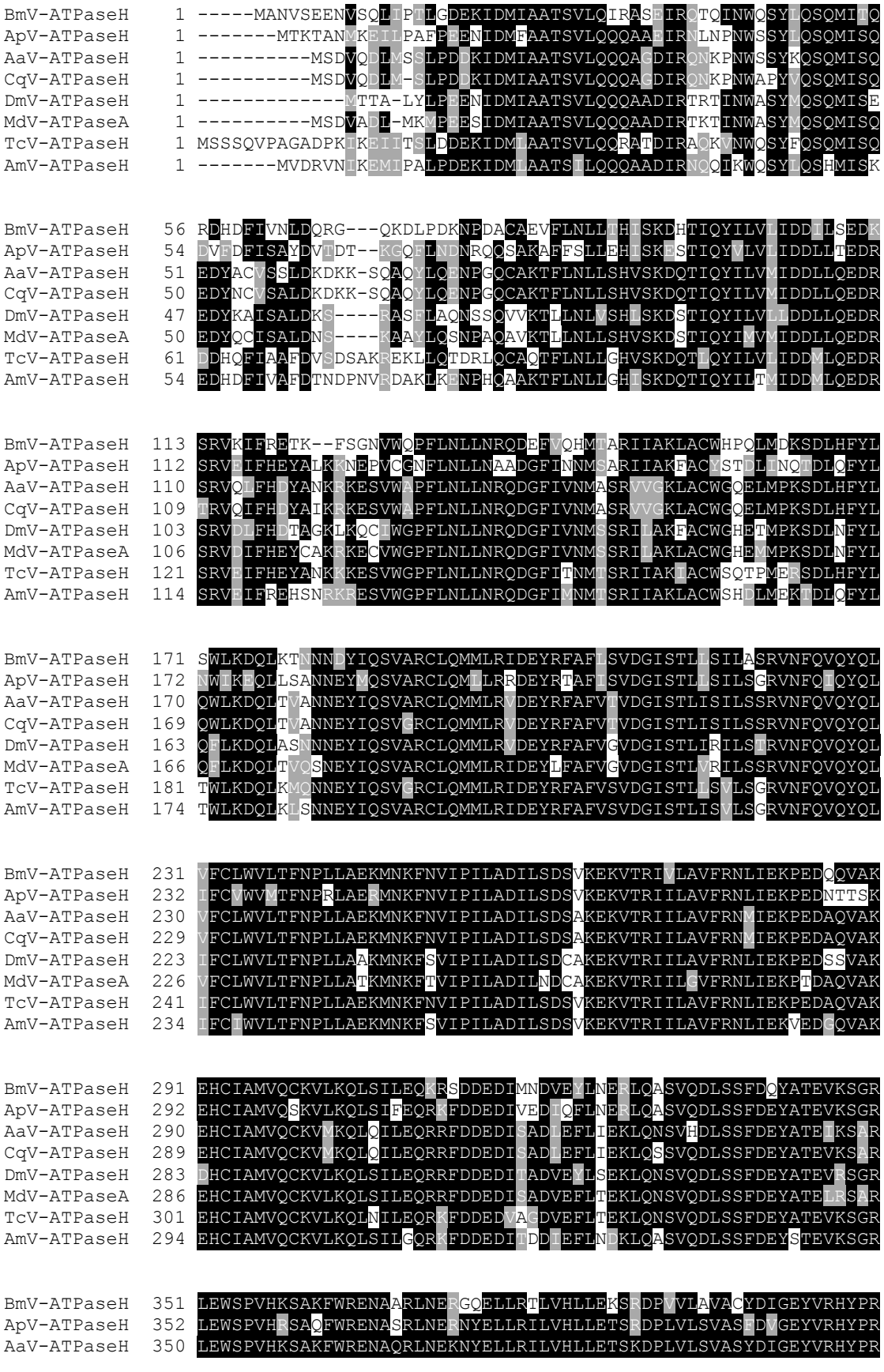
BmV-ATPaseH
ApV-ATPaseH
AaV-ATPaseH
CqV-ATPaseH
DmV-ATPaseH
MdV-ATPaseA
TcV-ATPaseH
AmV-ATPaseH

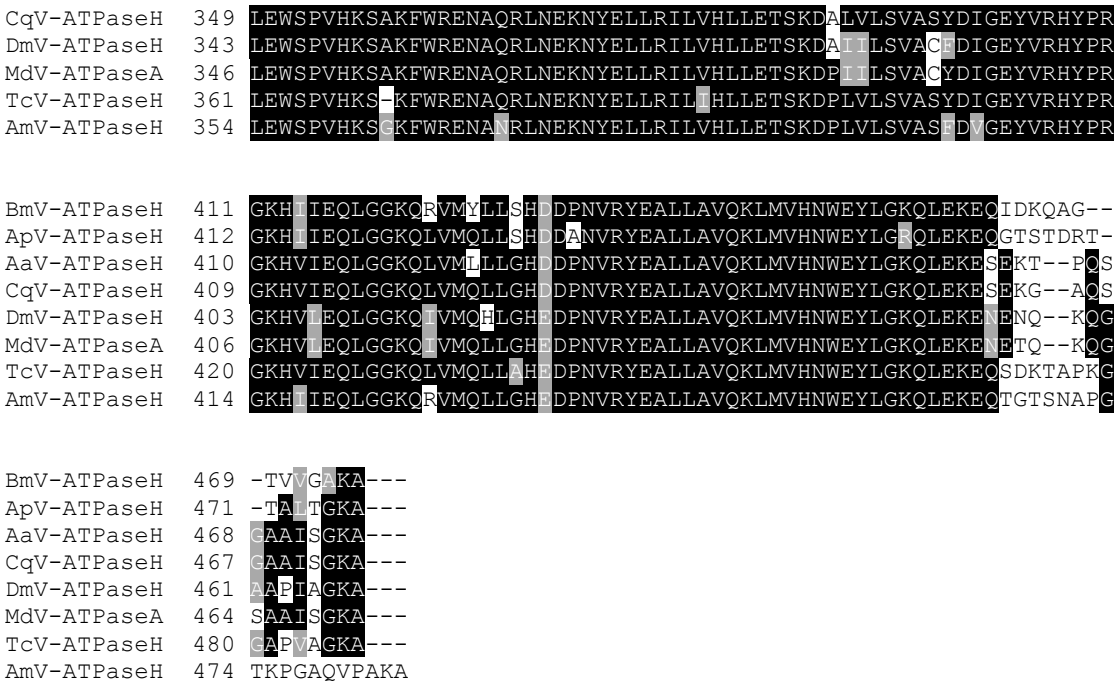

Figure 2.9. Multiple alignments of deduced amino acid sequences of V-ATPase subunit H (*Ae. aegypti, D. melanogaster, C. quinquefasciatus, M. domestica, B. mori, T. castaneum, A. mellifera, A. pisum*).

Chapter 3 - Molecular Characterization of Selected V-ATPase Genes in the Yellow Fever Mosquito *Aedes aegypti*

Abstract

Vacuolar ATPase (V-ATPase) is an important enzyme responsible for transportation of protons across membranes and acidification of intracellular compartments in eukaryotic cells. Although V-ATPases and their subunits have been widely studied in model organisms such as yeast and *Drosophila*, our understanding of their structure, function, and patterns of expression in mosquitoes is still very limited. In this study, I used RT-PCR to amplify partial sequences of selected V-ATPase subunits (A, D, and H) in the yellow fever mosquito, *Aedes aegypti*. Sequence analysis showed that these partial cDNAs covered approximately 30%, 76%, or 42% of the complete cDNA sequences of *V-ATPase A, V-ATPase D,* or *V-ATPase H,* respectively. Analyses of developmental and tissue-specific gene expressions using RT-qPCR showed that the selected V-ATPase genes had similar expression patterns across developmental stages (eggs; 1^{st}, 2^{nd}, 3^{rd}, and 4^{th} instar larvae; pupae; or adults), with highest expression in larval stages for each subunit. Similarly, V-ATPase subunits A, D, or H showed similar expression patterns in the different tissues examined in fourth instar larvae, with Malpighian tubules having the highest expression of all three. Interestingly, expression of subunits A, D, or H in different tissues of adults was highest in male hindgut versus Malpighian tubules in females. My results show the expression levels of different V-ATPase subunit genes vary in different genders, tissues and developmental stages.

Keywords: *Aedes aegypti*, gene expression patterns, sequence analysis, V-ATPase

3.1. Introduction

Vacuolar-ATPase (V-ATPase) is a multi-subunit enzyme that hydrolyzes ATP and transports H^+ across various biological membranes, generating electrochemical potentials (Beyenbach and Wieczorek, 2006). V-ATPases are widely distributed on intracellular vesicular membranes and at the plasma membrane in specific cell types (Forgac, 2007; Nishi and Forgac, 2002). Intracellular V-ATPases function to acidify endocytic and secretory organelles that are essential for endocytosis, receptor-ligand dissociation, and protein degradation (Maxson and Grinstein, 2014).

V-ATPases consist of as many as 12 different polypeptides that assemble to form two main ring structures, called the V_1 and V_0 domains (Beyenbach and Wieczorek, 2006). The V_1 domain is a peripheral complex of ~500 kDa that includes eight subunits (A, B, C, D, E, F, G, H) (Forgac, 1998) which interact with and hydrolyze ATP (O'Donnell, 2008). The catalytic ATP binding sites are located at the interfaces between the A and B subunits. Hydrolysis of ATP powers the rotation of the central stalk which includes subunits D and F. The peripheral stalk, which is composed of subunits C, E, G and H, prevents the movement of the A and B subunits during ATP hydrolysis (Maxson and Grinstein, 2014).

The V_0 domain is a membrane embedded complex of 150-250 kDa (O'Donnell, 2008) composed of at least four different subunits (a, d, c, e) (Forgac, 1998). Subunit c and its isoform c" form a ring, called the c-ring, where each subunit has a H^+ binding site on it (Beyenbach and Wieczorek, 2006). Subunit a is thought to allow the H^+ to reach and bind to one subunit of the c-ring (Meier et al., 2005). Subunit c functions as a rotor in the V_0 complex; however, the functions of subunits d and e remain to be elucidated. Hydrolysis of ATP causes rotation of V_0

and transports H^+ across the membrane. When the V_1 domain hydrolyzes only one ATP, this energy powers the 360° rotation of the V_0 domain (Cross and Müller, 2004).

In insects, most efforts have focused on V-ATPases in the model organisms, *Manduca sexta* or *Drosophila melanogaster*. The plasma membrane V-ATPase from *M. sexta* consists of at least 12 subunits (Wieczorek et al., 1999), with several subunits, G, a, c, d and e, being encoded by multiple genes in *M. sexta*. In contrast, subunits A, C, D, E, F, and H are to be encoded only by single genes. Moreover, multiple transcripts were identified for subunits B, G, c, and d suggesting that these subunits exist as multiple isoforms that could provide specialized functionality or be expressed in different tissues (Merzendorfer et al., 2000).

In *D. melanogaster*, genome-wide surveys have revealed that this V-ATPase has 14 subunits that are encoded by thirty-three genes in total (eight subunits are encoded by multiple genes). In addition, these subunits showed tissue-specific patterns of expression. Thirteen genes are specialized for epithelial roles and the disruption of any gene encoding a subunit of the tubule plasma membrane V-ATPase showed a transparent Malpighian tubule phenotype (Allan et al., 2005).

Aedes aegypti is one of the most important vectors of deadly diseases such as yellow fever, dengue fever, chikungunya, and Zika (Jentes et al., 2011; Leparc-Goffart et al., 2014; Musso and Gubler, 2016; Simmons et al., 2012). More than 3.5 billion people in over 125 countries are at risk of infection with dengue fever alone (Brady et al., 2012). Unfortunately, vaccines are not available for these diseases, thus, insecticide-based control of vectors is the most common practice for preventing disease. Insecticides are widely used to control *Ae. aegypti*; however, mosquitoes have developed resistance against many of the most common insecticides, including organophosphates and pyrethroids (Ranson et al., 2010). The rise in resistance in

vector mosquitoes requires the search for new target sites and new strategies to control vector mosquitoes. One such strategy, RNA interference, uses exogenous double-stranded RNA to suppress the transcript level of a specific target gene in the insect pest and has potential as a new control measure for mosquito vectors.

The mosquito V-ATPase functions to acidify endosomes, which is a crucial process for the entry of viruses such as dengue virus and the release of the viral genome from endosomes to the cytoplasm (Clyde et al., 2006; Nishi and Forgac, 2002). Another important function of V-ATPase in *Ae. aegypti* is providing the energy for secondary active transporters that are essential for osmoregulation and for the retention of ions, water, and nutrients (Bradley, 2008). Studies showed that V-ATPase is highly expressed in Malpighian tubules, which are essential for ion and water homeostasis at every stage of the mosquito life-cycle and are the major organ of salt and fluid balance (Beyenbach et al., 2010; Weng et al., 2003). These important functions showed that V-ATPase might be a good target for vector control strategies; however, there is very little information available on the expression patterns of V-ATPase in different tissues or different life stages that are critical for successful application of RNAi in pest control schemes.

I performed a detailed literature review in order to select the candidate V-ATPase genes in *Ae. aegypti*. Several subunits of V-ATPase, including subunits A, D, and H, were widely studied, which showed that targeting these genes in different insects using RNAi resulted in mortality or significant phenotypical changes. Subunits A, D, and H serve critical roles in the function of V-ATPases in binding and hydrolysis of ATP, coupling of ATP hydrolysis and proton translocation, and activation of ATP hydrolysis, respectively (Arata et al., 2002; Liu et al., 1997; MacLeod et al., 1998; Parra et al., 2000), and so may serve as excellent targets for RNAi experiments. However, V-ATPases have mostly been studied in *M. sexta* (Wieczorek et al.,

1999) or *D. melanogaster* (Allan et al., 2005), and very little information is available on the developmental and tissue-specific expression patterns in *Ae. aegypti*. Therefore, I analyzed the transcript levels of V-ATPase subunits A, D, and H in various tissues and developmental stages of *Ae. aegypti* in order to enhance future efforts focused on targeting these genes with RNAi.

3.2. Materials and Methods

3.2.1. Mosquito rearing and maintenance

Ae. aegypti, Liverpool-IB12 strain (MRA-735), a sub-strain of the Liverpool strain (LVP), were reared under standard insectary conditions at 27°C and 80% relative humidity, with a 12/12 h day/night light cycle, which was previously described by Clemons et al. (2010). This strain originated from West Africa and has been maintained at the Liverpool School of Tropical Medicine (LSTM) since 1936 in the United Kingdom. The Liverpool-IB12 strain was used in the genome sequencing project of *Ae. aegypti* (Nene et al., 2007).

Ae. aegypti mosquito eggs were obtained from BEI Resources (NIAID, NIH, Manassas, VA, USA). Eggs were received on a slice of filter paper and this paper was cut into small pieces of about 3-5 mm per side. These small papers were dipped into a 23 cm by 33 cm glass tray containing 500 ml of distilled water to allow the eggs to hatch. When the eggs hatched, the larvae were daily fed with finely ground dog food (Braga et al., 2005). Second instar larvae were split into a new tray filled with fresh water to reduce the larval density. Pupation occurred after the fourth instar larvae, and pupae were collected and transferred into screened cages to allow the adults emerge.

Adult mosquitoes were maintained on a 10% sucrose solution soaked into cotton balls. When female mosquitoes became three days old, they were fed with defibrinated sheep blood in

a glass feeder sealed with parafilm. The glass feeder was placed on top of the cage containing the adult mosquito and connected to a pump, circulating water at 37°C to keep the blood warm. Egg cups, filled with water and covered with filter paper, were placed into cages, allowing the females to lay eggs. Eggs were collected and placed into a dry petri dish and stored for up to three months.

3.2.2. RNA isolation and cDNA synthesis

I chose three subunits of V-ATPase (*V-ATPase A*, *V-ATPase D* and *V-ATPase H*), located in the V_1 domain, to explore their expression in *Ae. aegypti* tissues and developmental stages. Total RNA was isolated from seven different stages of *Ae. aegypti*, including egg, larvae (first-, second-, third- and fourth-instar), pupae, and adults. RNA was extracted using the TRIzol total RNA isolation kit (Invitrogen, Carlsbad, CA, USA) to study stage-specific expressions of V-ATPase genes.

Total RNA was also isolated from five different tissues (midgut, Malpighian tubule, hindgut, reproductive organ, and carcass) and one body part (head) of female, male, and larval *Ae. aegypti* for studying tissue-specific expression profiles using a similar protocol as above. Tissues were dissected from fourth-instar larvae, and three-day-old female and male adults in phosphate-buffered saline (1x PBS) solution. All isolated RNAs were quantified using a Nanophotometer P330 (Implen GmbH).

After quantification, one microgram of total RNA was treated with DNase I (Life Technologies, Carlsbad, CA, USA) to remove possible genomic DNA contamination. First strand cDNA was synthesized using the EasyScript™ cDNA Synthesis Kit (Applied Biological Materials, Richmond, Canada) with random primers and oligo (dT) in a 20-µl reaction. First

strand cDNA was subsequently used as a template to generate cDNA templates of each specific gene using PCR and gene-specific primers.

3.2.3. Molecular cloning and sequencing of selected V-ATPase subunits

Total RNA was isolated from third-instar *Ae. aegypti* larvae and first strand cDNA was prepared as above. The Primer Blast tool (NCBI) was used to design specific primers (Table 3.1.) for each of the selected genes based on their published mRNA sequences (CDS, Nene et al., 2007). PCR was performed using 2X PCR Taq Master Mix, (Applied Biological Materials) with thermal cycling conditions of an initial denaturation at 94°C for 10 min followed by 34 cycles at 94°C for 30 s, 55°C for 30 s, 72°C for 3 min, with a final extension at 72°C for 5 min. PCR products were resolved on a 1.5% agarose gel and visualized by staining the gel with SafeView™ (Applied Biological Materials) to determine the size of the amplicon and confirm that only a single band was present. The PCR products, which had the expected sizes, were directly purified from the gel using a PCR/Gel Extraction Kit (IBI Scientific, Peosta, IA, USA). Purified PCR products were ligated into pCRTM 2.1 TA cloning vectors (Life Technologies, Carlsbad, CA, USA). The ligation mixtures were used to transform *E. coli* cells using the Z-Competent E. coli transformation kit (Zymo Research, Orange, CA, USA). Plasmids were isolated from the bacterial culture and used for sequencing at Genewiz, LLC (South Plainfield, NJ, USA). The Molecular Evolutionary Genetics Analysis (MEGA7) software was used for analyzing the sequencing results. All sequences were aligned using Muscle alignment with default settings and then phylogenetic trees (shown in the previous chapter) were constructed using the maximum likelihood method.

3.2.4. Quantitative PCR analysis

To determine the relative expression levels of *V-ATPase A, D,* or *H* genes in different developmental stages or tissues, cDNA prepared from each above-mentioned sample was used as a template for quantitative PCR (qPCR) analysis. For each gene, 20-µl reactions were prepared with 1 µl cDNA, 0.6 µL each of forward and reverse primers (5 µM), and 10 µl Eva Green Master Mix, (Applied Biological Materials) on an iCycler iQ real-time PCR detection system (Bio-Rad Laboratories, Hercules, CA). qPCR primers used in this study were designed using NCBI- Primer Blast and are shown in Table 3.2. *Ae. aegypti* ribosomal protein 17 (*Rps17*) was used as a reference gene, which was previously tested for suitability by Soumaila Issa (2014). qPCR was performed with three biological replicates (each with two technical replicates) for each gene. The relative expression levels of the genes were analyzed using ΔΔCt method (Livak and Schmittgen, 2001).

3.3. Statistical analysis

For analyzing the relative expression levels of *V-ATPase A, D,* or *H* genes from different tissues and developmental stages of *Ae. aegypti*, I used one-way analysis of variance (ANOVA) followed by Tukey's HSD multiple comparisons tests to compare the means among the tissues or developmental stages. In this study, all statistical analyses were performed using MiniTab 17 statistical software (MiniTab, Inc., State College, PA). Additionally, SigmaPlot software was used as a graph creator.

3.4. Results

3.4.1. Sequencing of partial cDNAs of *V-ATPase A*, *D*, and *H* genes

In this study, I amplified the partial sequences of *V-ATPase A*, *V-ATPase D*, and *V-ATPase H* genes. Sequence analysis showed that the cDNA sequences were consistent with those available on NCBI. The partial cDNAs covered approximately 30%, 76%, or 42% of the full cDNAs of *V-ATPase A*, *V-ATPase D*, or *V-ATPase H*, respectively (Figures 3.1., 3.2., and 3.3.) (NCBI database accession numbers *XM_001659470.1*, *XM_001660376.1*, *XM_001651968.1*, for *V-ATPase A*, *D*, or *H*, respectively). When these partial sequences were blasted against all insect taxa, my results showed high identity to *Drosophila*, around 86, 76, or 80% for *V-ATPase A*, *D*, or *H* genes, respectively.

3.4.2. Developmental stage expression patterns

Stage-specific expression patterns of *V-ATPase A*, *V-ATPase D*, and *V-ATPase H* genes were determined in eggs (embryos), four different larval instars (1^{st}, 2^{nd}, 3^{rd} and 4^{th}), pupae, and adults by using RT-qPCR (Figure 3.4.). All selected V-ATPase genes were expressed in all developmental stages examined, and showed similar expression patterns. The relative transcript levels of the *V-ATPase A* gene was significantly higher in 1^{st} and 3^{rd} instar larvae when compared to pupae or adults. For *V-ATPase D*, transcript levels were significantly higher in 3^{rd} instar larvae compare to 1^{st} and 4^{th} instar larvae. In addition, the transcript levels of *V-ATPase H* were significantly higher in 1^{st} and 3^{rd} instar larvae than in embryos, pupae, or adults.

3.4.3. Tissue specific expression patterns in larvae

Tissue-specific expression profiles of *V-ATPase A, D,* or *H* genes were determined in four different larval tissues (midgut, Malpighian tubule, hindgut and carcass) and head of fourth instar larvae (Figure 3.5.). Although head is generally considered as a body part, I showed its relative expression along with the tissue types due to the technical difficulties associated with dissecting specific tissues from the mosquito head. All three V-ATPase genes showed similar expression patterns across the different tissues analyzed, but there were some significant differences in expression between specific tissues. The relative expression level of each selected V-ATPase genes was significantly higher in Malpighian tubule than in carcass or head, but was not significantly different compared to midgut or hindgut.

3.4.4. Tissue specific expression patterns in adults

Expression patterns of *V-ATPase A, D,* or *H* genes in adult female and male *Ae. aegypti* were analyzed in each of five different tissues including midgut, Malpighian tubule, hindgut, reproductive organs, and carcass (Figure 3.6.). Both in female and male, the selected V-ATPase genes showed similar expression patterns in different tissues. However, when I compared transcript levels of these subunits in female versus male *Ae. aegypti*, I observed a different pattern of expression in different tissues based on sex. In adult males, the relative transcript level of *V-ATPase A* gene was significantly higher in hindgut compared to midgut, reproductive organs, carcass, and head. Similarly, the relative transcript level for subunit H was higher in the hindgut than in any of the other tissues, whereas the relative transcript levels for the *V-ATPase D* gene were significantly higher in hindgut than carcass. In contrast, the relative transcript levels of

V-ATPase A, *D*, or *H* genes were significantly higher in Malpighian tubules than in any of the other tissues analyzed in adult females.

3.5. Discussion

V-ATPase is a critical multi-subunit enzyme that utilizes ATP to pump H^+ across biological membranes (Marshansky et al., 2014). Not surprisingly, each subunit has its own role in making this enzyme functional. V-ATPases have been widely studied in yeast and mammals; however, we know very little about the tissue or developmental stage-specific expression of each subunit or their specific functions in insects. These studies are critical in understanding their role in insect development and survival as well as in evaluating the suitability of V-ATPase genes as targets for RNAi-based insect control strategies.

In this study, I evaluated the relative transcript levels of *V-ATPase A*, *V-ATPase D*, and *V-ATPase H* genes at different developmental stages and in different tissues. My results showed that these three V-ATPase genes are expressed in all developmental stages in *Ae. aegypti*. In addition, high transcript levels of V-ATPase genes were observed in larval stages compared to other developmental stages. Expression patterns were similar for each subunit in different larval tissues, but the highest expression for each selected V-ATPase subunit was observed in Malpighian tubule when compared to carcass or head in fourth instar larva. Similar expression patterns were also observed for each subunit in female or male adult tissues, but when I compared expression patterns in female versus male mosquitoes, my data showed that for each selected V-ATPase subunit, the highest expression level was observed in Malpighian tubule versus other tissues in female adults, whereas in male adults the highest expression was observed in hindgut when compared to carcass.

Larval and adult mosquitoes live in different environments with varying requirements, particularly those surrounding osmoregulation and excretion (Li et al., 2017). Larval and pupal developmental stages of the mosquito occur in water where they are immersed in a hypotonic environment (Bradley, 1987; Marusalin et al., 2012). In contrast, adult mosquitoes are terrestrial organisms that have to deal with rapid dehydration. In addition, adult females feed on blood and excrete about 40% of the blood within 1-2 hours (Drake et al., 2010; Williams et al., 1983). My results showed that the highest expression of V-ATP subunits was obtained in larval stages of *Ae. aegypti*. Similar results were reported for *Drosophila* larval stages (Allan et al., 2005). Previous studies showed that V-ATPase enzymes are localized at the apical membrane of principal cells and energized the membrane and secondary transporters in Malpighian tubules of the mosquito, *Ae. aegypti* (Beyenbach, 2001; Beyenbach and Piermarini, 2011). Another study also showed that V-ATPase subunits A, B, a, c" were highly expressed in larval midgut of *Drosophila* (Overend et al., 2016). Here, I found that each V-ATPase subunit examined in this study showed high expression in larval tissues; midgut, Malpighian tubule, and hindgut. In addition, my results showed that the highest expression of selected V-ATPase genes was observed in Malpighian tubules in female adults. Similar results were reported previously for V-ATPase subunit B in Malpighian tubules of *Ae. aegypti* (Weng et al., 2003).

V-ATPases are found in the plasma membrane and within the membranes of many organelles in every eukaryotic cell (Forgac, 2007; Kane, 2006). Here, I found that all selected V-ATPase genes were expressed in different tissues in larval, male, and female mosquitoes. In *Drosophila*, the V-ATPase subunit A is encoded by three genes (*vha68-1*, *vha68-2*, *vha68-3*) that showed different expressions in different tissues. *Vha68-2* is expressed in gut, Malpighian tubules, ceaca, and muscles, whereas the *vha68-1* is restricted to hindgut (Allan et al., 2005). In

my study, I showed that subunit A, which is encoded by a single gene, was highly expressed in Malpighian tubules of female *Ae. aegypti* as compared with the other two genes. Furthermore, in female mosquito, the highest transcript levels of V-ATPase genes were observed in Malpighian tubules. This expression pattern is consistent with the need of female mosquitoes to excrete large amounts of urine through their Malpighian tubules after blood feeding (Clements, 1992). Similarly, male mosquitoes do not feed on blood and likely instead rely on V-ATPase expression in the hindgut to satisfy their excretory needs.

References

Allan, A.K., Du, J., Davies, S.A., Dow, J.A.T., 2005. Genome-wide survey of V-ATPase genes in *Drosophila* reveals a conserved renal phenotype for lethal alleles. Physiol. Genomics 22, 128-138.

Arata, Y., Baleja, J.D., Forgac, M., 2002. Localization of subunits D, E, and G in the yeast V-ATPase complex using cysteine-mediated cross-linking to subunit B. Biochemistry 41, 11301-11307.

Beyenbach, K.W., 2001. Energizing epithelial transport with the vacuolar H+-ATPase. News Physiol. Sci. 16, 145-151.

Beyenbach, K.W., Piermarini, P.M., 2011. Transcellular and paracellular pathways of transepithelial fluid secretion in Malpighian (renal) tubules of the yellow fever mosquito *Aedes aegypti*. Acta Physiol. 202, 387–407.

Beyenbach, K.W., Skaer, H., Dow, J.A.T., 2010. The developmental, molecular, and transport biology of Malpighian tubules. Annu. Rev. Entomol. 55, 351-374.

Beyenbach, K.W., Wieczorek, H., 2006. The V-type H+ ATPase: molecular structure and function, physiological roles and regulation. J. Exp. Biol. 209, 577-589.

Bradley, T.J., 2008. Active transport in insect recta. J. Exp. Biol. 211, 835-836.

Bradley, T.J., 1987. Physiology of osmoregulation in mosquitoes. Annu. Rev. Entomol. 32, 439–462.

Brady, O.J., Gething, P.W., Bhatt, S., Messina, J.P., Brownstein, J.S., Hoen, A.G., Moyes, C.L., Farlow, A.W., Scott, T.W., Hay, S.I., 2012. Refining the global spatial limits of dengue virus transmission by evidence-based consensus. PLoS Negl. Trop. Dis. 6, e1760.

Braga, I.A., Mello, C.B., Peixoto, A.A., Valle, D., 2005. Evaluation of methoprene effect on *Aedes aegypti* (Diptera: Culicidae) development in laboratory conditions. Mem. Inst. Oswaldo Cruz. 100, 435-440.

Clements, A.N., 1992. The Biology of Mosquitoes. Chapman and Hall, London.

Clemons, A., Mori, A., Haugen, M., Severson, D.W., Duman-Scheel, M., 2010. *Aedes aegypti*: culturing and egg collection. Cold Spring Harbor Protoc. 2010: pdb.prot5507.

Clyde, K., Kyle, J.L., Harris, E., 2006. Recent advances in deciphering viral and host determinants of dengue virus replication and pathogenesis. J. Virol. 80, 11418-11431.

Cross, R.L., Müller, V., 2004. The evolution of A-, F-, and V-type ATP synthases and ATPases: reversals in function and changes in the H+/ATP coupling ratio. FEBS Lett. 576, 1-4.

Drake, L.L., Boudko, D.Y., Marinotti, O., Carpenter, V.K., Dawe, A.L., Hansen, I.A., 2010. The Aquaporin gene family of the yellow fever mosquito, *Aedes aegypti*. PLoS ONE 5, e15578.

Forgac, M., 2007. Vacuolar ATPases: rotary proton pumps in physiology and pathophysiology. Nat. Rev. Mol. Cell Biol. 8, 917-929.

Forgac, M., 1998. Structure, function and regulation of the vacuolar (H+)-ATPases. FEBS Lett. 440, 258-263.

Jentes, E.S., Poumerol, G., Gershman, M.D., Hill, D.R., Lemarchand, J., Lewis, R.F., Staples, J.E., Tomori, O., Wilder-Smith, A., Monath, T.P., 2011. The revised global yellow fever risk map and recommendations for vaccination, 2010: consensus of the Informal WHO Working Group on Geographic Risk for Yellow Fever. Lancet Infect. Dis. 11, 622-632.

Kane, P.M., 2006. The where, when, and how of organelle acidification by the yeast vacuolar H+-ATPase. Microbiol. Mol. Biol. Rev. 70, 177–191.

Leparc-Goffart, I., Nougairede, A., Cassadou, S., Prat, C., de Lamballerie, X., 2014. Chikungunya in the Americas. The Lancet 383, 514.

Li, Y., Piermarini, P.M., Esquivel, C.J., Drumm, H.E., Schilkey, F.D., Hansen, I.A., 2017. RNA-seq comparison of larval and adult Malpighian tubules of the yellow fever mosquito *Aedes aegypti* reveals life stage-specific changes in renal function. Front. Physiol. 8, 283.

Liu, Q., Leng, X., Newman, P.R., Vasilyeva, E., Kane, P.M., Forgac, M., 1997. Site-directed mutagenesis of the yeast V-ATPase A subunit. J. Biol. Chem. 272, 11750-11756.

Livak, K.J., Schmittgen, T.D., 2001. Analysis of relative gene expression data using real-time quantitative PCR and the 2(−Delta Delta C(T)) method. Methods 25, 402-408.

MacLeod, K.J., Vasilyeva, E., Baleja, J.D., Forgac, M., 1998. Mutational analysis of the nucleotide binding sites of the yeast vacuolar proton-translocating ATPase. J. Biol. Chem. 273, 150-156.

Marshansky, V., Rubinstein, J.L., Gruber, G., 2014. Eukaryotic V-ATPase: novel structural findings and functional insights. Biochim. Biophys. Acta 1837, 857–879.

Marusalin, J., Matier, B.J., Rheault, M.R., Donini, A., 2012. Aquaporin homologs and water transport in the anal papillae of the larval mosquito, *Aedes aegypti*. J. Comp. Physiol. B Biochem. Syst. Environ. Physiol. 182, 1047–1056.

Maxson, M.E., Grinstein, S., 2014. The vacuolar-type H+-ATPase at a glance – more than a proton pump. J. Cell. Sci. 127, 4987-4993.

Meier, T., Polzer, P., Diederichs, K., Welte, W., Dimroth, P., 2005. Structure of the rotor ring of F-Type Na+-ATPase from *Ilyobacter tartaricus*. Science 308, 659-662.

Merzendorfer, H., Reineke, S., Zhao, X., Jacobmeier, B., Harvey, W.R., Wieczorek, H., 2000. The multigene family of the tobacco hornworm V-ATPase: novel subunits a, C, D, H, and putative isoforms. Biochim. Biophys. Acta 1467, 369-379.

Musso, D., Gubler, D.J., 2016. Zika virus. Clin. Microbiol. Rev. 29, 487-524.

Nene, V., Wortman, J.R., Lawson, D., Haas, B., Kodira, C., Tu, Z., Loftus, B., Xi, Z., Megy, K., Grabherr, M., Ren, Q., Zdobnov, E.M., Lobo, N.F., Campbell, K.S., Brown, S.E., Bonaldo, M.F., Zhu, J., Sinkins, S.P., Hogenkamp, D.G., Amedeo, P., Arensburger, P., Atkinson, P.W., Bidwell, S., Biedler, J., Birney, E., Bruggner, R.V., Costas, J., Coy, M.R., Crabtree, J., Crawford, M., deBruyn, B., DeCaprio, D., Eiglmeier, K., Eisenstadt, E., El-Dorry, H., Gelbart, W.M., Gomes, S.L., Hammond, M., Hannick, L.I., Hogan, J.R., Holmes, M.H., Jaffe, D., Johnston, J.S., Kennedy, R.C., Koo, H., Kravitz, S., Kriventseva, E.V., Kulp, D., LaButti, K., Lee, E., Li, S., Lovin, D.D., Mao, C., Mauceli, E., Menck, C.F.M., Miller, J.R., Montgomery, P., Mori, A., Nascimento, A.L., Naveira, H.F., Nusbaum, C., O'Leary, S., Orvis, J., Pertea, M., Quesneville, H., Reidenbach, K.R., Rogers, Y., Roth, C.W., Schneider, J.R., Schatz, M., Shumway, M., Stanke, M., Stinson, E.O., Tubio, J.M.C., VanZee, J.P., Verjovski-Almeida, S., Werner, D., White, O., Wyder, S., Zeng, Q., Zhao, Q., Zhao, Y., Hill, C.A., Raikhel, A.S., Soares, M.B., Knudson, D.L., Lee, N.H., Galagan, J., Salzberg, S.L., Paulsen, I.T., Dimopoulos, G., Collins, F.H., Birren, B., Fraser-Liggett, C., Severson, D.W., 2007. Genome sequence of *Aedes aegypti*, a major arbovirus vector. Science 316, 1718-1723.

Nishi, T., Forgac, M., 2002. The vacuolar (H+)-ATPases — nature's most versatile proton pumps. Nat. Rev. Mol. Cell Biol. 3, 94-103.

O'Donnell, M., 2008. Insect excretory mechanisms, in: Simpson, S.J. (Eds.), Advances in Insect Physiology. Vol. 35. Academic Press, New York, pp. 1-122.

Overend, G., Luo, Y., Henderson, L., Douglas, A.E., Davies, S.A., Dow, J.A., 2016. Molecular mechanism and functional significance of acid generation in the *Drosophila* midgut. Sci. Rep. 6, 27242.

Parra, K.J., Keenan, K.L., Kane, P.M., 2000. The H subunit (Vma13p) of the yeast V-ATPase inhibits the ATPase activity of cytosolic V1 complexes. J. Biol. Chem. 275, 21761-21767.

Ranson, H., Burhani, J., Lumjuan, N., Black IV, W.C., 2010. Insecticide resistance in dengue vectors. TropIKA.net 1, 0-0.

Simmons, C.P., Farrar, J.J., Nguyen, V.V., Wills, B., 2012. Dengue. N. Engl. J. Med. 366, 1423-1432.

Soumaila Issa, M., 2014. Molecular characterization and functional analysis of cytochrome P450 genes in the yellow fever mosquito *Aedes aegypti* (Diptera: Culicidae). MSc thesis, Manhattan, Kansas State University.

Weng, X., Huss, M., Wieczorek, H., Beyenbach, K.W., 2003. The V-type H+-ATPase in Malpighian tubules of *Aedes aegypti*: localization and activity. J. Exp. Biol. 206, 2211-2219.

Wieczorek, H., Grüber, G., Harvey, W.R., Huss, M., Merzendorfer, H., 1999. The plasma membrane H+-V-ATPase from tobacco hornworm midgut. J. Bioenerg. Biomembr. 31, 67-74.

Williams, J.C., Hagedorn, H.H., Beyenbach, K.W., 1983. Dynamic changes in flow rate and composition of urine during the post blood meal diuresis in *Aedes aegypti*. J. Comp. Physiol. B Biochem. Syst. Environ. Physiol. 153, 257–266.

Table 3.1. RT-PCR primers used for sequencing in this study.

Gene Name	Primer 5' - 3'	Primer Length (base)	Tm (°C)	Product size (bp)
V-ATPaseA	F:CAGCGTCCACTGAAGGACAT	20	61	912
	R:GACGATGGACACCGAACCTT	20	62	
V-ATPaseD	F:AAAGGTCACGGGTTGCTGAA	20	63	912
	R:ACGTCCTCCAAACCACGAAG	20	62	
V-ATPaseH	F:CCATGTCCGACGTTCAGGAT	20	63	824
	R:GCTGCTTCATGACCTTGCAC	20	62	

>V-ATPaseA

TTTTCATTCCTCTCCTCGAAGTGCACAGGTTGGCCAGTCTTTCAGTCAGTCAGTCTTGTGATAC
CATTTTGCTTCGCTCGGTGTGTGGAGTTTGCATTTTTCCCATCCCATCTCTCTCGACAACTGCA
GCACCTAAGAGCAGAAGGAAGCAGAGCAGGAGGAACGGATCGTAACA**ATG**TCCACCCTGAAGAA
GATCTCCGATGAGGACCGCGAGTCCAAATTCGGATATGTGTTCGCCGTATCCGGTCCTGTCGTC
ACGGCCGAGCGGATGTCCGGTTCGGCTATGTACGAGTTGGTCCGCGTCGGTTACTACGAGCTGG
TCGGTGAGATCATCCGTTTGGAAGGTGACATGGCCACCATCCAGGTATACGAGGAAACCTCCGG
TGTCACCGTCGGCGATCCCGTGCTGCGTACCGGCAAGCCCCTCTCCGTCGAACTCGGTCCAGGT
ATTATGGGTAGCATCTTTGACGGTATC**CAGCGTCCACTGAAGGACATTAACGAACTGACCAGCT**
CGATCTACATCCCGAAGGGTGTGAACATTCCCTGCTTGTCCCGTACCCAGAGCTGGGGATTCAA
CCCCTTGAACGTAAAGGTTGGCTCTCACATCACCGGAGGAGATCTGTACGGTTTGGTGCACGAG
AATACCCTGGTCAAGCACAAGCTGTTGGTCCCGCCACGCGCCAAGGGTACAGTTCGTTACATTG
CTCCACCCGGCAACTACACCGTCGACGACATCATTCTGGAGACGGAATTCGACGGTGAGATCAA
CAAGTGGTCTATGTTGCAGGTGTGGCCCGTGCGTCAGCCACGTCCAGTGACTGAGAAGTTGCCC
GCCAATCATCCTCTGCTGACTGGTCAGCGTGTGTTGGATTCGCTGTTCCCTTGTGTCCAGGGTG
GTACCACTGCCATCCCCGGAGCTTTCGGTTGCGGTAAGACTGTCATCTCGCAGGCCCTGTCCAA
GTACTCCAACTCCGATGTCATTATCTACGTCGGTTGCGGAGAACGTGGTAACGAAATGTCTGAA
GTATTGCGTGATTTCCCTGAGCTGTCGGTTGAGATTGACGGTGTTACGGAGTCCATCATGAAGC
GTACCGCGCTGGTTGCCAACACCTCCAACATGCCTGTCGCTGCTCGTGAAGCTTCCATCTACAC
CGGTATTACCTTGTCCGAGTACTTCCGTGATATGGGTTACAACGTATCCATGATGGCTGACTCG
ACCTCTCGTTGGGCCGAAGCTCTTCGAGAAATTTCCGGTCGTCTGGCTGAGATGCCTGCCGATT
CCGGTTATCCTGCCTACCTGGGTGCACGTTTGGCCTCCTTCTACGAGCGTGCCGGTCGTGTCAA
GTGTCTCGGTAACCCTGAACGTGAAGGTTCGGTGTCCATCGTCGGTGCCGTATCGCCCCCTGGT
GGTGATTTCTCCGATCCCGTCACATCCGCCACCCTTGGTATCGTACAGGTGTTCTGGGGTCTGG
ACAAGAAACTGGCCCAGCGTAAGCATTTCCCCTCGATCAACTGGTTGATCTCCTACAGCAAGTA
CATGCGCGCCCTTGATGACTTCTACGATAAGAACTTCCAGGAGTTTGTCCCACTGCGTACCAAG
GTTAAGGAGATCCTGCAGGAGGAAGAAGATTTGTCCGAAATTGTGCAGCTGGTCGGTAAGGCAT
CGCTGGCAGAAACCGATAAGATCACCCTTGAGGTAGCCAAGCTGCTCAAGGATGATTTCCTGCA
GCAGAACTCGTACTCGGCGTACGATCGATTCTGTCCGTTCTACAAGACGGTCGGTATGCTGCGA
AACATGATCGGATTCTACGATATGGCTCGCCACGCCGTCGAAACCACCGCCCAGTCGGAGAACA
AGATCACCTGGAACGTGATCCGTGACTCGATGGGCAACATCCTGTACCAGCTGTCGTCGATGAA
GTTCAAGGACCCAGTGAAGGATGGCGAAGCGAAGATCAAGGCCGATTTCGACCAACTGTACGAA
GACCTGCAGCAGGCGTTCCGCAACCTGGAAGAT**TAA**ATTCTCCCGCACATTCGTGGTCTCTTCA
ATGCGAAATTCCTTGAAACAGTTTTATTGTTTTCAGTAAACATAGCAAAGAAATGTTCGTAGCA
TAGTGCAAACAAAACATCAAAATGAGAAACACGAAACACAGCAAAAGTGTAGGGCCCTCCTTGG
CATCATGATCAACCAACAACATCCATTAAGTAAAATGCTTCTAGGTCACCATTTTACAGGCGTA
TTTAGGTTGAAACATTTATTTACACAAATTATTGCAAGAAAAAAGATTAAGAGAACAAATCTAT
AAAGCGAGTGTAACATATACATTTAGAAACGGCGAAACACTACAACAACTACAGAACACACGGC
AGAACAGAAACAAATTTTAGTAGGTAAGTGATATTGCAAGTGTTGTCCGACGGCGTAGGAAAAG
GTTAGCGAACGGAATAACGTTCAATCGGAAATTGTCTTCGAAAGTTTTCCGCTTGCATGCGTGT
CTCAAATGCGAATAAAACGTATAAACAATCGTGGTGAAACTTAACATCAGTGATGATATAATCA

AAGGGGATTAAAATGAAACACGTGGACAAAAGATCTATAAAGCAAAACTCTCAGCTAGAATAGT
TCATGACGTCGCGAAGCGTACTATAAATAGAATAATATCTAAACCACGGTTAATGGGAAAATAA
GAAGAAACTTTCGATTGAGCTATGTTATAGAAACTTATCCATGTATGATTGTATAAGATCGCTA
ATTAATCGTATAAGAAATAACAGAAAACAAGTTTTATTATAGGTGTAAGCCAATCAAGTTGTTA
TATCAGTTTAAATATTATTTAGTGAATATAGTTTTACTTTTAATTTTGTAGTGTCGTTTTTCCA
TCGGTAGGATCGGAAACGAGAATCGATGATTGATTGACTGTTGGCAAATGAAATGAAAGTTAAA
TTTATTATGCTTTTTTGTTTGTGTGAACAGAATTGAAGAGCCGCCGCGTCGTTTCGGTCAATGC
AAGCGACCGACGGCTCGTATCTGTCTTGTACATTTTTGTCGATGAGCAGAAAATATATGAGAAT
AAAACCCTCTAAAAAATTGCATTCCGCGTAAACTGT

Figure 3.1. Nucleotide sequence of the cDNA encoding V-ATPase subunit A.

The sequence represents the full-length cDNA. The partially sequenced cDNA is highlighted in bold, pink letters. PCR and qPCR primers are marked with yellow and green, respectively. Start and stop codons are shown in bold, red letters.

>***V-ATPaseD***

GAAAACATCAGAAAAAATTCATTTGATCTTGTGACCCGTTTTGCGCTGGTTGGTTGATTGGTGT
TTCGCGGACCGAAAGAAATAATAAACTTGCAAAA**ATG**TCGTCCAAGGATCGAATCCCGATTTTC
CCATCCCGAGGTGCCCAGATGCAGATGAAGGCCCGTCTGGCAGGAGCCCAC**AAAGGTCACGGGT**
TGCTGAAGAAGAAGGCCGATGCCCTCCAGATGAGGTTCCGGATGATCCTTAGCAAAATTATCGA
GACCAAAACGTTGATGGGAGAAGTGATGAAGGAAGCTGCCTTTTCGCTGGCTGAGGCCAAGTTC
TTGTCCGGAGACTTCAACCAGGTGGTGCTGCAGAATGTCACCAAGGCTCAAATCAAGATCCGCA
CCAAGAGGGACAACGTGGCGGGAGTCACGCTACCAGTTTTCGAGTCATACCAGGATGGCAGCGA
TACCTATGAGCTGACCGGTCTAGCCAAGGGTGGCCAACAGATGCAGAAGCTGAAGAAAAACTAC
CAGAGCGCCGTGAAGCTGCTGGTGGAGCTTGCGTCGCTGCAGACGTCCTTCGTGACTTTGGATG
AAGTCATCAAAATTACCAACAGACGAGTTAACGCCATCGA**GCACGTTATTATCCCTCGCATTC**A
TCGTACTTTGGCTTACATTATCTCGGAGTTAGATGAACTGGAACGTGAAGAATTCTACCGTTTG
AAGAAGATTCAGGACAAAAAACGAATTGCAAAGAAAAAGGAAGAGGCTCGCAAAGCAGCCCTTT
TGGAAAACGGAGTTGATGTACGAGATCATGCTAATCTCCTCGACGAAGGCGATGATGACATTTT
GTTC**TAA**GATGTTTATTCCCAACGGGCAGCGGCGTACAAGTTCGGTGAAAGCATGGGACAGTCG
CAACTTCTAACAAAGCGGATTGTGAATGCTTTTATGAAAAGTTCATTCCCTTCTAAGTGTAGAT
CAACAGTAAACGGTTTTGAGTAG**CTTCGTGGTTTGGAGGACGT**ATATGTAACAAGTGTATTTTT
TTTTTGTTTTCTTTTTCAATCTAGGTTAGATGATTCTATTTGCGTATTATGCGCAAAAAATACA
GCATATAAATTATAAACGGATTATTATAGAATAAATGTTATCGATAAGCATA

Figure 3.2. Nucleotide sequence of the cDNA encoding V-ATPase subunit D.

The sequence represents the full-length cDNA. The partially sequenced cDNA is highlighted in bold, pink letters. PCR and qPCR primers are marked with yellow and green, respectively. Start and stop codons are shown in bold, red letters.

>***V-ATPaseH***

GCAAGTCATATGACATTCAGCTGCGACGGGAATTTTTCACTGTCGACTGTCTCTGGCTTGCGAG
GTCCTCTGTCTAATCGAACGAAAAGAAATCGGAAAATCTGTCCATTTTACCAGCGTTTGTGAAC
TTTTTTCTGTTCCATCGTAAGCTCGACCACTACCGGAAA**CCATGTCCGACGTTCAGGATCTGAT**
GTCGTCCCTGCCGGACGACAAAATTGATATGATCGCTGCGACCAGCGTTTTGCAGCAGCAGGCA
GGAGATATCCGCCAGAACAAGCCAAACTGGTCCTCATACAAGCAGTCCCAGATGATCTCCCAGG
AGGACTATGCCTGCGTGAGCAGTCTGGACAAGGACAAGAAGTCCCAGGCTCAGTACCTGCAGGA
GAATCCAGGTCAATGCGCCAAGACGTTCCTGAATCTGCTGTCGCACGTTTCCAAGGACCAGACG
ATCCAGTACATCCTGGTCATGATCGATGATCTGCTGCAGGAGGACCGTTCCCGGGTACAGCTGT
TCCACGACTACGCCAACAAGCGCAAGGAAAGCGTCTGGGCCCCGTTCCTGAATCTGCTGAACCG
CCAGGACGGATTCATTGTGAATATGGCCTCGCGTGTTGTTGGCAAGTTGGCTTGCTGGGGCCAG
GAGCTGATGCCCAAATCCGATCTGCACTTCTATCTGCAGTGGCTGAAGGATCAGCTGACCGTTG
CGAACAATGAATATATCCAATCGGTGGCCCGTTGCCTGCAGATGATGCTTCGCGTTGACGAGTA
CCGCTTTGCGTTCGTTACAGTTGATGGAATCAGCACGTTGATCAGCATCCTGTCATCTCGGGTG
AACTTCCAGGTTCAATACCAGCTGGTGTTCTGCTTGTGGGTGCTCACGTTCAACCCACTGCTGG
CGGAGAAGATGAACAAGTTCAACGTGATTCCGATCCTGGCCGACATCCTGAGCGACAGTGCCAA
GGAGAAGGTCACCCGTATCATCTTGGCCGTGTTCCGCAACATGATCGAAAAACCGGAAGACGCG
CAGGTCGCCAAGGAGCACTGCATTGCCATGGTCCAGTGCAAGGTCATGAAGCAGCTGCAGATTC
TGGAGCAGCGCCGTTTCGACGACGAGGACATCAGTGCCGATCTGGAGTTCCTCATCGAGAAGCT
GCAGAACTCCGTGCAT**GATCTGAGCTCGTTCGATGAGTA**CGCCACGGAGATCAAGAGCGCCCGC
TTGGAGTGGTCGCCGGTGCACAAATCGGCCAAGTTCTGGCGCGAGAATGCCCAGCGCTTGAACG
AGAAGAACTACGAACTGCTCC**GTATTCTGGTGCATTTGCTGGAG**ACTTCCAAGGACCCCCTGGT
GCTGTCCGTTGCTAGCTACGACATCGGAGAATACGTTCGTCACTACCCGAGAGGAAAGCACGTT
ATTGAACAACTGGGTGGAAAACAGTTGGTCATGCTTCTGCTCGGCCATGACGACCCGAATGTTC
GCTATGAGGCCCTGCTTGCCGTCCAGAAGCTGATGGTGCACAACTGGGAATACCTCGGCAAACA
GCTGGAGAAGGAAAGCGAGAAGACACCCCAATCCGGGGCCGCTATCAGTGGAAAGGCT**TAG**AAA
GCTTCCTGCCGCAATTTCGGAACTCGTTGTTAAATCTGTTCGTGAGTTTAGTTTTGTTGTTGAC
AATTTTAGTTAAAATCCCTTACCGATCGAAATTTATTGCGCGTATTCAGCTTGCGTATGGAAGC
ATTACATTCCCTTTAGCTTCAGTTTTTTTACTCGTTTGTCATGTTCTGGAATATATGAGAAGGT
TCTTTGGATACGTTGGAGAAGAAAAAGATTGTATATATCAAATTGCGTGAAAACTAACACAATT
TCAATCAACTATTATTCGATTTCTCTGGTATAATATTGAACCAACCATCAAGAAGATTGTTTTA
GTGCAAAAAAAAAAACAGCTTCGGCTGTTTATAAGAAATATGTATTTATAAGAATGATGTATTA
TTGATCAAAATGATGTTTTAGTGGTAAGCTTTTGTCTGGTGGAATGTGTAGTTTTAAAGAACAT
CCGTAATGGTAATAGAAACAGCTTATTAAAAACTACGCCCAACACCTAGAAACATATTACATAA
AAATAATCGTGAGCAACAAACTGTATTGCCGTAATAAAGTATCGTTGTACGATG

Figure 3.3. Nucleotide sequence of the cDNA encoding V-ATPase subunit H.

The sequence represents the full-length cDNA. The partially sequenced cDNA is highlighted in bold, pink letters. PCR and qPCR primers are marked with yellow and green, respectively. Start and stop codons are shown in bold, red letters.

Table 3.2. qPCR primers used for expression profiles in this study.

Gene Name	Primer 5' - 3'	Primer Length (base)	Tm (°C)	Product size (bp)
V-ATPaseA	F: CTCCAACTCCGATGTCATTATC	22	60.00	124
	R: CTTCATGATGGACTCCGTAAC	21	60.00	
V-ATPaseD	F:GCACGTTATTATCCCTCGCATTG	23	60.36	175
	R:TCGTACATCAACTCCCTTTTCCA	23	59.67	
V-ATPaseH	F:GATCTGAGCTCGTTCGATGAGTA	23	59.75	156
	R:CTCCAGCAAATGCACCAGAATAC	23	60.18	

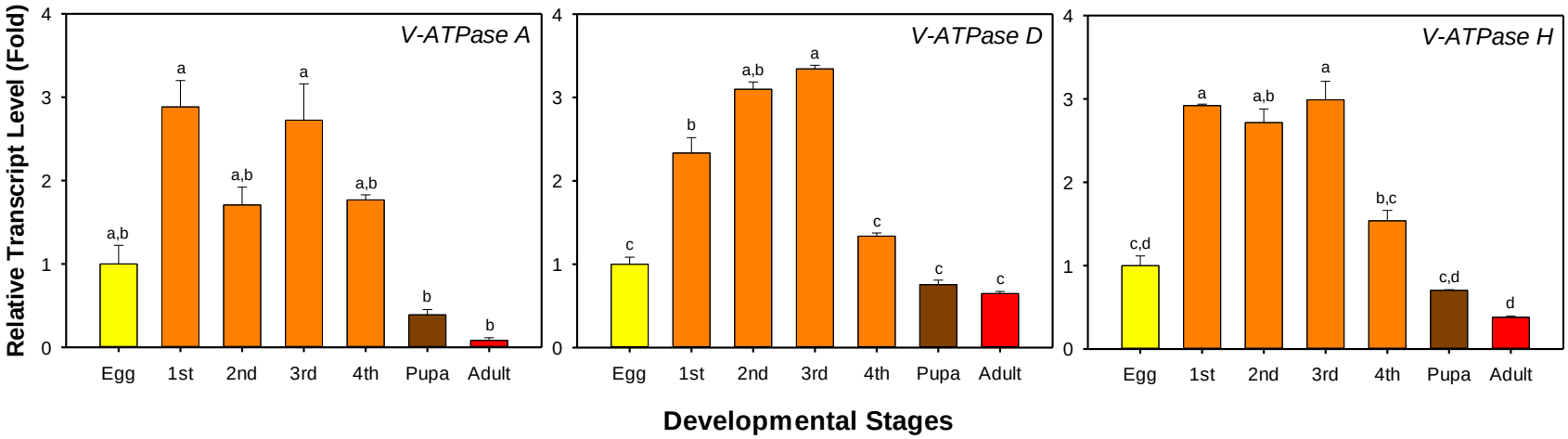

Figure 3.4. The relative transcript levels of *V-ATPase A, V-ATPase D and V-ATPase H* genes in different developmental stages of the mosquito.

Ae. aegypti Rps17 was used as a reference gene. Transcript levels were expressed as relative fold changes as compared to the levels in eggs. Data are presented as the mean ± standard error. Different letters on the bars indicate statistically significant differences as evaluated by ANOVA followed by Tukey's multiple comparison test ($P < 0.05$).

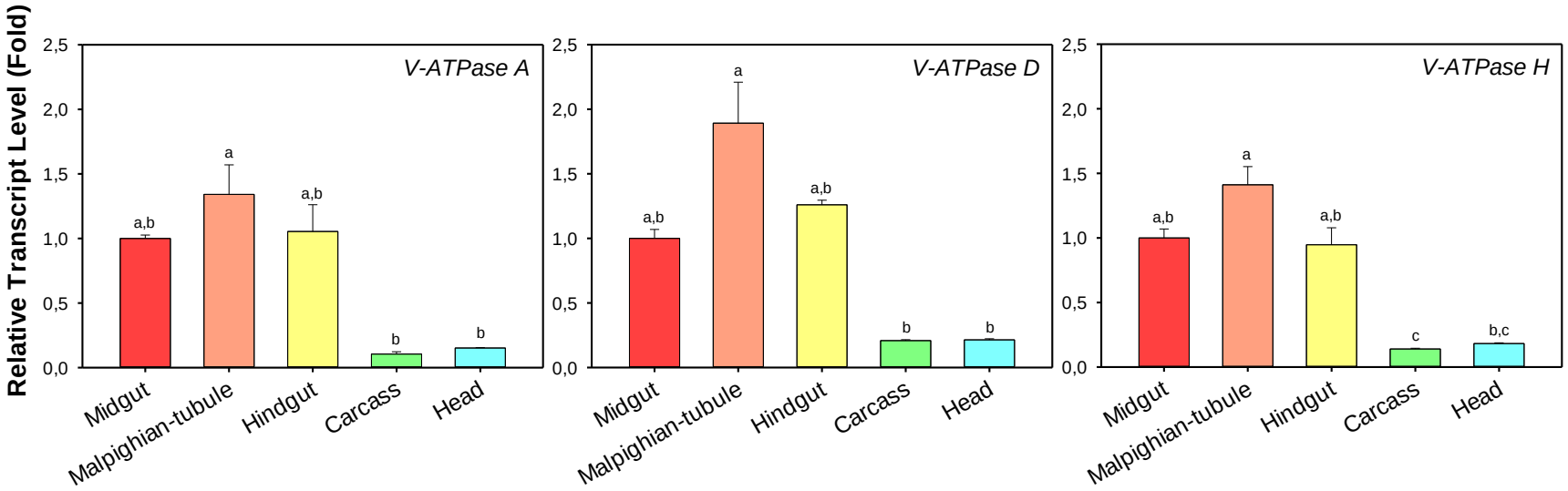

Figure 3.5. The relative transcript levels of *V-ATPase A, V-ATPase D and V-ATPase H* genes in different tissues or head from fourth-instar larvae.

Ae. aegypti Rps17 was used as a reference gene. Transcript levels were expressed as relative fold changes as compared to the levels in midgut. Data are presented as the mean ± standard error. Different letters on the bars indicate statistically significant differences as evaluated by ANOVA followed by Tukey's multiple comparison test ($P < 0.05$).

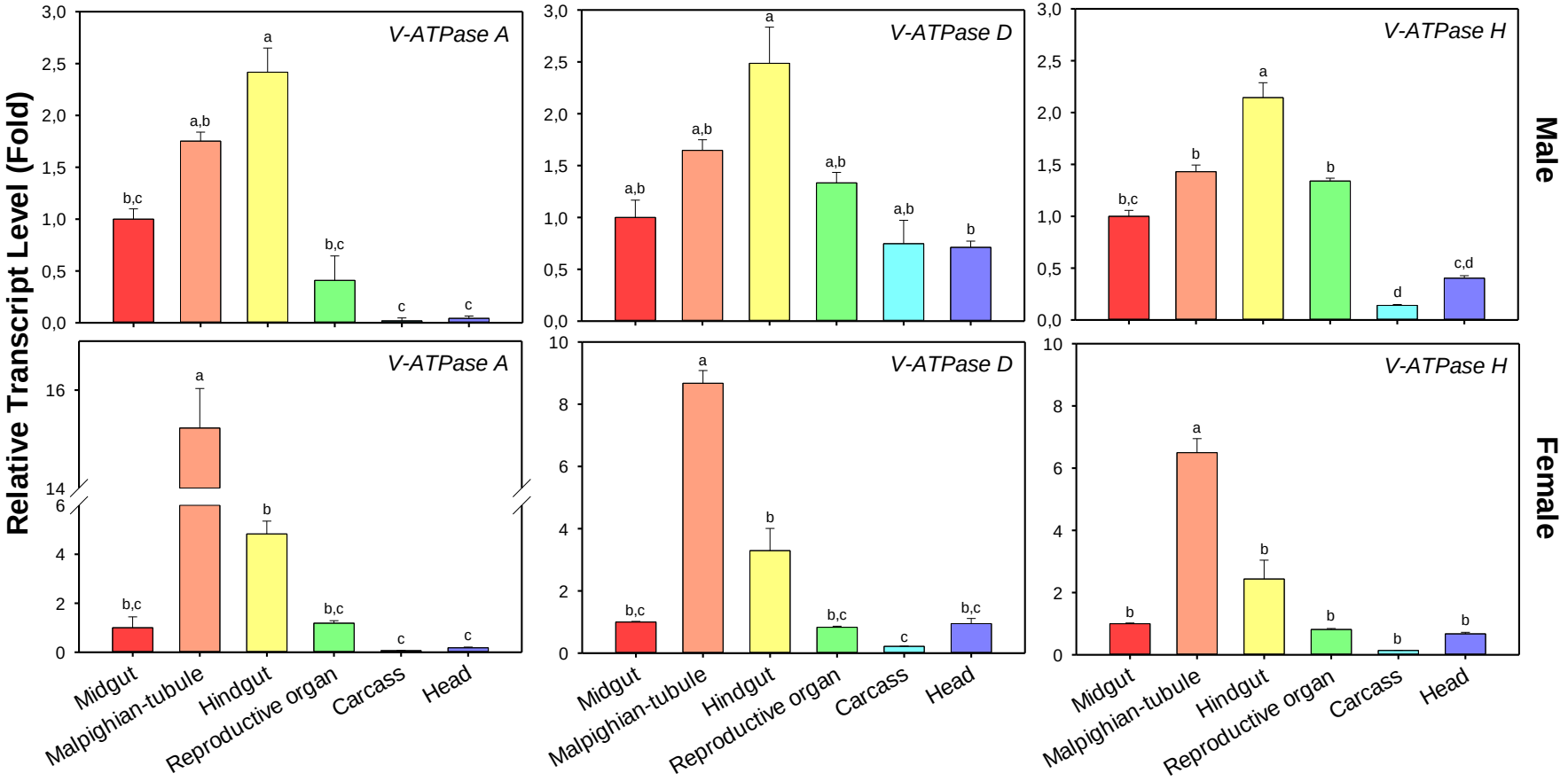

Figure 3.6. The relative transcript levels of *V-ATPase A*, *V-ATPase D and V-ATPase H* genes in different tissues from male or female adults.

Ae. aegypti Rps17 was used as a reference gene. Transcript levels were expressed as relative fold changes as compared to the levels in midgut. Data are presented as the mean ± standard error. Different letters on the bars indicate statistically significant differences as evaluated by ANOVA followed by Tukey's multiple comparison test ($P < 0.05$).

Chapter 4 - Suppression of Selected V-ATPase Subunit Transcripts in *Aedes aegypti* Larvae by Oral Delivery of dsRNA/Chitosan Nanoparticles

Abstract

Vacuolar-ATPase (V-ATPase) is an essential enzyme that is located in the plasma membrane for pumping protons and regulating the pH in various cell types. In insects, V-ATPase energizes epithelial transport that permits the retention of ions, water, and nutrients, and has been used as an efficacious target for RNAi in insects other than *Aedes aegypti*. In this study, I examined the efficiency of RNAi of V-ATPase subunits A, D, or H in *Ae. aegypti* larvae through feeding with dsRNA/chitosan nanoparticles. My results showed that transcript levels of the selected V-ATPase subunit genes were significantly suppressed (by 27.3 to 70.4%) as compared with those of the larvae fed dseGFP/chitosan nanoparticles. Peak suppression of V-ATPase A, D, or H transcripts occurred on the fifth day, where transcript levels were suppressed by 66.0, 27.3, or 70.4%, respectively, as compared with those of the control. Additionally, I examined the mortality for all selected V-ATPase subunits, but mortality was only observed in larvae fed dsRNA/chitosan nanoparticles targeting V-ATPase D. Mortality after feeding of subunit D dsRNA/chitosan nanoparticles was observed beginning on day 3 and increased to to a total of 14.8% mortality on day 6. These results showed that oral delivery of dsRNA/chitosan nanoparticles significantly suppressed target gene transcript levels in *Ae. aegypti* larvae, but further increases in RNAi efficiency appear to be necessary in order to see higher larval mortality using oral delivery of dsRNA/chitosan nanoparticles.

Keywords: *Aedes aegypti*, chitosan nanoparticles, mortality, RNA interference, V-ATPase

4.1. Introduction

Vacuolar H^+-ATPases (V-ATPase) are ATP-dependent proton pumps that acidify various intracellular compartments such as lysosomes, secretory vesicles, and endosomes in eukaryotic cells. They also pump protons across the plasma membrane and regulate pH in various cell types (Beyenbach and Wieczorek, 2006; Cotter et al., 2015; Nishi and Forgac, 2002; Wieczorek et al., 1999). Furthermore, V-ATPases energize epithelial transport aiding in the retention of ions, water, and nutrients in insects (Beyenbach and Piermarini, 2009; Bradley, 2008).

Aedes aegypti is an important vector that transmits deadly diseases, including Zika, dengue fever, yellow fever, and chikungunya (Jentes et al., 2011; Leparc-Goffart et al., 2014; Musso and Gubler, 2016; Simmons et al., 2012), which affect more than 3.5 billion people in over 125 countries (Brady et al., 2012). Since vaccines are not available for any of these diseases except yellow fever, insecticide-based vector control is the most common and effective practice for preventing disease. As a result, *Ae. aegypti* has developed resistance against many of the most common insecticides, including organophosphates and pyrethroids (Ranson et al., 2010). This rise in resistance to traditional control schemes for mosquitoes necessitates the development of new target sites and control strategies to continue to manage vector mosquito populations.

RNA interference (RNAi) is an innate post-transcriptional process that uses complementary double-stranded RNA (dsRNA) to suppress expression of messenger RNA (mRNA) transcripts (Fire et al., 1998). Used as a genetic tool, RNAi has allowed modulation of expression of specific mRNA transcripts and elucidate the biological, developmental, or physiological functions of their resulting proteins in many experimental systems, including insects (Bellés, 2010). In addition to its utility in experimental applications, RNAi also has enormous potential for use in novel and sustainable pest management strategies for control of

specific insect pests with little or no non-target effects (Burand and Hunter, 2013; Huvenne and Smagghe, 2010). Accordingly, I examined using RNAi to suppress expression of selected V-ATPase genes (*V-ATPase A, V-ATPase D*, and *V-ATPase H*) in *Ae. aegypti* in order to determine the suitability of these targets for use in pest control.

4.2. Materials and Methods

4.2.1. Mosquito rearing

Ae. aegypti Liverpool-IB12 strain (MRA-735), the sub-strain of the Liverpool strain (LVP), was reared under standard insectary conditions at 27°C and 80% relative humidity, with a 12/12 h day/night light cycle, which was previously described by Clemons et al. (2010). Mosquito eggs were purchased from BEI Resources (NIAID, NIH, Manassas, VA, USA). These eggs were received on a slice of filter paper and this paper was cut into small pieces of about 3-5 mm per side. These small papers were dipped into a 23 cm by 33 cm glass tray containing 500 ml of distilled water to allow the eggs to hatch. When the eggs hatched, the larvae were daily fed with finely ground dog food (Braga et al., 2005). Second instar larvae were split into a new tray filled with fresh water to reduce the larval density. Pupation occurred after the fourth instar larvae, and pupae were collected and transferred into screened cages to allow the adults emerge.

While mosquito larvae were fed on ground dog food, adult mosquitoes were fed either on 10% sucrose or on defibrinated sheep blood. When female mosquitoes became three days old, they were fed with defibrinated sheep blood in a glass feeder sealed with parafilm. The glass feeder was placed on top of the cage containing the adult mosquito and connected to a pump, circulating water at 37°C to keep the blood warm. Egg cups, filled with water and covered with

filter paper, were placed into cages, allowing the females to lay eggs. Eggs were collected and placed into a dry petri dish and stored for up to three months.

4.2.2. dsRNA synthesis

pCRTM 2.1 TA clones containing *Ae. aegypti V-ATPase A, V-ATPase D,* or *V-ATPase H* cDNA fragments were used as templates for synthesis of dsRNA using the HiScribe™ T7 RNA synthesis kit (*New England Lab*, Woburn, MA, USA) following the manufacturer's instructions. PCR amplification was performed using 95°C for 2 min followed by 30 cycles of 95°C for 30 s, 59°C for 30s, and 72°C for 5 min, with a final 10 min extension time at 72°C. dsRNA targeting V-ATPase subunits or eGFP transcripts were produced using gene specific primers which also included T7 promoter sequences (Table 4.1.). Primers were designed using the E-RNAi web server (http://www.dkfz.de/signaling/e-rnai3/) (Horn and Boutros, 2010). The synthesized dsRNAs were resuspended in nuclease-free water and quantified with a Nanophotometer P330 (Implen GmbH) before being stored at −20°C until use. Five microliters of 10-fold dilutions of each dsRNA were examined on a 1% agarose gel to check dsRNA size.

4.2.3. Preparation of dsRNA/chitosan nanoparticles and larval feeding

Since feeding dsRNA directly to mosquitoes had not been successfully used to significantly silence gene expression, Zhang et al. (2010b) developed a technique for feeding the mosquito larvae (*Anopheles gambiae*) dsRNA/chitosan-based nanoparticles to increase the RNAi efficiency. This procedure was used in the current study for preparation of dsRNA/chitosan nanoparticles and larval feeding with little modification, and will only be briefly described here. Chitosan from crab shells (Cat. No. C3646-25G, ≥75 deacetylated; Sigma-Aldrich, Milwaukee,

WI, USA) was dissolved in 0.1 M sodium acetate buffer (0.1 M sodium acetate, 0.1 M acetic acid, pH 4.5) to make a 0.02% (w/v) working chitosan solution. In order to produce the dsRNA/chitosan based complexes, 100 µl chitosan solution was mixed with 32 µg dsRNA (in 100 µL 100 mM sodium sulfate buffer, pH 4.5). The mixture was heated to 55°C for one min, and then vortexed for 30 s and centrifuged at 13,000 g for 10 min. After discarding the supernatant, the nanoparticles were mixed with 6 mg of ground larval food and subsequently coated with pre-melted 2% agarose in deionized H_2O. This mixture was left to set at room temperature to form a gel containing the larval food and nanoparticles. The gel was subsequently cut into small pieces prior to feeding the mosquito larvae.

Feeding assays were performed using 15-20 newly-hatched, age-synchronized larvae that were fed with whole diet containing dsRNA/chitosan nanoparticles daily, for six consecutive days. Chitosan-based nanoparticles containing eGFP dsRNA were prepared and fed to the mosquito larvae as a control. Total RNA was isolated 1, 3, 5, and 6 days after initiation of feeding from 15-20 larvae per treatment, and used to assess the effects of dsRNA feeding on gene transcript level. The experiments were performed with three biological replicates for each gene.

4.2.4. RNA isolation and cDNA synthesis

Total RNA was isolated from 3 mosquito larvae per treatment at each time point (1, 3, 5, or 6 days) using TRIzol total RNA isolation kit (Invitrogen, Carlsbad, CA, USA). All isolated total RNAs were quantified using a Nanophotometer P330 (Implen GmbH). After quantification, 1.0 µg of total RNA were treated with DNase I (Life Technologies, Carlsbad, CA, USA) to remove possible genomic DNA contamination. First strand cDNA was synthesized using the

EasyScript™ cDNA synthesis kit (Applied Biological Materials, Richmond, Canada) with random primers and oligo (dT) in a 20-µl reaction according to the manufacturer's instructions.

4.2.5. Quantitative PCR analysis

cDNAs synthesized above were used as a template for quantitative PCR (qPCR) analysis. The PCR reactions contained 1 µl of cDNA, 0.6 µL each of forward and reverse primers (5 µM), 10 µl Eva Green Master Mix, (Applied Biological Materials) in a total volume of 20 µl. The *Ae. aegypti* ribosomal protein 17 (*Rps17*) was used as a reference gene and was previously validated by Soumaila Issa (2014). For negative controls, larvae were fed on eGFP dsRNA/chitosan nanoparticles. qPCR was performed with three biological and two technical replicates for each gene. The relative transcript levels of each gene were analyzed using the ΔΔCt method (Livak and Schmittgen, 2001).

4.3. Results

4.3.1. RNAi of V-ATPase subunits A, D, or H in mosquito larvae

To examine the efficiency of RNAi in *Ae. aegypti* larvae, dsRNA/chitosan nanoparticles targeting V-ATPase subunits A, D, or H were fed to mosquito larvae in ground dog food. My results showed that transcript levels of the selected V-ATPase subunits were significantly reduced to 27.3 to 70.4% of that of control (Figure 4.1.). Peak suppression of V-ATPase A, D, or H transcripts occurred on the fifth day, where transcript levels were suppressed by 66.0, 27.3, or 70.4%, respectively, as compared with the control. Interestingly, the decrease in V-ATPase A or D transcripts were sharply reduced on the sixth day compared to the fifth day, but the reductions in transcript levels were still significant when compared with that of control.

In addition to gene expression, larvae fed dsRNA/chitosan nanoparticles were also evaluated for mortality and phenotypical changes. Whereas no mortality or other phenotypes were observed in larvae fed dsRNA/chitosan nanoparticles targeting V-ATPase A or H gene, feeding of dsRNA/chitosan nanoparticles targeting subunit D caused mortality starting on day 3, with cumulative mortality by the sixth day of 14.8% (Table 4.2.). After dsRNA feeding against *V-ATPase D*, I observed phenotypic changes on some of the dead larvae. These changes were mainly seen as color changes throughout the body. For instance, dark color was observed in the last four segments, where the Malpighian tubules and hindgut are located, in eight of the larvae that died (Figure 4.2.).

4.4. Discussion

The critical roles of V-ATPase in endocytosis, protein degradation, acidification and other cellular processes, as well as its expression in gut and Malpighian tubules (Patrick et al., 2006) make it a potential target for developing RNAi-based strategies for insect pest management. Accordingly, we set out to determine if we could suppress the transcripts of V-ATPase subunits A, D, or H in *Ae. aegypti* by feeding larvae with dsRNA/chitosan nanoparticles to target each of these genes. I found that the transcripts at 1, 3, 5, and 6 days were decreased by 9.2, 26.5, 66, and 41.4%, respectively, for subunit A; 3.7, 18.6, 27.3, and 17.6% for subunit D; and 6.7, 8, 70.4, and 32.4% for subunit H. Peak suppression of transcript levels occurred after larvae were fed for five days for all three genes examined. However, levels of suppression decreased on day 6. It is not known why the suppression levels decreased even though the larvae had been continuously fed with the dsRNA/chitosan nanoparticles targeting each of these genes.

This change in suppression of transcript level may be associated with 4th instar larvae preparing for the pupal moult, which can occur soon as early as day 5 or as late as day 10.

To our knowledge, this is the first study to show that the expression of several V-ATPase subunit genes can be suppressed by feeding *Ae. aegypti* larvae with dsRNA/chitosan nanoparticles. Other researchers have suppressed other genes in mosquitoes or V-ATPase subunit genes in other insect species. For instance, previous studies showed that V-ATPase transcript levels can be successfully suppressed through oral delivery or injection of dsRNA and this caused mortality or phenotypical changes in different insects including *Diabrotica virgifera virgifera* (Baum et al., 2007), *Tribolium castaneum* (Whyard et al., 2009), *Ae. aegypti* (Coy et al., 2012), *Peregrinus maidis* (Yao et al., 2013), *Bemisia tabaci* (Thakur et al., 2014), *Helicoverpa armigera* (Mao et al., 2015), and *Aethina tumida* (Powell et al., 2017).

Previous studies showed that chitin synthase gene expression was suppressed around 60% in *Anopheles gambiae* after dsRNA/chitosan nanoparticles feeding and this caused significant mortalities in the presence of an insecticide or another chemical (Zhang et al., 2010b). Another study demonstrated that *V-ATPase A* transcripts were significantly suppressed after feeding with sucrose meal which included dsRNA in adult female *Ae. aegypti*, but they did not observe increased mortality associated with dsRNA feeding (Coy et al., 2012). In my study, I did not observe any mortality for V-ATPase subunits A or H. Larval mortality was observed after dsRNA feeding against V-ATPase subunit D, but this effect was not statistically significant from control (Table 4.2.).

This preliminary study showed that it is feasible to suppress the expression of selected V-ATPase subunit genes in *Ae. aegypti* larvae by feeding dsRNA/chitosan nanoparticles for a relatively extended period of time (e.g., 5 days). Whereas suppression of transcripts for subunits

A or H was similar (around 70%), only limited reduction in transcript levels was observed with dsRNA targeting V-ATPase subunit D, and very little larval mortality was observed in any of the treatments. These results are similar to those previously obtained in *Anopheles gambiae* larvae, where RNAi by feeding dsRNA targeting chitin synthase 1 (*AgCHS1*) caused a 62.8% depletion of target transcripts (Zhang et al., 2010b). No direct mortality was observed as a result of dsRNA treatment unless an insecticide or other chemical was used to challenge the larvae. In contrast, injection of dsRNA in 2nd instar nymphs of the migratory locust (*Locusta migratoria*) caused an 80% decrease in chitin synthase 1 transcript levels with 95.6% mortality (Zhang et al., 2010a). These results suggest that the difference in mortality after RNAi targeting chitin synthase 1 gene between *L. migratoria* nymphs and *An. gambiae* larvae is potentially caused by different levels of suppression of the target gene transcripts, and that significantly higher suppression of transcript levels is necessary in *Ae. aegypti* to induce larval mortality. Accordingly, further research is necessary to improve the efficiency of RNAi in *Ae. aegypti* to improve larval mortality and use V-ATPase subunit genes as targets in mosquito vector control.

References

Baum, J.A., Bogaert, T., Clinton, W., Heck, G.R., Feldmann, P., Ilagan, O., Johnson, S., Plaetinck, G., Munyikwa, T., Pleau, M., Vaughn, T., Roberts, J., 2007. Control of coleopteran insect pests through RNA interference. Nat. Biotech. 25, 1322-1326.

Bellés, X., 2010. Beyond *Drosophila*: RNAi in vivo and functional genomics in insects. Annu. Rev. Entomol. 55, 111-128.

Beyenbach, K.W., Piermarini, P., 2009. Osmotic and ionic regulation in insects. in: Evans, D.H. (Eds.), Osmotic and Ionic Regulation: Cells and Animals. CRC Press, Boca Raton, FL, pp. 231-293.

Beyenbach, K.W., Wieczorek, H., 2006. The V-type H+ ATPase: molecular structure and function, physiological roles and regulation. J. Exp. Biol. 209, 577-589.

Bradley, T.J., 2008. Active transport in insect recta. J. Exp. Biol. 211, 835-836.

Brady, O.J., Gething, P.W., Bhatt, S., Messina, J.P., Brownstein, J.S., Hoen, A.G., Moyes, C.L., Farlow, A.W., Scott, T.W., Hay, S.I., 2012. Refining the global spatial limits of dengue virus transmission by evidence-based consensus. PLoS Negl. Trop. Dis. 6, e1760.

Braga, I.A., Mello, C.B., Peixoto, A.A., Valle, D., 2005. Evaluation of methoprene effect on *Aedes aegypti* (Diptera: Culicidae) development in laboratory conditions. Mem. Inst. Oswaldo Cruz. 100, 435-440.

Burand, J.P., Hunter, W.B., 2013. RNAi: future in insect management. J. Invertebr. Pathol. 112, S68-S74.

Clemons, A., Mori, A., Haugen, M., Severson, D.W., Duman-Scheel, M., 2010. *Aedes aegypti*: culturing and egg collection. Cold Spring Harbor Protoc. 2010: pdb.prot5507.

Cotter, K., Stransky, L., McGuire, C., Forgac, M., 2015. Recent insights into the structure, regulation and function of the V-ATPases. Trends Biochem. Sci. 40, 611-622.

Coy, M.R., Sanscrainte, N.D., Chalaire, K.C., Inberg, A., Maayan, I., Glick, E., Paldi, N., Becnel, J.J., 2012. Gene silencing in adult *Aedes aegypti* mosquitoes through oral delivery of double-stranded RNA. J. Appl. Entomol. 136, 741-748.

Fire, A., Xu, S., Montgomery, M.K., Kostas, S.A., Driver, S.E., Mello, C.C., 1998. Potent and specific genetic interference by double-stranded RNA in *Caenorhabditis elegans*. Nature 391, 806-811.

Horn, T., Boutros, M., 2010. E-RNAi: a web application for the multi-species design of RNAi reagents—2010 update. Nucleic Acids Res. 38, W332-W339.

Huvenne, H., Smagghe, G., 2010. Mechanisms of dsRNA uptake in insects and potential of RNAi for pest control: a review. J. Insect Physiol. 56, 227-235.

Jentes, E.S., Poumerol, G., Gershman, M.D., Hill, D.R., Lemarchand, J., Lewis, R.F., Staples, J.E., Tomori, O., Wilder-Smith, A., Monath, T.P., 2011. The revised global yellow fever risk map and recommendations for vaccination, 2010: consensus of the Informal WHO Working Group on Geographic Risk for Yellow Fever. Lancet Infect. Dis. 11, 622-632.

Leparc-Goffart, I., Nougairede, A., Cassadou, S., Prat, C., de Lamballerie, X., 2014. Chikungunya in the Americas. The Lancet 383, 514.

Livak, K.J., Schmittgen, T.D., 2001. Analysis of relative gene expression data using real-time quantitative PCR and the 2(−Delta Delta C(T)) method. Methods 25, 402-408.

Mao, J., Zhang, P., Liu, C., Zeng, F., 2015. Co-silence of the coatomer *β* and *v-ATPase A* genes by siRNA feeding reduces larval survival rate and weight gain of cotton bollworm, *Helicoverpa armigera*. Pestic. Biochem. Physiol. 118, 71-76.

Musso, D., Gubler, D.J., 2016. Zika virus. Clin. Microbiol. Rev. 29, 487-524.

Nishi, T., Forgac, M., 2002. The vacuolar (H+)-ATPases — nature's most versatile proton pumps. Nat. Rev. Mol. Cell Biol. 3, 94-103.

Patrick, M.L., Aimanova, K., Sanders, H.R., Gill, S.S., 2006. P-type Na+/K+-ATPase and V-type H+-ATPase expression patterns in the osmoregulatory organs of larval and adult mosquito *Aedes aegypti*. J. Exp. Biol. 209, 4638-4651.

Powell, M.E., Bradish, H.M., Gatehouse, J.A., Fitches, E.C., 2017. Systemic RNAi in the small hive beetle *Aethina tumida* Murray (Coleoptera: Nitidulidae), a serious pest of the European honey bee *Apis mellifera*. Pest Manag. Sci. 73, 53-63.

Ranson, H., Burhani, J., Lumjuan, N., Black IV, W.C., 2010. Insecticide resistance in dengue vectors. TropIKA.net 1, 0-0.

Simmons, C.P., Farrar, J.J., Nguyen, V.V., Wills, B., 2012. Dengue. N. Engl. J. Med. 366, 1423-1432.

Soumaila Issa, M., 2014. Molecular characterization and functional analysis of cytochrome P450 genes in the yellow fever mosquito *Aedes aegypti* (Diptera: Culicidae). MSc thesis, Manhattan, Kansas State University.

Thakur, N., Upadhyay, S.K., Verma, P.C., Chandrashekar, K., Tuli, R., Singh, P.K., 2014. Enhanced whitefly resistance in transgenic tobacco plants expressing double stranded RNA of *v-ATPase A* gene. PLoS ONE 9, e87235.

Whyard, S., Singh, A.D., Wong, S., 2009. Ingested double-stranded RNAs can act as species-specific insecticides. Insect Biochem. Mol. Biol. 39, 824-832.

Wieczorek, H., Grüber, G., Harvey, W.R., Huss, M., Merzendorfer, H., 1999. The plasma membrane H+-V-ATPase from tobacco hornworm midgut. J. Bioenerg. Biomembr. 31, 67-74.

Yao, J., Rotenberg, D., Afsharifar, A., Barandoc-Alviar, K., Whitfield, A.E., 2013. Development of RNAi methods for *Peregrinus maidis*, the corn planthopper. PLoS ONE 8, e70243.

Zhang, J., Liu, X., Zhang, J., Li, D., Sun, Y., Guo, Y., Ma, E., Zhu, K.Y., 2010a. Silencing of two alternative splicing-derived mRNA variants of chitin synthase 1 gene by RNAi is lethal to the oriental migratory locust, *Locusta migratoria manilensis* (Meyen). Insect Biochem. Mol. Biol. 40, 824-833.

Zhang, X., Zhang, J., Zhu, K.Y., 2010b. Chitosan/double-stranded RNA nanoparticle-mediated RNA interference to silence chitin synthase genes through larval feeding in the African malaria mosquito (*Anopheles gambiae*). Insect Mol. Biol. 19, 683-693.

Table 4.1. Double-stranded RNA primers used in this study. T7 promoters are underlined.

Gene Name	Primer 5' - 3'	Primer Length (base)	Tm (°C)	Product size (bp)
V-ATPaseA	F: taatacgactcactatagggAGCGTCCACTGAAGGACATT	20	59.73	236
	R: taatacgactcactatagggGGGTGGAGCAATGTAACGAA	20	60.89	
V-ATPaseD	F: taatacgactcactatagggGAGGTGCCCAGATGCAGAT	19	61.22	266
	R: taatacgactcactatagggCACGTTGTCCCTCTTGGTG	19	60.14	
V-ATPaseH	F: taatacgactcactatagggGTTGCCTGCAGATGATGCT	19	59.97	238
	R: taatacgactcactatagggGTGACCTTCTCCTTGGCACT	20	59.31	

Table 4.2. Mortality rate of larvae after feeding with dsRNA/chitosan nanoparticles.

There is no significant difference between mortality caused by dseGFP and dsV-ATPase D treatments. Two-tailed student t-test was performed (P=0.09).

	Cumulative mortality (%)			
Day	1	3	5	6
dseGFP	0	0	0	0
dsV-ATPase D	0	5.7 ± 3.3	13.2 ± 7.6	14.8 ± 8.6

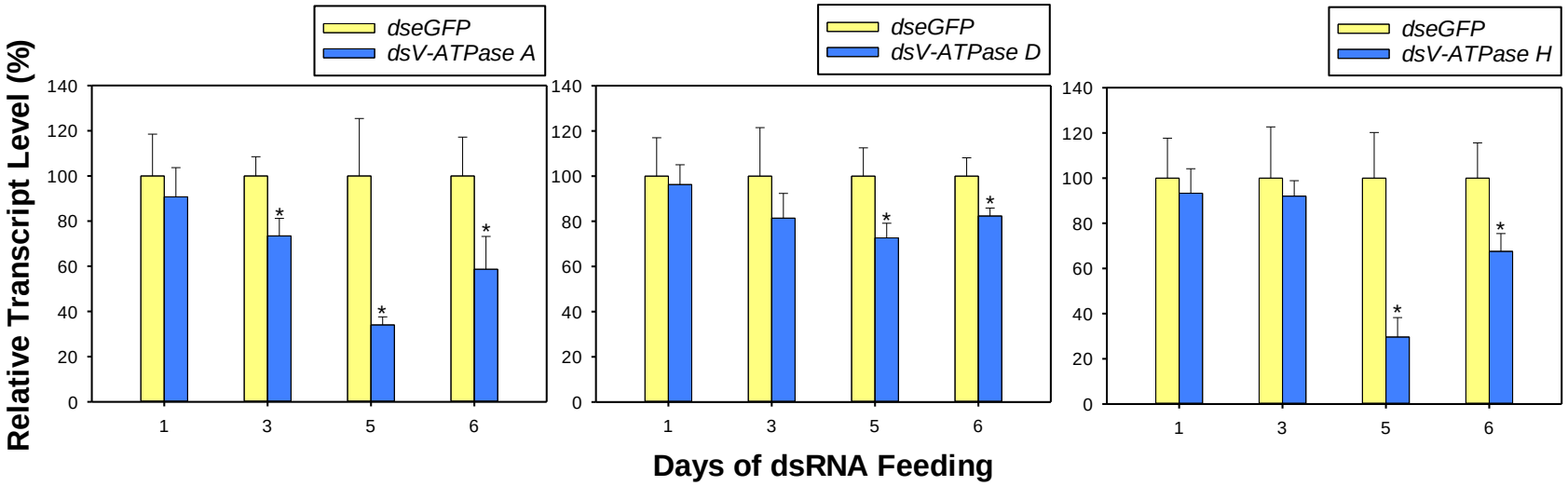

Figure 4.1. Suppression of *V-ATPase A*, *D*, or *H* subunit transcript levels in *Ae. aegypti* larvae fed dsRNA/chitosan nanoparticles.

Data are presented as the mean ± SE of three biological replicates (each with two technical replicates). 1, 3, 5, or 6 on the x-axis generally include 1st-, 2nd-, 3rd-, or 4th-instar larvae, respectively. * indicates significant differences in transcript levels of V-ATPase subunit genes between larvae fed dsRNA/chitosan nanoparticles targeting V-ATPase subunit genes (treatment) and dsRNA/chitosan nanoparticles prepared with dseGFP (control) according to Student's *t*-test ($P<0.05$).

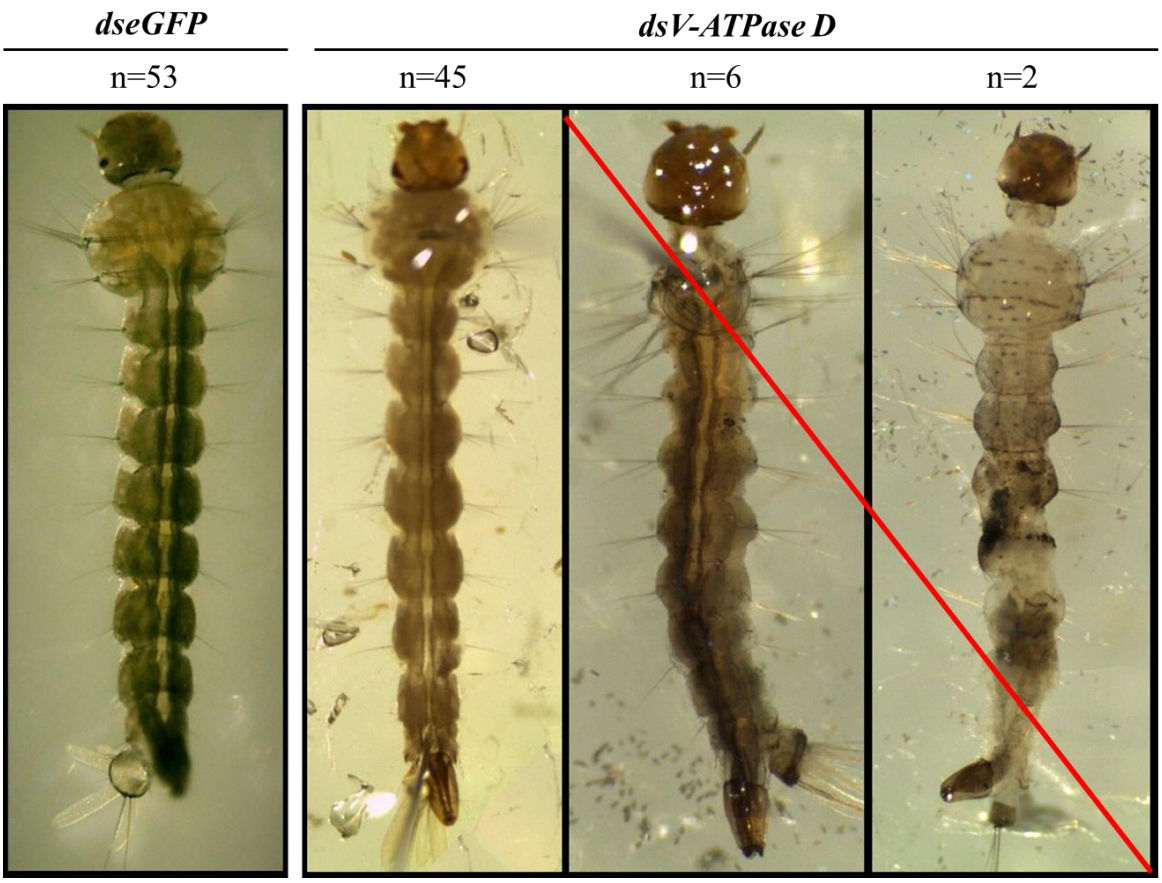

Figure 4.2. The phenotypic effects of dsRNA/chitosan nanoparticles specific to *V-ATPase D* or eGFP on *Ae. aegypti* larvae.

Mosquito larvae were continuously fed with dseGFP, or dsV-ATPaseD nanoparticles for 5 days. All mosquito larvae fed with dseGFP developed normally, but larvae fed with dsV-ATPaseD showed 14.8% cumulative mortality after 6 days and showed phenotypical changes such as color change throughout the body.

Appendix A - Bioinformatic and Phylogenetic Data

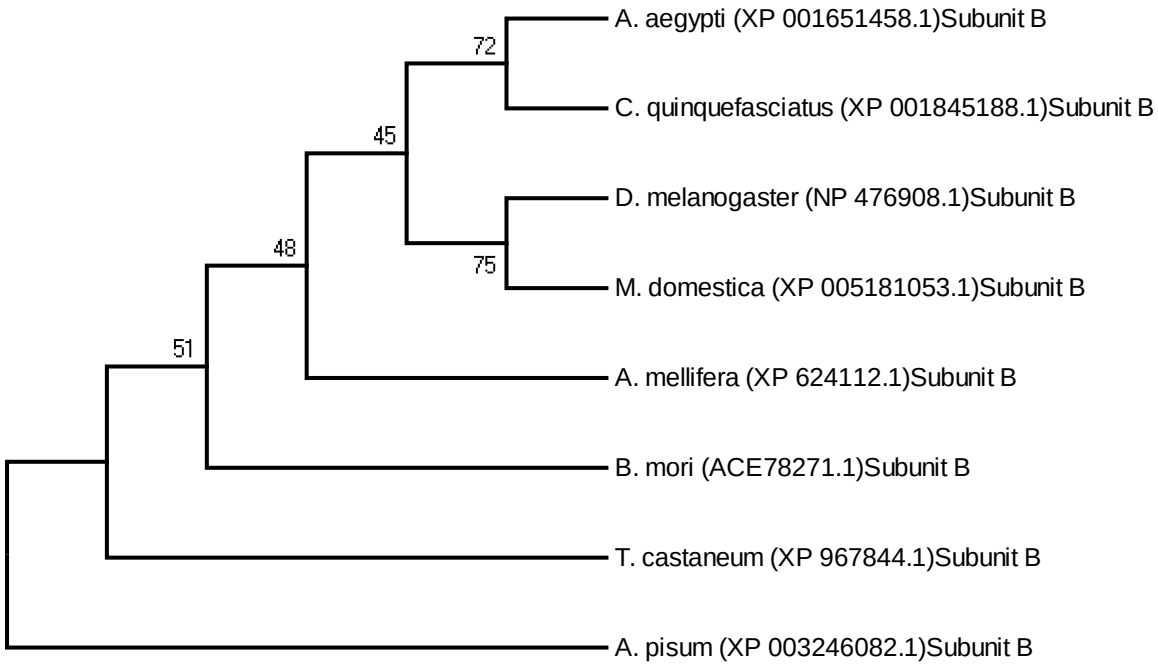

Figure A.1. Phylogenetic relationship of the deduced amino acid sequences of *V-ATPase B* gene.

This rooted phylogenetic tree was constructed using the maximum likelihood method. Nodes indicate bootstrap values calculated with 1000 replications.

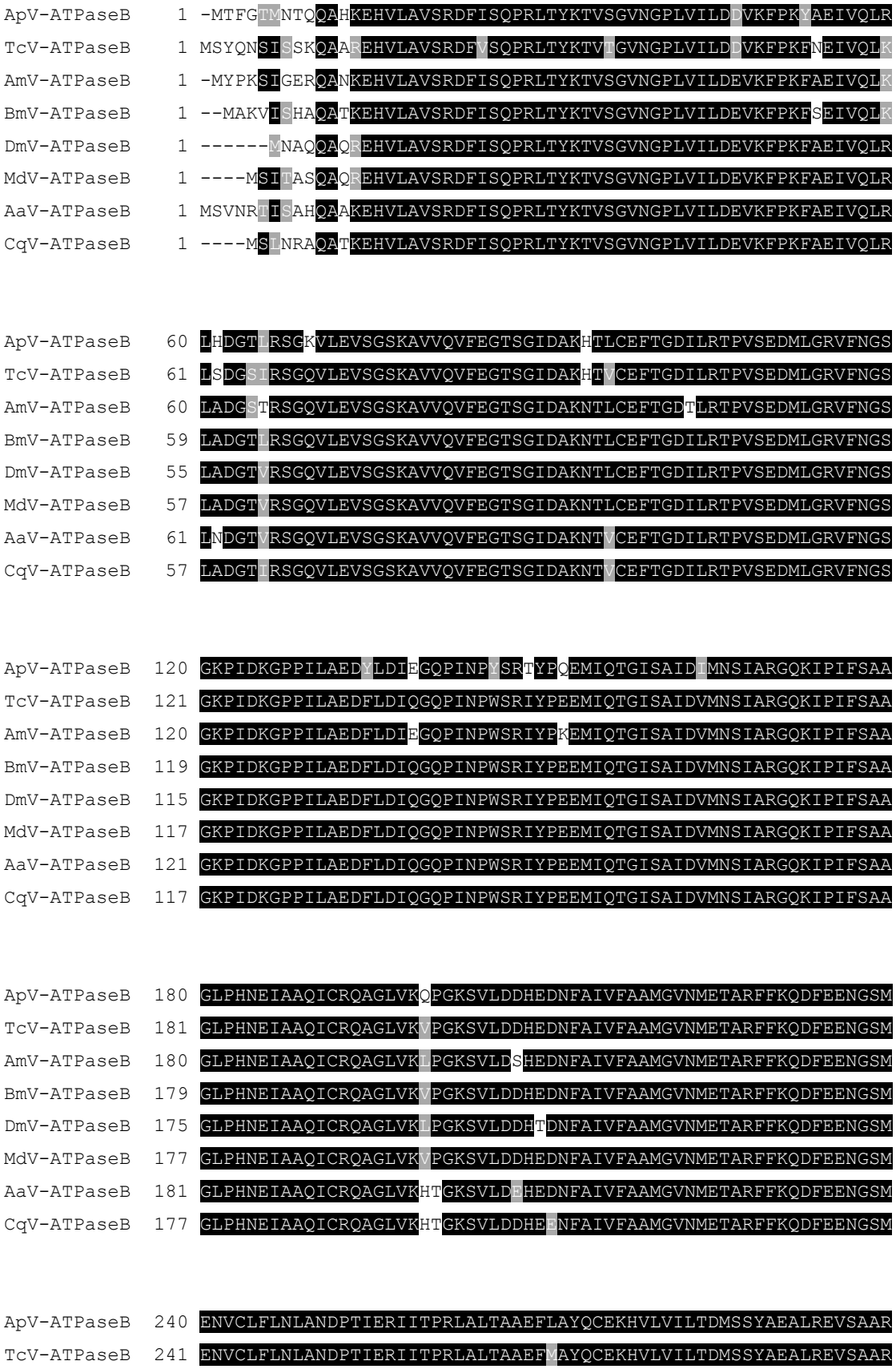
ApV-ATPaseB 1 -MTFGTMNTQQAHKEHVLAVSRDFISQPRLTYKTVSGVNGPLVILDDVKFPKYAEIVQLR
TcV-ATPaseB 1 MSYQNSISSKQAAREHVLAVSRDFVSQPRLTYKTVTGVNGPLVILDDVKFPKFNEIVQLK
AmV-ATPaseB 1 -MYPKSIGERQANKEHVLAVSRDFISQPRLTYKTVSGVNGPLVILDEVKFPKFAEIVQLK
BmV-ATPaseB 1 --MAKVISHAQATKEHVLAVSRDFISQPRLTYKTVSGVNGPLVILDEVKFPKFSEIVQLK
DmV-ATPaseB 1 ------MNAQQAQREHVLAVSRDFISQPRLTYKTVSGVNGPLVILDEVKFPKFAEIVQLR
MdV-ATPaseB 1 ----MSITASQAQREHVLAVSRDFISQPRLTYKTVSGVNGPLVILDEVKFPKFAEIVQLR
AaV-ATPaseB 1 MSVNRTISAHQAAKEHVLAVSRDFISQPRLTYKTVSGVNGPLVILDEVKFPKFAEIVQLR
CqV-ATPaseB 1 ----MSINRAQATKEHVLAVSRDFISQPRLTYKTVSGVNGPLVILDEVKFPKFAEIVQLR
ApV-ATPaseB 60 LHDGTIRSGKVLEVSGSKAVVQVFEGTSGIDAKHTLCEFTGDILRTPVSEDMLGRVFNGS
TcV-ATPaseB 61 LSDGSIRSGQVLEVSGSKAVVQVFEGTSGIDAKHTVCEFTGDILRTPVSEDMLGRVFNGS
AmV-ATPaseB 60 LADGSTRSGQVLEVSGSKAVVQVFEGTSGIDAKNTLCEFTGDTLRTPVSEDMLGRVFNGS
BmV-ATPaseB 59 LADGTIRSGQVLEVSGSKAVVQVFEGTSGIDAKNTLCEFTGDILRTPVSEDMLGRVFNGS
DmV-ATPaseB 55 LADGTVRSGQVLEVSGSKAVVQVFEGTSGIDAKNTLCEFTGDILRTPVSEDMLGRVFNGS
MdV-ATPaseB 57 LADGTVRSGQVLEVSGSKAVVQVFEGTSGIDAKNTLCEFTGDILRTPVSEDMLGRVFNGS
AaV-ATPaseB 61 LNDGTVRSGQVLEVSGSKAVVQVFEGTSGIDAKNTVCEFTGDILRTPVSEDMLGRVFNGS
CqV-ATPaseB 57 LADGTIRSGQVLEVSGSKAVVQVFEGTSGIDAKNTVCEFTGDILRTPVSEDMLGRVFNGS
ApV-ATPaseB 120 GKPIDKGPPILAEDYLDIEGQPINPYSRTYPQEMIQTGISAIDTMNSIARGQKIPIFSAA
TcV-ATPaseB 121 GKPIDKGPPILAEDFLDIQGQPINPWSRIYPEEMIQTGISAIDVMNSIARGQKIPIFSAA
AmV-ATPaseB 120 GKPIDKGPPILAEDFLDIEGQPINPWSRIYPKEMIQTGISAIDVMNSIARGQKIPIFSAA
BmV-ATPaseB 119 GKPIDKGPPILAEDFLDIQGQPINPWSRIYPEEMIQTGISAIDVMNSIARGQKIPIFSAA
DmV-ATPaseB 115 GKPIDKGPPILAEDFLDIQGQPINPWSRIYPEEMIQTGISAIDVMNSIARGQKIPIFSAA
MdV-ATPaseB 117 GKPIDKGPPILAEDFLDIQGQPINPWSRIYPEEMIQTGISAIDVMNSIARGQKIPIFSAA
AaV-ATPaseB 121 GKPIDKGPPILAEDFLDIQGQPINPWSRIYPEEMIQTGISAIDVMNSIARGQKIPIFSAA
CqV-ATPaseB 117 GKPIDKGPPILAEDFLDIQGQPINPWSRIYPEEMIQTGISAIDVMNSIARGQKIPIFSAA
ApV-ATPaseB 180 GLPHNEIAAQICRQAGLVKQPGKSVLDDHEDNFAIVFAAMGVNMETARFFKQDFEENGSM
TcV-ATPaseB 181 GLPHNEIAAQICRQAGLVKVPGKSVLDDHEDNFAIVFAAMGVNMETARFFKQDFEENGSM
AmV-ATPaseB 180 GLPHNEIAAQICRQAGLVKLPGKSVLDSHEDNFAIVFAAMGVNMETARFFKQDFEENGSM
BmV-ATPaseB 179 GLPHNEIAAQICRQAGLVKVPGKSVLDDHEDNFAIVFAAMGVNMETARFFKQDFEENGSM
DmV-ATPaseB 175 GLPHNEIAAQICRQAGLVKLPGKSVLDDHTDNFAIVFAAMGVNMETARFFKQDFEENGSM
MdV-ATPaseB 177 GLPHNEIAAQICRQAGLVKVPGKSVLDDHEDNFAIVFAAMGVNMETARFFKQDFEENGSM
AaV-ATPaseB 181 GLPHNEIAAQICRQAGLVKHTGKSVLDEHEDNFAIVFAAMGVNMETARFFKQDFEENGSM
CqV-ATPaseB 177 GLPHNEIAAQICRQAGLVKHTGKSVLDDHEENFAIVFAAMGVNMETARFFKQDFEENGSM
ApV-ATPaseB 240 ENVCLFLNLANDPTIERIITPRLALTAAEFLAYQCEKHVLVILTDMSSYAEALREVSAAR
TcV-ATPaseB 241 ENVCLFLNLANDPTIERIITPRLALTAAEFMAYQCEKHVLVILTDMSSYAEALREVSAAR

```
AmV-ATPaseB  240 ENVCLFLNLANDPTIERIITPRLALTAAEFLAYQCEKHVLVILTDMSSYAEALREVSAAR
BmV-ATPaseB  239 ENVCLFLNLANDPTIERIITPRLALTAAEFLAYQCEKHVLVILTDMSSYAEALREVSAAR
DmV-ATPaseB  235 ENVCLFLNLANDPTIERIITPRLALTAAEFLAYQCEKHVLVILTDMSSYAEALREVSAAR
MdV-ATPaseB  237 ENVCLFLNLANDPTIERIITPRLALTAAEFLAYQCEKHVLVILTDMSSYAEALREVSAAR
AaV-ATPaseB  241 ENVCLFLNLANDPTIERIITPRLALTAAEFLAYQCEKHVLVILTDMSSYAEALREVSAAR
CqV-ATPaseB  237 ENVCLFLNLANDPTIERIITPRLALTAAEFLAYQCEKHVLVILTDMSSYAEALREVSAAR

ApV-ATPaseB  300 EEVPGRRGFPGYMYTDLATIYERAGRVEGRNGSITQIPILTMPNDDITHPIPDLTGYITE
TcV-ATPaseB  301 EEVPGRRGFPGYMYTDLATIYERAGRVEGRNGSITQIPILTMPNDDITHPIPDLTGYITE
AmV-ATPaseB  300 EEVPGRRGFPGYMYTDLATIYERAGRVEGRNGSITQIPILTMPNDDITHPIPDLTGYITE
BmV-ATPaseB  299 EEVPGRRGFPGYMYTDLATIYERAGRVEGRNGSITQIPILTMPNDDITHPIPDLTGYITE
DmV-ATPaseB  295 EEVPGRRGFPGYMYTDLATIYERAGRVEGRNGSITQIPILTMPNDDITHPIPDLTGYITE
MdV-ATPaseB  297 EEVPGRRGFPGYMYTDLATIYERAGRVEGRNGSITQIPILTMPNDDITHPIPDLTGYITE
AaV-ATPaseB  301 EEVPGRRGFPGYMYTDLATIYERAGRVEGRNGSITQIPILTMPNDDITHPIPDLTGYITE
CqV-ATPaseB  297 EEVPGRRGFPGYMYTDLATIYERAGRVEGRNGSITQIPILTMPNDDITHPIPDLTGYITE

ApV-ATPaseB  360 GQIYVDRQLHNRQIYPPINVLPSLSRLMKSAIGEGMTRKDHSDVSNQLYACYAIGKDVQA
TcV-ATPaseB  361 GQIYVDRQLHNRQIYPPTNVLPSLSRLMKSAIGEGMTRKDHSDVSNQLYACYAIGKDVQA
AmV-ATPaseB  360 GQIYVDRQLHNRQIYPPVNVLPSLSRLMKSAIGEGWTRKDHSDVSNQLYACYAIGKDVQA
BmV-ATPaseB  359 GQIYVDRQLHNRQIYPPVNVLPSLSRLMKSAIGEGMTRKDHSDVSNQLYACYAIGKDVQA
DmV-ATPaseB  355 GQIYVDRQLHNRQIYPPVNVLPSLSRLMKSAIGEGMTRKDHSDVSNQLYACYAIGKDVQA
MdV-ATPaseB  357 GQIYVDRQLHNRQIYPPVNVLPSLSRLMKSAIGEGMTRKDHSDVSNQLYACYAIGKDVQA
AaV-ATPaseB  361 GQIYVDRQLHNRQIYPPVNVLPSLSRLMKSAIGEGMTRKDHSDVSNQLYACYAIGKDVQA
CqV-ATPaseB  357 GQIYVDRQLHNRQIYPPVNVLPSLSRLMKSAIGEGMTRKDHSDVSNQLYACYAIGKDVQA
ApV-ATPaseB  420 MKAVVGEEALTPDDLLYLEFLTKFEKNFITQGNYENRTVFESLDIGWQLLRIFPKEMLKR
TcV-ATPaseB  421 MKAVVGEEALTPDDLLYLEFLSKFEKNFITQGSYENRTVFESLDIGWQLLRIFPKEMLKR
AmV-ATPaseB  420 MKAVVGEEALTPDDLLYLEFLSKFEKNFISQGSYENRTVFESLDIGWQLLRIFPKEMLKR
BmV-ATPaseB  419 MKAVVGEEALTPDDLLYLEFLTKFEKNFITQGNYENRTVFESLDIGWQLLRIFPKEMLKR
DmV-ATPaseB  415 MKAVVGEEALTPDDLLYLEFLTKFEKNFISQGNYENRTVFESLDIGWQLLRIFPKEMLKR
MdV-ATPaseB  417 MKAVVGEEALTPDDLLYLEFLTKFEKNFISQGNYENRTVFESLDIGWQLLRIFPKEMLKR
AaV-ATPaseB  421 MKAVVGEEALTPDDLLYLEFLTKFEKNFISQGNYENRTVFESLDIGWQLLRIFPKEMLKR
CqV-ATPaseB  417 MKAVVGEEALTPDDLLYLEFLSKFEKNFISQGNYENRTVFESLDIGWQLLRIFPKEMLKR

ApV-ATPaseB  480 VPAATLAEFYPRDSRPK
TcV-ATPaseB  481 IPAATLAEFYPRDSRH-
AmV-ATPaseB  480 IPTNILAEFYPRDSRH-
BmV-ATPaseB  479 IPASTLAEFYPRDSRH-
DmV-ATPaseB  475 IPASILAEFYPRDSRH-
MdV-ATPaseB  477 IPASILAEFYPRDSRH-
```

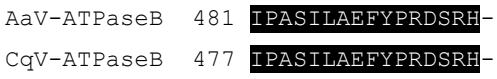

Figure A.2. Multiple alignments of amino acid sequences of V-ATPase subunit B (*Ae. aegypti, D. melanogaster, C. quinquefasciatus, M. domestica, B. mori, T. castaneum, A. mellifera, A. pisum*).

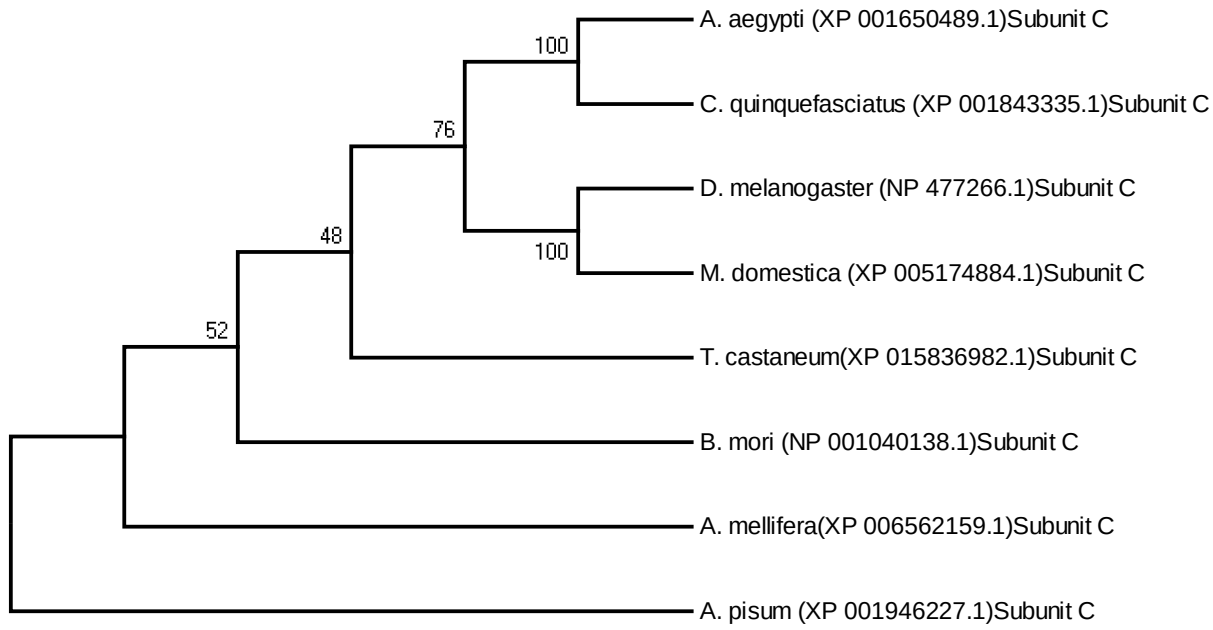

Figure A.3. Phylogenetic relationship of the deduced amino acid sequences of *V-ATPase C* gene.

This rooted phylogenetic tree was constructed using the maximum likelihood method. Nodes indicate bootstrap values calculated with 1000 replications.

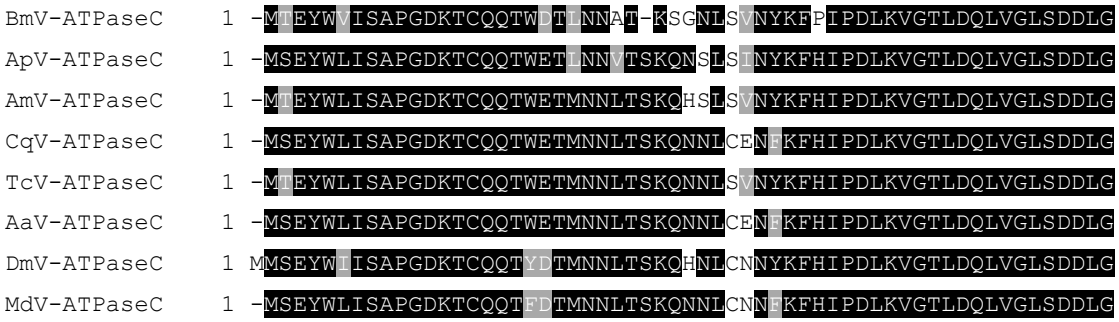
BmV-ATPaseC 1 -MTEYWVISAPGDKTCQQTWDTLNNAT-KSGNLSVNYKFPIPDLKVGTLDQLVGLSDDLG
ApV-ATPaseC 1 -MSEYWLISAPGDKTCQQTWETLNNVTSKQNSLSINYKFHIPDLKVGTLDQLVGLSDDLG
AmV-ATPaseC 1 -MTEYWLISAPGDKTCQQTWETMNNLTSKQHSLSVNYKFHIPDLKVGTLDQLVGLSDDLG
CqV-ATPaseC 1 -MSEYWLISAPGDKTCQQTWETMNNLTSKQNNLCENFKFHIPDLKVGTLDQLVGLSDDLG
TcV-ATPaseC 1 -MTEYWLISAPGDKTCQQTWETMNNLTSKQNNLSVNYKFHIPDLKVGTLDQLVGLSDDLG
AaV-ATPaseC 1 -MSEYWLISAPGDKTCQQTWETMNNLTSKQNNLCENFKFHIPDLKVGTLDQLVGLSDDLG
DmV-ATPaseC 1 MMSEYWIISAPGDKTCQQTYDTMNNLTSKQHNLCNNYKFHIPDLKVGTLDQLVGLSDDLG
MdV-ATPaseC 1 -MSEYWLISAPGDKTCQQTFDTMNNLTSKQNNLCNNFKFHIPDLKVGTLDQLVGLSDDLG


BmV-ATPaseC 59 KLDTFVEGVTRKVAQYLGEVLEDQRDKLHENLMANN----------
ApV-ATPaseC 60 KLDSFVDQVTHKVASYLGEVLEDQRDKLQENLMANN----------
AmV-ATPaseC 60 KLDTYVEQITRKVATYLGEVLEDQRDKLHENLLANN----------
CqV-ATPaseC 60 KLDAYVEQSTRKIASYLGDVLEDQRDKLYENLQANNNEVDPDE----------
TcV-ATPaseC 60 KLDAFVEQVTRKVSSYLGEVLEDQRDKLQENLMANNSGRPP----------
AaV-ATPaseC 60 KLDAYVEQSTRKIASYLGDVLEDQRDKLYENLQANNSNFIFMGVFDTVFCIELNYIRPRH
DmV-ATPaseC 61 KLDTYVEQITRKVANYLGEVLEDQRDKLHENLMANN----------
MdV-ATPaseC 60 KLDTYVEQITRKVAAYLGEVLEDQRDKLHENLLANN----------

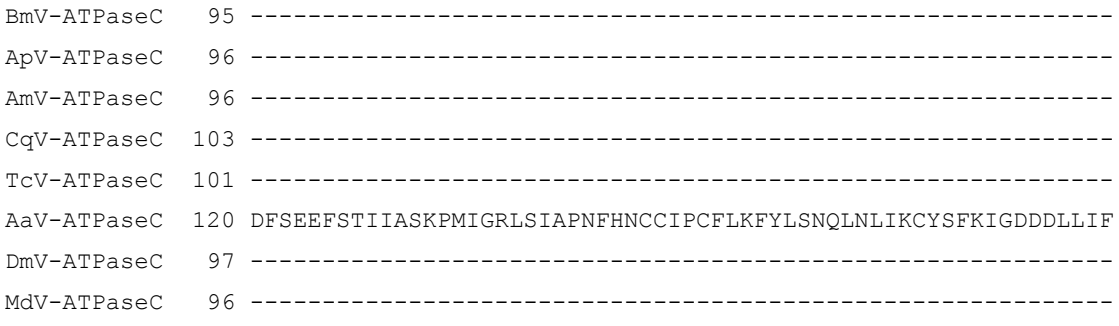
BmV-ATPaseC 95 ----------
ApV-ATPaseC 96 ----------
AmV-ATPaseC 96 ----------
CqV-ATPaseC 103 ----------
TcV-ATPaseC 101 ----------
AaV-ATPaseC 120 DFSEEFSTIIASKPMIGRLSIAPNFHNCCIPCFLKFYLSNQLNLIKCYSFKIGDDDLLIF
DmV-ATPaseC 97 ----------
MdV-ATPaseC 96 ----------

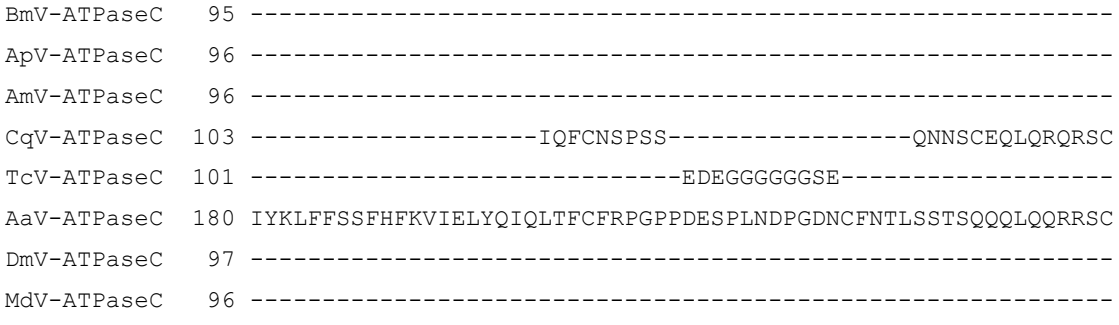
BmV-ATPaseC 95 ----------
ApV-ATPaseC 96 ----------
AmV-ATPaseC 96 ----------
CqV-ATPaseC 103 ----------IQFCNSPSS----------QNNSCEQLQRQRSC
TcV-ATPaseC 101 ----------EDEGGGGGGSE----------
AaV-ATPaseC 180 IYKLFFSSFHFKVIELYQIQLTFCFRPGPPDESPLNDPGDNCFNTLSSTSQQQLQQRRSC
DmV-ATPaseC 97 ----------
MdV-ATPaseC 96 ----------

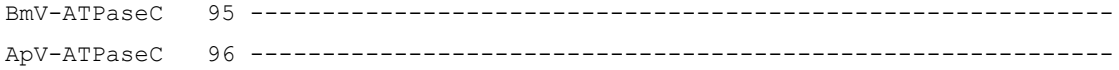
BmV-ATPaseC 95 ----------
ApV-ATPaseC 96 ----------

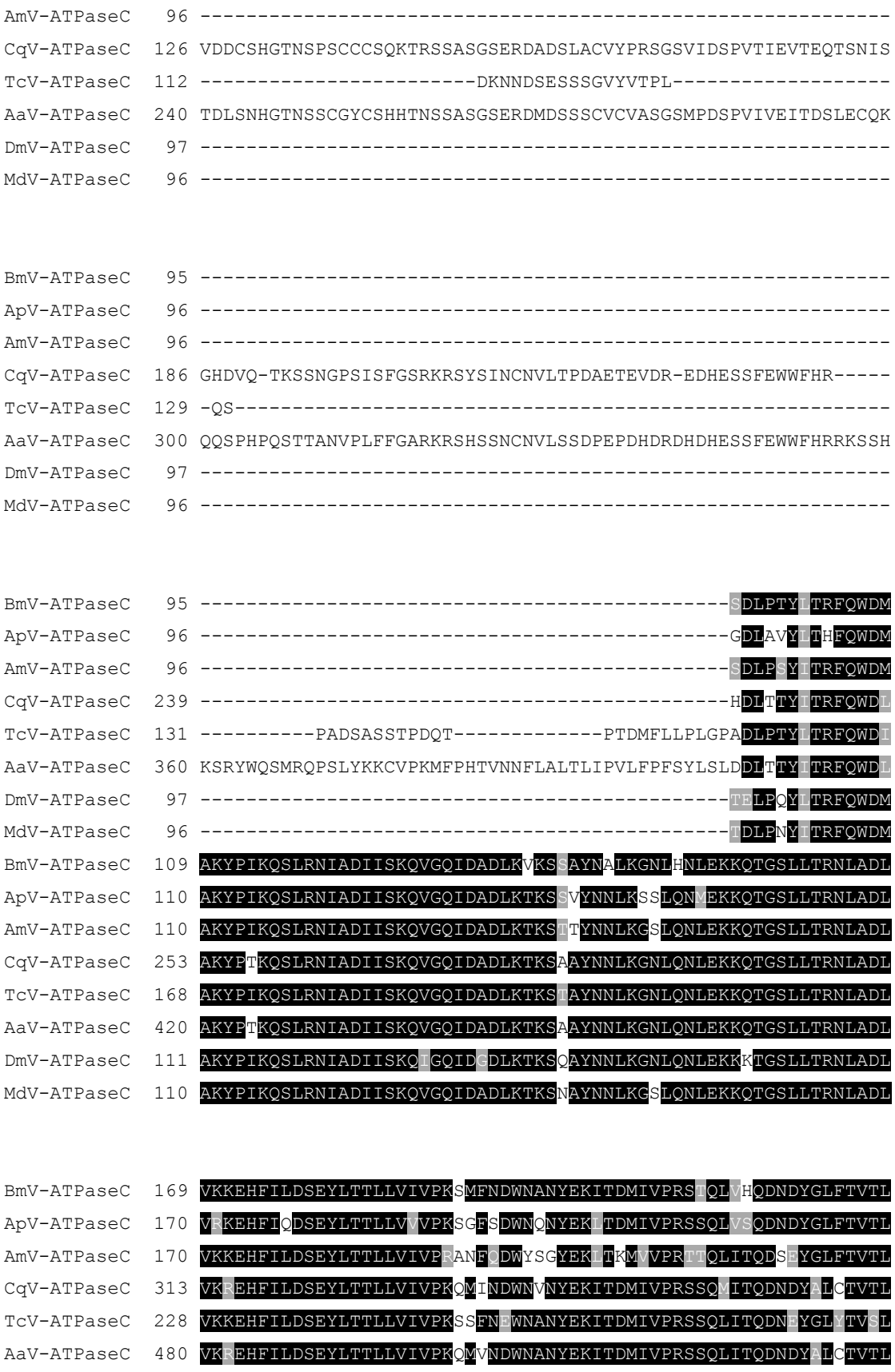
AmV-ATPaseC 96
CqV-ATPaseC 126 VDDCSHGTNSPSCCCSQKTRSSASGSERDADSLACVYPRSGSVIDSPVTIEVTEQTSNIS
TcV-ATPaseC 112 DKNNDSESSSGVYVTPL
AaV-ATPaseC 240 TDLSNHGTNSSCGYCSHHTNSSASGSERDMDSSSCVCVASGSMPDSPVIVEITDSLECQK
DmV-ATPaseC 97
MdV-ATPaseC 96
BmV-ATPaseC 95
ApV-ATPaseC 96
AmV-ATPaseC 96
CqV-ATPaseC 186 GHDVQ-TKSSNGPSISFGSRKRSYSINCNVLTPDAETEVDR-EDHESSFEWWFHR
TcV-ATPaseC 129 -QS
AaV-ATPaseC 300 QQSPHPQSTTANVPLFFGARKRSHSSNCNVLSSDPEPDHDRDHDHESSFEWWFHRRKSSH
DmV-ATPaseC 97
MdV-ATPaseC 96
BmV-ATPaseC 95 SDLPTYLTRFQWDM
ApV-ATPaseC 96 GDLAVYLTHFQWDM
AmV-ATPaseC 96 SDLPSYITRFQWDM
CqV-ATPaseC 239 HDLTTYITRFQWDL
TcV-ATPaseC 131 PADSASSTPDQT PTDMFLLPLGPADLPTYITRFQWDI
AaV-ATPaseC 360 KSRYWQSMRQPSLYKKCVPKMFPHTVNNFLALTLIPVLFPFSYLSLDDLTTYITRFQWDL
DmV-ATPaseC 97 TPLPQYITRFQWDM
MdV-ATPaseC 96 TDLPNYITRFQWDM
BmV-ATPaseC 109 AKYPIKQSLRNIADIISKQVGQIDADLKVKSSAYNALKGNLHNLEKKQTGSLLTRNLADL
ApV-ATPaseC 110 AKYPIKQSLRNIADIISKQVGQIDADLKTKSSVYNNLKSSLQNMEKKQTGSLLTRNLADL
AmV-ATPaseC 110 AKYPIKQSLRNIADIISKQVGQIDADLKTKSTTYNNLKGSLQNLEKKQTGSLLTRNLADL
CqV-ATPaseC 253 AKYPTKQSLRNIADIISKQVGQIDADLKTKSAAYNNLKGNLQNLEKKQTGSLLTRNLADL
TcV-ATPaseC 168 AKYPIKQSLRNIADIISKQVGQIDADLKTKSTAYNNLKGNLQNLEKKQTGSLLTRNLADL
AaV-ATPaseC 420 AKYPTKQSLRNIADIISKQVGQIDADLKTKSAAYNNLKGNLQNLEKKQTGSLLTRNLADL
DmV-ATPaseC 111 AKYPIKQSLRNIADIISKQIGQIDGDLKTKSQAYNNLKGNLQNLEKKKTGSLLTRNLADL
MdV-ATPaseC 110 AKYPIKQSLRNIADIISKQVGQIDADLKTKSNAYNNLKGSLQNLEKKQTGSLLTRNLADL
BmV-ATPaseC 169 VKKEHFILDSEYLTTLLVIVPKSMFNDWNANYEKITDMIVPRSTQLVHQDNDYGLFTVTL
ApV-ATPaseC 170 VRKEHFIQDSEYLTTLLVVVPKSGFSDWNQNYEKITDMIVPRSSQLVSQDNDYGLFTVTL
AmV-ATPaseC 170 VKKEHFILDSEYLTTLLVIVPRANFQDWYSGYEKITKMVVPRTTQLITQDSEYGLFTVTL
CqV-ATPaseC 313 VKREHFILDSEYLTTLLVIVPKQMINDWNVNYEKITDMIVPRSSQMITQDNDYALCTVTL
TcV-ATPaseC 228 VKKEHFILDSEYLTTLLVIVPKSSFNEWNANYEKITDMIVPRSSQLITQDNEYGLYTVSL
AaV-ATPaseC 480 VKREHFILDSEYLTTLLVIVPKQMVNDWNANYEKITDMIVPRSSQLITQDNDYALCTVTL

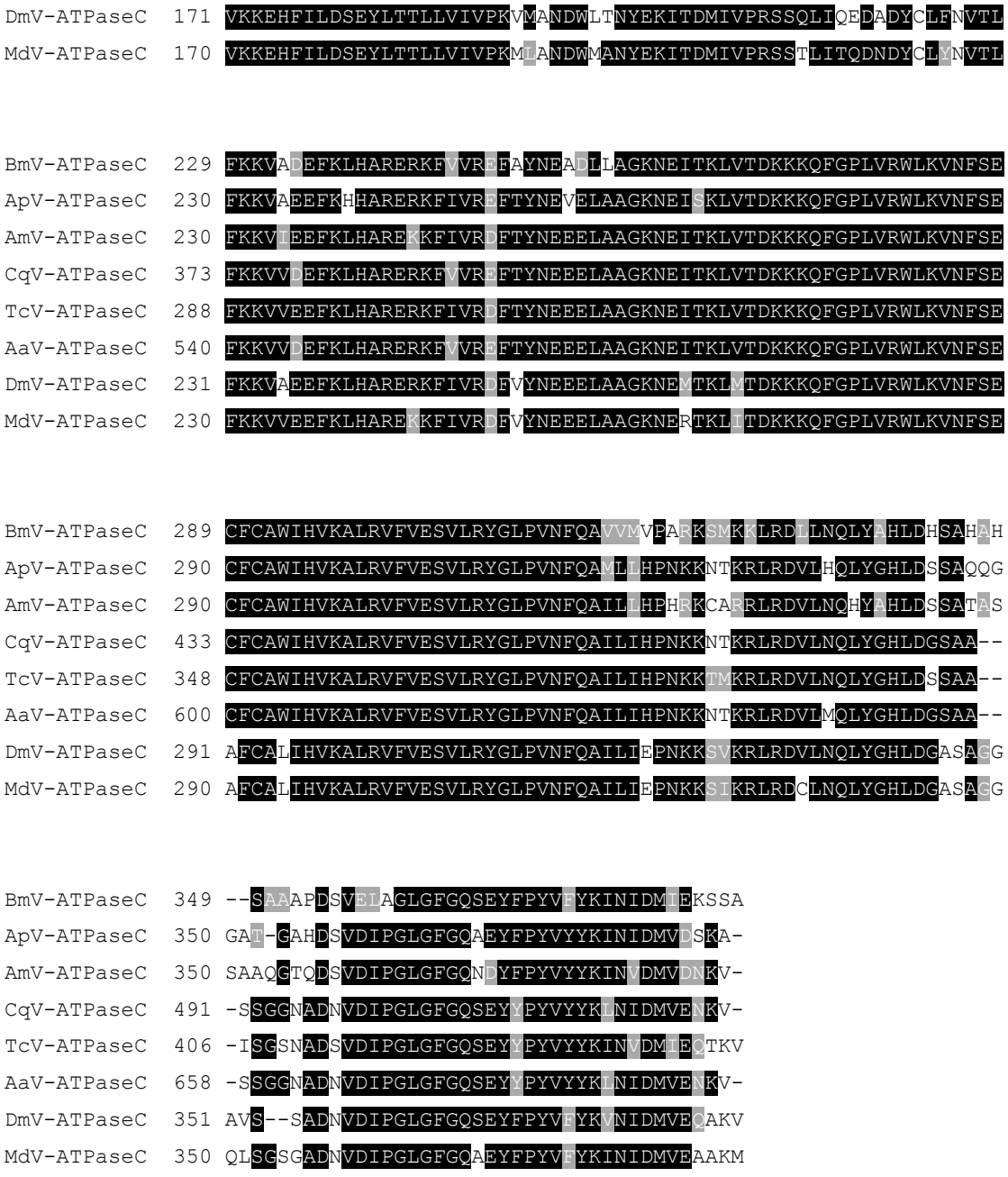

Figure A.4. Multiple alignments of amino acid sequences of V-ATPase subunit C (*Ae. aegypti, D. melanogaster, C. quinquefasciatus, M. domestica, B. mori, T. castaneum, A. mellifera, A. pisum*).

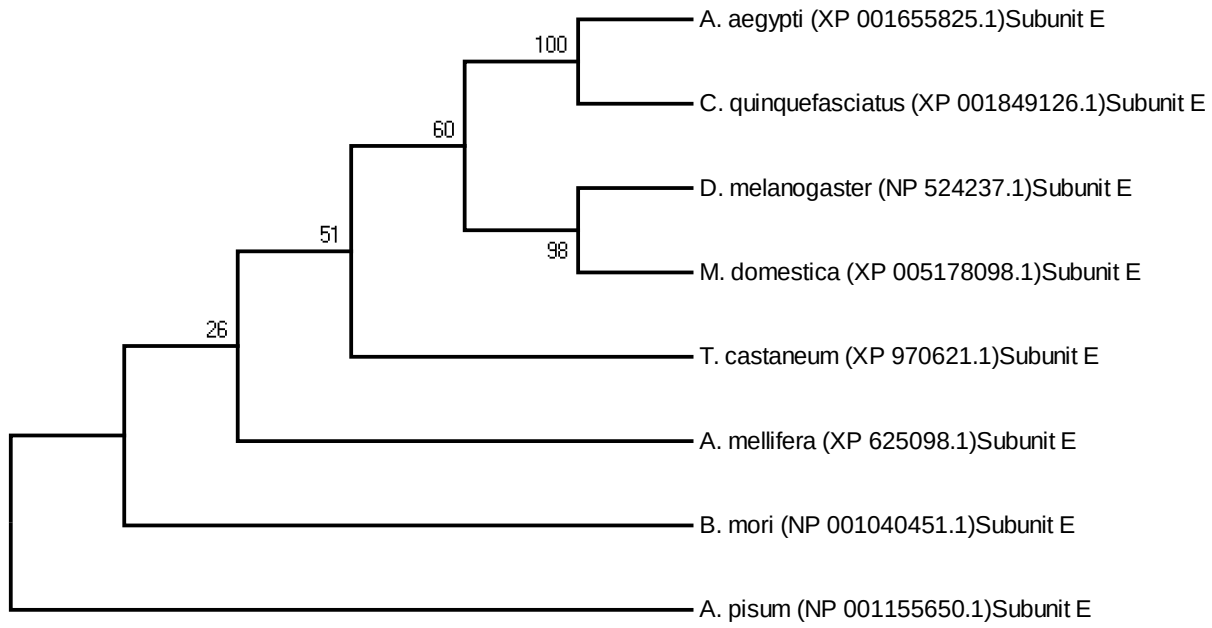

Figure A.5. Phylogenetic relationship of the deduced amino acid sequences of *V-ATPase E* gene.

This rooted phylogenetic tree was constructed using the maximum likelihood method. Nodes indicate bootstrap values calculated with 1000 replications.

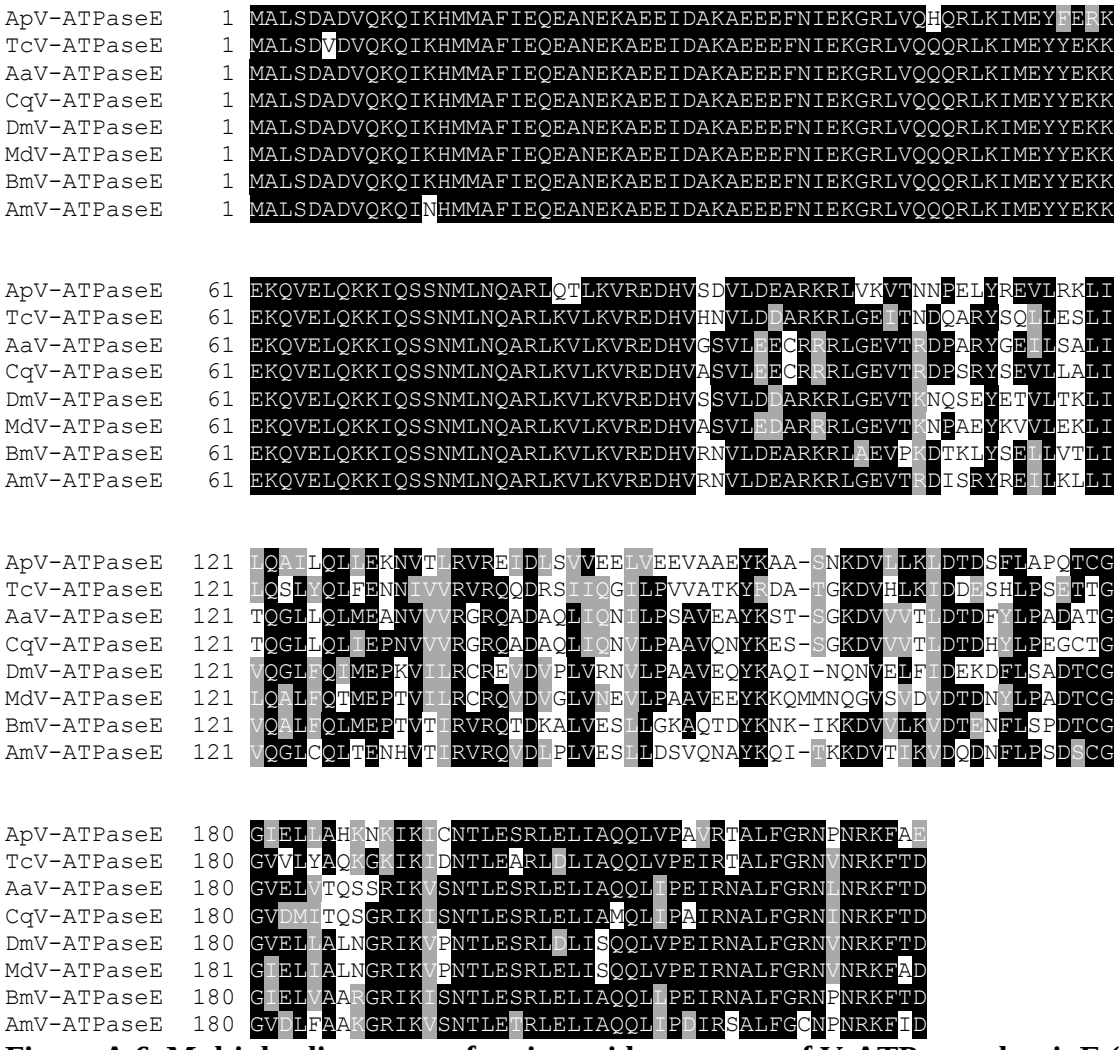

Figure A.6. Multiple alignments of amino acid sequences of V-ATPase subunit E (*Ae. aegypti, D. melanogaster, C. quinquefasciatus, M. domestica, B. mori, T. castaneum, A. mellifera, A. pisum*).

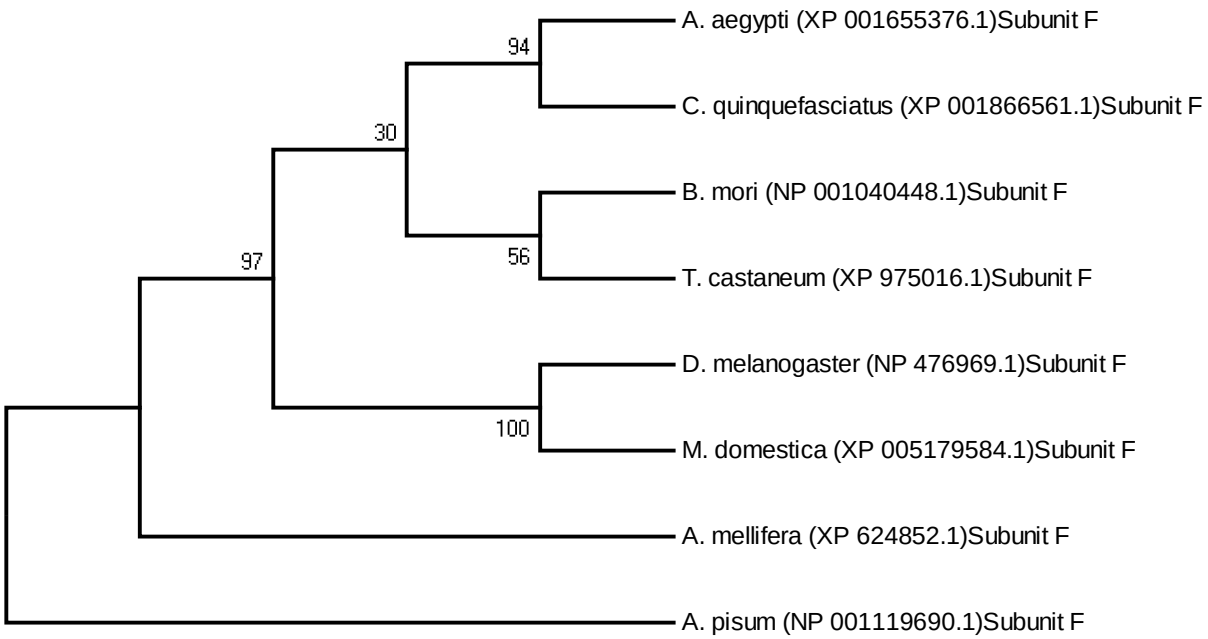

Figure A.7. Phylogenetic relationship of the deduced amino acid sequences of *V-ATPase F* gene.

This rooted phylogenetic tree was constructed using the maximum likelihood method. Nodes indicate bootstrap values calculated with 1000 replications.

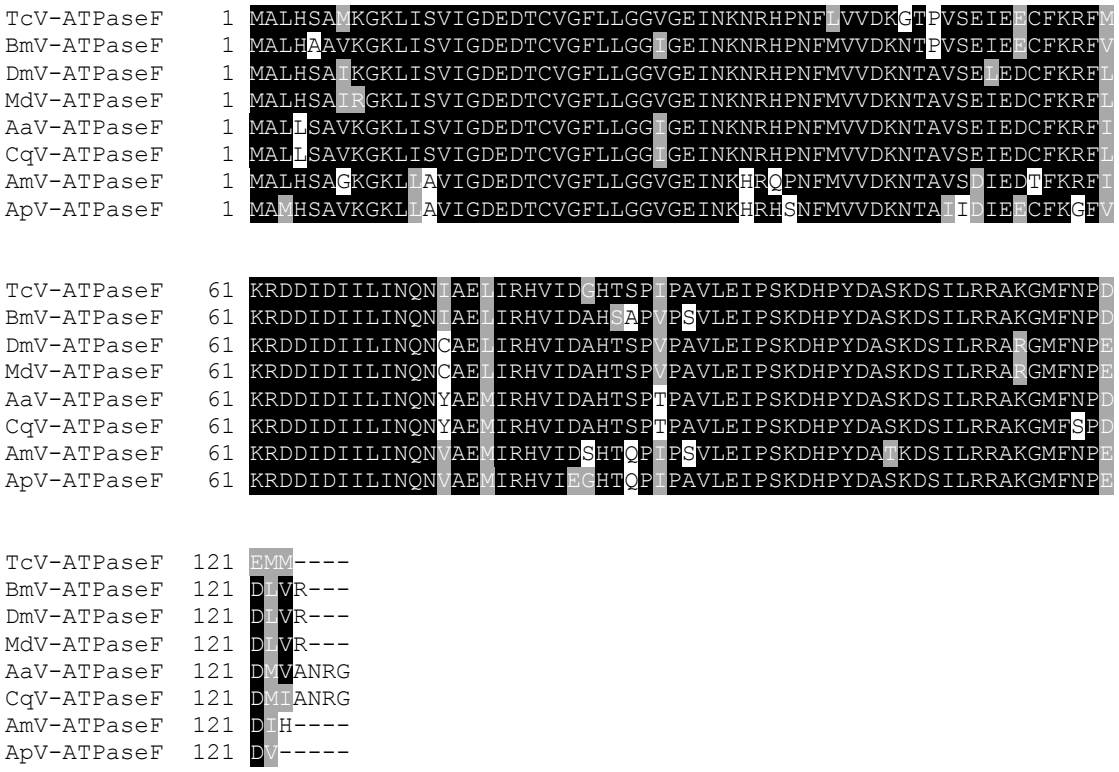

Figure A.8. Multiple alignments of amino acid sequences of V-ATPase subunit F (*Ae. aegypti, D. melanogaster, C. quinquefasciatus, M. domestica, B. mori, T. castaneum, A. mellifera, A. pisum*).

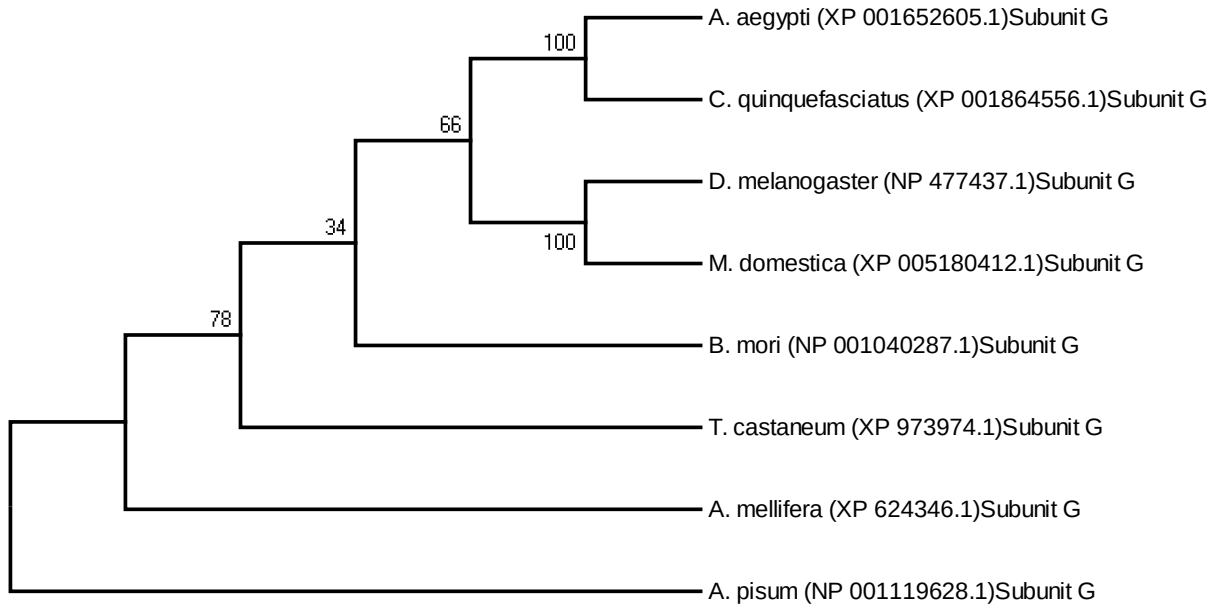

Figure A.9. Phylogenetic relationship of the deduced amino acid sequences of *V-ATPase G* gene.

This rooted phylogenetic tree was constructed using the maximum likelihood method. Nodes indicate bootstrap values calculated with 1000 replications.

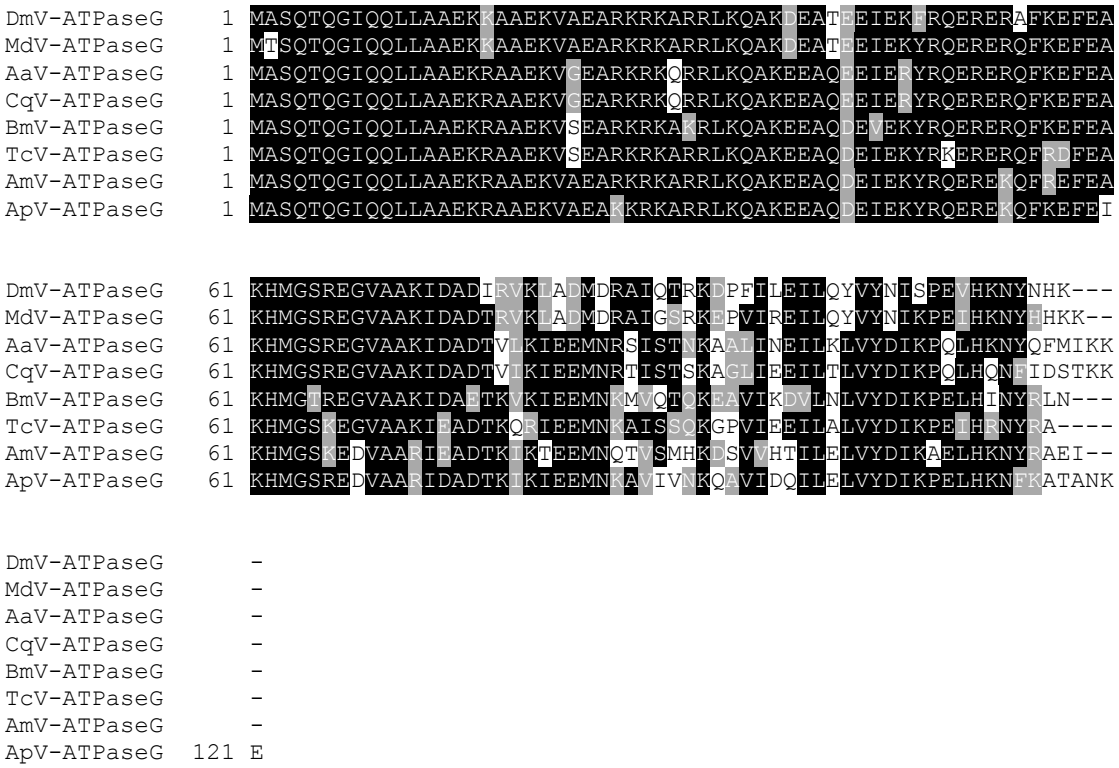

Figure A.10. Multiple alignments of amino acid sequences of V-ATPase subunit G (*Ae. aegypti, D. melanogaster, C. quinquefasciatus, M. domestica, B. mori, T. castaneum, A. mellifera, A. pisum*).

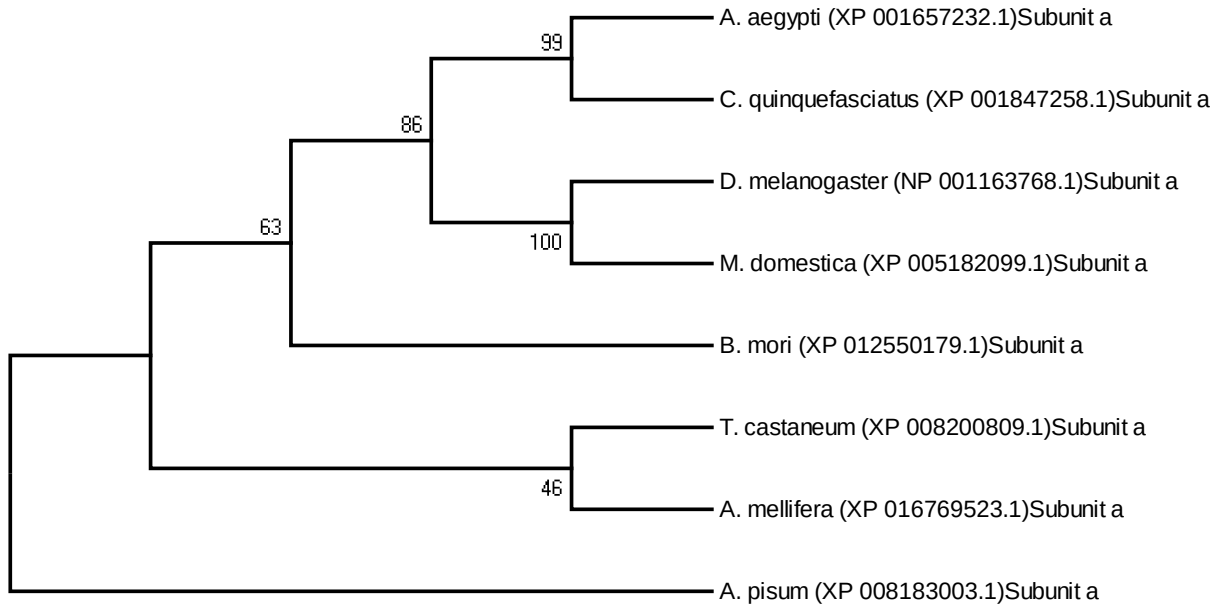

Figure A.11. Phylogenetic relationship of the deduced amino acid sequences of *V-ATPase-a* gene.

This rooted phylogenetic tree was constructed using the maximum likelihood method. Nodes indicate bootstrap values calculated with 1000 replications.

```
TcV-ATPase-a     1 MASLFRSAEMTLCQLFLQSEAAYACVSELGELGLVQFRDLNPDVNVFQRKFVNEVRRCDE
ApV-ATPase-a     1 MGSLFRSEEMALCQLFLQSEAAYACVSELGELGLVQFRDLNPDVNAFQRKFVSEVRRCDE
BmV-ATPase-a     1 MGSLFRSEQMTLCQLFLQSEAAYACVSELGELGLVQFRDLNPDVNAFQRKFVNEVRRCDE
AmV-ATPase-a     1 MGSLFRSEEMTLCQLFLQSEAAYACVSELGELGLVQFRDLNPDVNAFQRKFVNEVRRCDE
AaV-ATPase-a     1 MGSLFRSEEMTLCQLFLQSEAAYACVSELGELGLVQFRDLNPDVNAFQRKFVNEVRRCDE
CqV-ATPase-a     1 MGSLFRSEEMTLCQLFLQSEAAYACVSELGELGLVQFRDLNPDVNAFQRKFVNEVRRCDE
DmV-ATPase-a     1 MGSLFRSEEMALCQLFLQSEAAYACVSELGELGLVQFRDLNPDVNAFQRKFVNEVRRCDE
MdV-ATPase-a     1 MGSLFRSEEMTLCQLFLQSEAAYACVSELGELGLVQFRDLNPDVNAFQRKFVNEVRRCDE

TcV-ATPase-a    61 MERKLRYLEKEIKKDGIPMLDTGENPEAPQPREMIDLEATFEKLENELREVNQNAEALKR
ApV-ATPase-a    61 MERKLRYLEKEIKKDGIPMLDTGENPEAPQPREMIDLEATFEKLENELREVNHNAEALKR
BmV-ATPase-a    61 MERKLRYLEKEIKKDGIPMLDTGENPEAPQPREMIDLEATFEKLENELREVNQNAETLKR
AmV-ATPase-a    61 MERKLRYLEKEIKKDGIPMLDTGENPEAPQPREMIDLEATFEKLENELREVNQNAETLKR
AaV-ATPase-a    61 MERKLRYLEKEIKKDGIPMLDTGESPEAPQPREMIDLEATFEKLENELREVNQNAEALKR
CqV-ATPase-a    61 MERKLRYLEKEIKKDGIPMLDTGESPEAPQPREMIDLEATFEKLENELREVNQNAEALKR
DmV-ATPase-a    61 MERKLRYLEKEIKKDGIPMLDTGESPEAPQPREMIDLEATFEKLENELREVNQNAEALKR
MdV-ATPase-a    61 MERKLRYLEKEIKKDGIPMLDTGESPEAPQPREMIDLEATFEKLENELREVNQNAEALKR

TcV-ATPase-a   121 NFLELTELKQILRKTQVFFDEHE-GGANPTESMTRALISDDSIARQSTLGPVQLGFPEKQ
ApV-ATPase-a   121 NFLELTELKHILRKTQVFFDEQE-GGLHPTESMTRALISDDSIARQVNAGPVQLGF----
BmV-ATPase-a   121 NFLELTELKHILRKTQVFFDEQEHAGLNPTESMTRALISDDNIARQTALGPVQLGF----
AmV-ATPase-a   121 NFLELTELKHILRKTQVFFDEQEHAGLNPTESMTRALISDDNIARQTALGPVQLGF----
AaV-ATPase-a   121 NFLELTELKHILRKTQVFFDEQEGGMH-TTESMTRALITDESRTGGKTMGPVQLGFLEKS
CqV-ATPase-a   121 NFLELTELKHILRKTQVFFDEMADSHR-EEEQV-NLLGDEGIRAGGAG------------
DmV-ATPase-a   121 NFLELTELKHILRKTQVFFDEQEGGLNHTTESMTRALITDEVRTAGASMGPVQLGFMEKS
MdV-ATPase-a   121 NFLELTELKHILRKTQVFFDEQEGGLNTTTESMTRALITDEVRT-GHSMGPVQLGFMEKS

TcV-ATPase-a   180 FESEEEFPCFVAGVILRERIPAFERMLWRACRGNVFLRQAEIETPLEDPSTGDQVYKSVF
ApV-ATPase-a   176 ----------VAGVILRERIPAFERMLWRACRGNVFLRQAEIETPLEDPSTGDQVHKSVF
BmV-ATPase-a   177 ----------VAGVILRERIPAFERMLWRACRGNVFLRQAEIETPLEDPSTGDQVFKSVF
AmV-ATPase-a   177 ----------VAGVILRERIPAFERMLWRACRGNVFLRQAEIETPLEDPSTGDQVFKSVF
AaV-ATPase-a   180 QEPEEEYLPCFVAGVILRERLPAFERMLWRACRGNVFLRQAMIESPLEDPSTGDKVYKSVF
CqV-ATPase-a   167 AQGQNLKLGFVAGVILRERLPAFERMLWRACRGNVFLRQAVIDSALEDPSNGDKVYKSVF
DmV-ATPase-a   181 IERREDYLPCFVAGVISREKLPAFERMLWRACRGNVFLRQAMIESPLEDPTNGDQVYKSVF
MdV-ATPase-a   180 NERREDYYPCFVAGVISREKLPAFERMLWRACRGNVFLRQAMIESPLEDPSNGDQVYKSVF

TcV-ATPase-a   240 IIFFQGDQLKTRVKKICEGFRATLYPCPEAPGDRREMAMGVMTRIEDLNTVLGQTQDHRH
ApV-ATPase-a   226 IIFFQGDQLKSRVRKICEGFRATLYPCPEAPSQRREMAMGVMTRIEDLNTVLGQTQDHRH
```

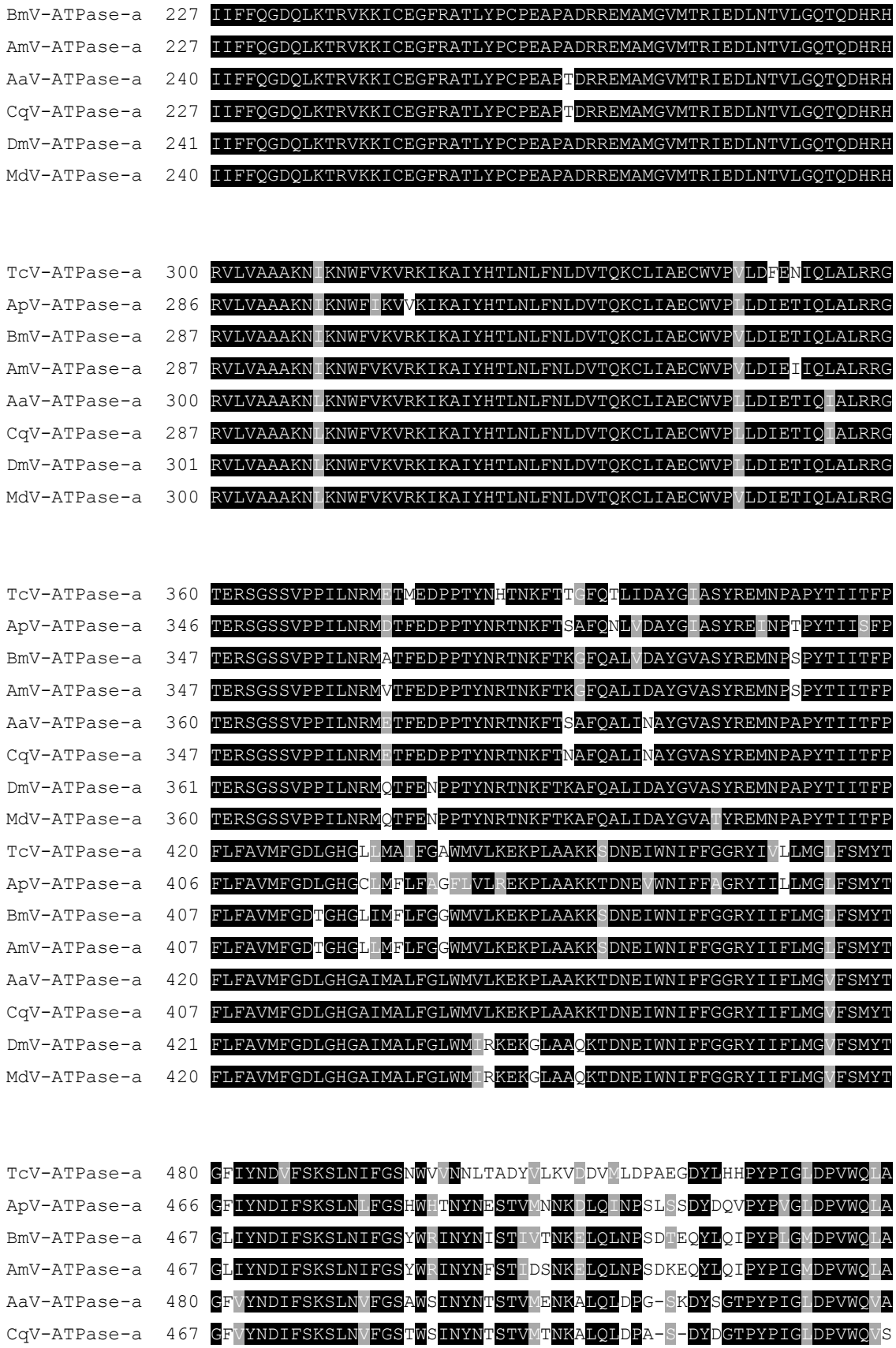
BmV-ATPase-a 227 IIFFQGDQLKTRVKKICEGFRATLYPCPEAPADRREMAMGVMTRIEDLNTVLGQTQDHRH
AmV-ATPase-a 227 IIFFQGDQLKTRVKKICEGFRATLYPCPEAPADRREMAMGVMTRIEDLNTVLGQTQDHRH
AaV-ATPase-a 240 IIFFQGDQLKTRVKKICEGFRATLYPCPEAPTDRREMAMGVMTRIEDLNTVLGQTQDHRH
CqV-ATPase-a 227 IIFFQGDQLKTRVKKICEGFRATLYPCPEAPTDRREMAMGVMTRIEDLNTVLGQTQDHRH
DmV-ATPase-a 241 IIFFQGDQLKTRVKKICEGFRATLYPCPEAPADRREMAMGVMTRIEDLNTVLGQTQDHRH
MdV-ATPase-a 240 IIFFQGDQLKTRVKKICEGFRATLYPCPEAPADRREMAMGVMTRIEDLNTVLGQTQDHRH
TcV-ATPase-a 300 RVLVAAAKNIKNWFVKVRKIKAIYHTLNLFNLDVTQKCLIAECWVPVLDFENIQLALRRG
ApV-ATPase-a 286 RVLVAAAKNIKNWFIKVVKIKAIYHTLNLFNLDVTQKCLIAECWVPLLDIETIQLALRRG
BmV-ATPase-a 287 RVLVAAAKNIKNWFVKVRKIKAIYHTLNLFNLDVTQKCLIAECWVPVLDIETIQLALRRG
AmV-ATPase-a 287 RVLVAAAKNIKNWFVKVRKIKAIYHTLNLFNLDVTQKCLIAECWVPVLDIEIIQLALRRG
AaV-ATPase-a 300 RVLVAAAKNIKNWFVKVRKIKAIYHTLNLFNLDVTQKCLIAECWVPILDIETIQIALRRG
CqV-ATPase-a 287 RVLVAAAKNIKNWFVKVRKIKAIYHTLNLFNLDVTQKCLIAECWVPILDIETIQIALRRG
DmV-ATPase-a 301 RVLVAAAKNIKNWFVKVRKIKAIYHTLNLFNLDVTQKCLIAECWVPILDIETIQLALRRG
MdV-ATPase-a 300 RVLVAAAKNIKNWFVKVRKIKAIYHTLNLFNLDVTQKCLIAECWVPVLDIETIQLALRRG
TcV-ATPase-a 360 TERSGSSVPPILNRMETMEDPPTYNHTNKFTTGFQTLIDAYGIASYREMNPAPYTIITFP
ApV-ATPase-a 346 TERSGSSVPPILNRMDTFEDPPTYNRTNKFTSAFQNLVDAYGIASYREINPTPYTIISFP
BmV-ATPase-a 347 TERSGSSVPPILNRMATFEDPPTYNRTNKFTKGFQALVDAYGVASYREMNPSPYTIITFP
AmV-ATPase-a 347 TERSGSSVPPILNRMVTFEDPPTYNRTNKFTKGFQALIDAYGVASYREMNPSPYTIITFP
AaV-ATPase-a 360 TERSGSSVPPILNRMPTFEDPPTYNRTNKFTSAFQALINAYGVASYREMNPAPYTIITFP
CqV-ATPase-a 347 TERSGSSVPPILNRMPTFEDPPTYNRTNKFTNAFQALINAYGVASYREMNPAPYTIITFP
DmV-ATPase-a 361 TERSGSSVPPILNRMQTFENPPTYNRTNKFTKAFQALIDAYGVASYREMNPAPYTIITFP
MdV-ATPase-a 360 TERSGSSVPPILNRMQTFENPPTYNRTNKFTKAFQALIDAYGVAIYREMNPAPYTIITFP
TcV-ATPase-a 420 FLFAVMFGDLGHGLLMAIFGAWMVLKEKPLAAKKSDNEIWNIFFGGRYIVLLMGLFSMYT
ApV-ATPase-a 406 FLFAVMFGDLGHGCLMFLFAGFLVLREKPLAAKKTDNEVWNIFFAGRYIILLMGLFSMYT
BmV-ATPase-a 407 FLFAVMFGDTGHGLIMFLFGGWMVLKEKPLAAKKSDNEIWNIFFGGRYIIFLMGLFSMYT
AmV-ATPase-a 407 FLFAVMFGDTGHGLLMFLFGGWMVLKEKPLAAKKSDNEIWNIFFGGRYIIFLMGLFSMYT
AaV-ATPase-a 420 FLFAVMFGDLGHGAIMALFGLWMVLKEKPLAAKKTDNEIWNIFFGGRYIIFLMGVFSMYT
CqV-ATPase-a 407 FLFAVMFGDLGHGAIMALFGLWMVLKEKPLAAKKTDNEIWNIFFGGRYIIFLMGVFSMYT
DmV-ATPase-a 421 FLFAVMFGDLGHGAIMALFGLWMIRKEKGLAAQKTDNEIWNIFFGGRYIIFLMGVFSMYT
MdV-ATPase-a 420 FLFAVMFGDLGHGAIMALFGLWMIRKEKGLAAQKTDNEIWNIFFGGRYIIFLMGVFSMYT
TcV-ATPase-a 480 GFIYNDVFSKSLNIFGSNWVVNNLTADYVLKVDDVMLDPAEGDYLHHPYPIGLDPVWQLA
ApV-ATPase-a 466 GFIYNDIFSKSLNLFGSHWHTNYNESTVMNNKDLQTNESLSSDYDQVPYPVGLDPVWQIA
BmV-ATPase-a 467 GLIYNDIFSKSLNIFGSYWRINYNISTIVTNKELQLNESDIEQYLQIPYPLGMDPVWQLA
AmV-ATPase-a 467 GLIYNDIFSKSLNIFGSYWRINYNFSTIDSNKELQLNPSDKEQYLQIPYPIGMDPVWQLA
AaV-ATPase-a 480 GFVYNDIFSKSLNVFGSAWSINYNTSTVMENKALQLDEG-SKDYSGTPYPIGLDPVWQVA
CqV-ATPase-a 467 GFVYNDIFSKSLNVFGSTWSINYNTSTVMTNKALQLDEA-S-DYDGTPYPIGLDPVWQVS

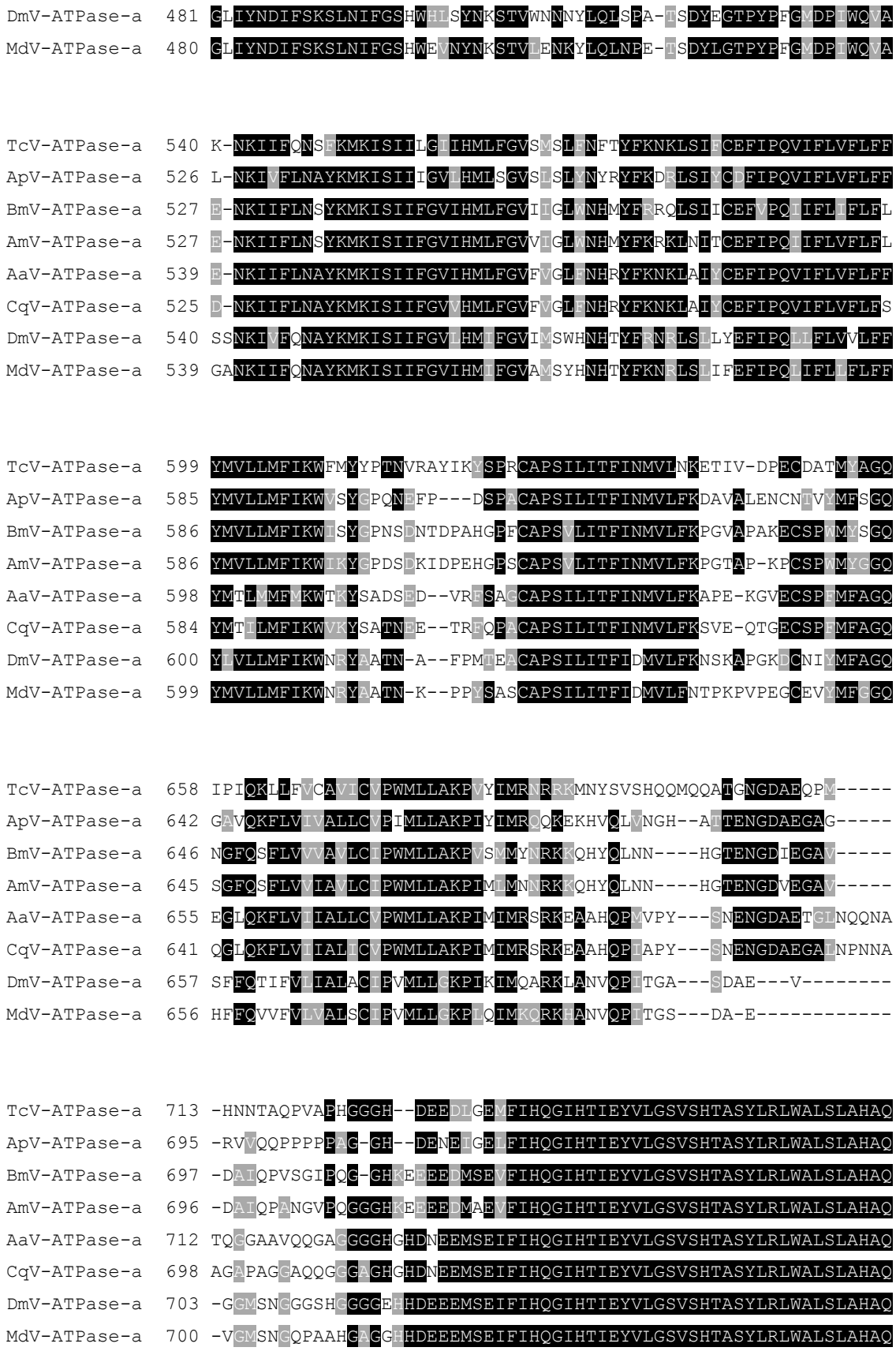
DmV-ATPase-a 481 GLIYNDIFSKSLNIFGSHWHLSYNKSTVWNNNYLQLSPA-TSDYEGTPYPFGMDPIWQVA
MdV-ATPase-a 480 GLIYNDIFSKSLNIFGSHWEVNYNKSTVLENKYLQLNPE-TSDYLGTPYPFGMDPIWQVA
TcV-ATPase-a 540 K-NKIIFQNSFKMKISIILGIIHMLFGVSMSLFNFTYFKNKLSICEFIPQVIFLVFLFF
ApV-ATPase-a 526 L-NKIVFLNAYKMKISIIIGVLHMLSGVSLSLYNYRYFKDRLSIYCDFIPQVIFLVFLFF
BmV-ATPase-a 527 E-NKIIFLNSYKMKISIIFGVIHMLFGVIIGLWNHMYFRRQLSIICEFVPQIIFLIFLFL
AmV-ATPase-a 527 E-NKIIFLNSYKMKISIIFGVIHMLFGVVIGLWNHMYFKRKLNITCEFIPQIIFLVFLFL
AaV-ATPase-a 539 E-NKIIFLNAYKMKISIIFGVIHMLFGVFVGLFNHRYFKNKLAIYCEFIPQVIFLVFLFF
CqV-ATPase-a 525 D-NKIIFLNAYKMKISIIFGVVHMLFGVFVGLFNHRYFKNKLAIYCEFIPQVIFLVFLFS
DmV-ATPase-a 540 SSNKIVFQNAYKMKISIIFGVLHMIFGVIMSWHNHTYFRNRLSILYEFIPQLIFLVVLFF
MdV-ATPase-a 539 GANKIIFQNAYKMKISIIFGVIHMIFGVAMSYHNHTYFKNRLSLIFEFIPQIIFLIFLFF
TcV-ATPase-a 599 YMVLLMFIKWFMYYPTNVRAYIKYSPRCAPSILITFINMVINKETIV-DPECDATMYAGQ
ApV-ATPase-a 585 YMVLLMFIKWVSYGPQNEFP---DSPACAPSILITFINMVLFKDAVALENCNIVYMFSGQ
BmV-ATPase-a 586 YMVLLMFIKWISYGPNSDNTDPAHGPFCAPSVLITFINMVLFKPGVAPAKECSPWMYSGQ
AmV-ATPase-a 586 YMVLLMFIKWIKYGPDSDKIDPEHGPSCAPSVLITFINMVLFKPGTAP-KPCSPWMYGGQ
AaV-ATPase-a 598 YMTLLMFMKWTKYSADSED--VRFSAGCAPSILITFINMVLFKAPE-KGVECSPFMFAGQ
CqV-ATPase-a 584 YMTILMFIKWVKYSATNEE--TRFQPACAPSILITFINMVLFKSVE-QTGECSPFMFAGQ
DmV-ATPase-a 600 YLVLLMFIKWNRYAATN-A--FPMTEACAPSILITFIDMVLFKNSKAPGKDCNIYMFAGQ
MdV-ATPase-a 599 YMVLLMFIKWNRYAATN-K--PPYSASCAPSILITFIDMVLFNTPKPVPEGCEVYMFGGQ
TcV-ATPase-a 658 IPIQKLLFYCAVICVPWMLLAKPVYIMRNRRKMNYSVSHQQMQQATGNGDAEQPM-----
ApV-ATPase-a 642 GAVQKFLVIVALLCVPIMLLAKPIYIMRQQKEKHVQLVNGH--AITENGDAEGAG-----
BmV-ATPase-a 646 NGFQSFLVVVAVLCIPWMLLAKPVSMMYNRKKQHYQLNN----HGTENGDIEGAV-----
AmV-ATPase-a 645 SGFQSFLVVIAVLCIPWMLLAKPIMLMNNRKKQHYQLNN----HGTENGDVEGAV-----
AaV-ATPase-a 655 EGLQKFLVIIALLCVPWMLLAKPIMIMRSRKEAAHQPMVPY---SNENGDAETGLNQQNA
CqV-ATPase-a 641 QGLQKFLVIIALICVPWMLLAKPIMIMRSRKEAAHQPIAPY---SNENGDAEGALNPNNA
DmV-ATPase-a 657 SFFQTIFVIIALACIPVMLLGKPIKIMQARKLANVQPITGA---SDAE---V--------
MdV-ATPase-a 656 HFFQVVFVLVALSCIPVMLLGKPLQIMKQRKHANVQPITGS---DA-E----------
TcV-ATPase-a 713 -HNNTAQPVAPHGGGH--DEEDLGEMFIHQGIHTIEYVLGSVSHTASYLRLWALSLAHAQ
ApV-ATPase-a 695 -RVVQQPPPPPAG-GH--DENEIGELFIHQGIHTIEYVLGSVSHTASYLRLWALSLAHAQ
BmV-ATPase-a 697 -DAIQPVSGIPQG-GHKEEEEDMSEVFIHQGIHTIEYVLGSVSHTASYLRLWALSLAHAQ
AmV-ATPase-a 696 -DAIQPANGVPQGGGGHKEEEEDMAEVFIHQGIHTIEYVLGSVSHTASYLRLWALSLAHAQ
AaV-ATPase-a 712 TQGAAAVQQGAGGGGHGHDNEEMSEIFIHQGIHTIEYVLGSVSHTASYLRLWALSLAHAQ
CqV-ATPase-a 698 AGAPAGGAQQGGGAGHGHDNEEMSEIFIHQGIHTIEYVLGSVSHTASYLRLWALSLAHAQ
DmV-ATPase-a 703 -GGMSNGGGSHGGGGEHHDEEEMSEIFIHQGIHTIEYVLGSVSHTASYLRLWALSLAHAQ
MdV-ATPase-a 700 -VGMSNGQPAAHGAGGHHDEEEMSEIFIHQGIHTIEYVLGSVSHTASYLRLWALSLAHAQ

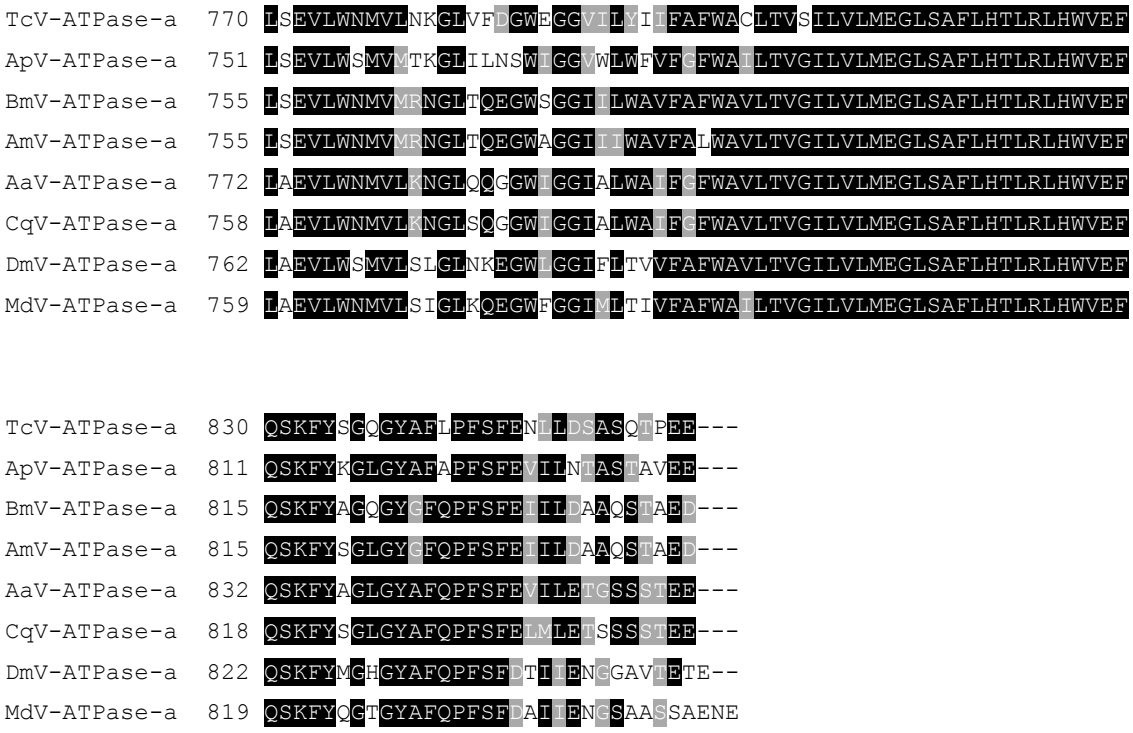

Figure A.12. Multiple alignments of amino acid sequences of V-ATPase subunit a (*Ae. aegypti, D. melanogaster, C. quinquefasciatus, M. domestica, B. mori, T. castaneum, A. mellifera, A. pisum*).

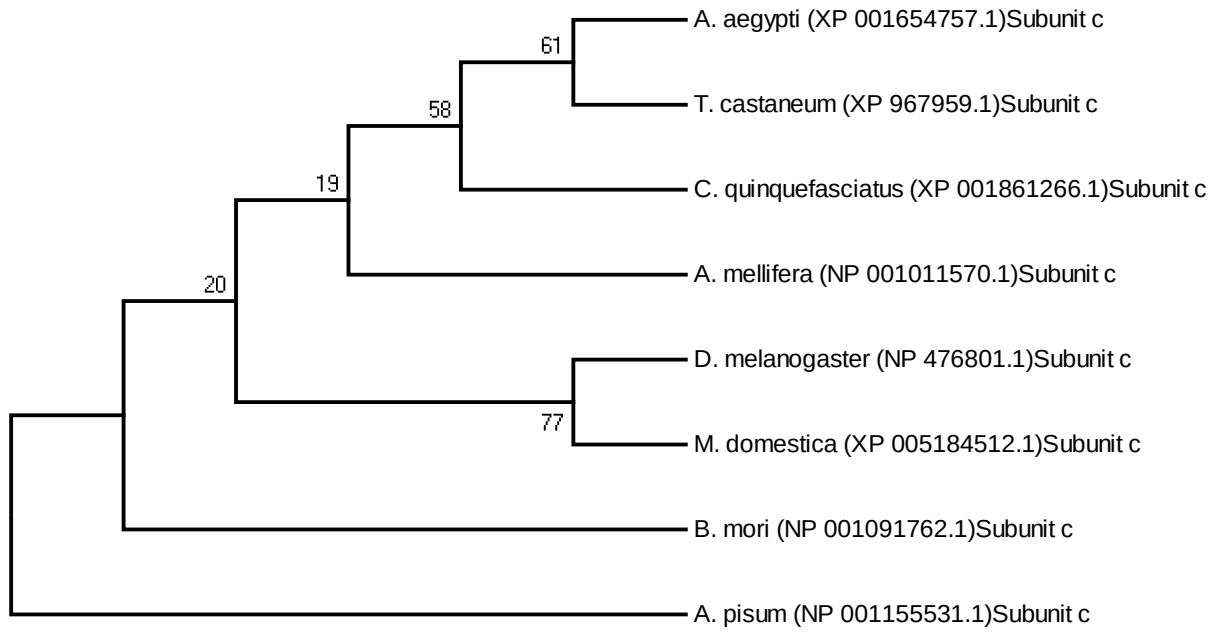

Figure A.13. Phylogenetic relationship of the deduced amino acid sequences of *V-ATPase-c* gene.

This rooted phylogenetic tree was constructed using the maximum likelihood method. Nodes indicate bootstrap values calculated with 1000 replications.

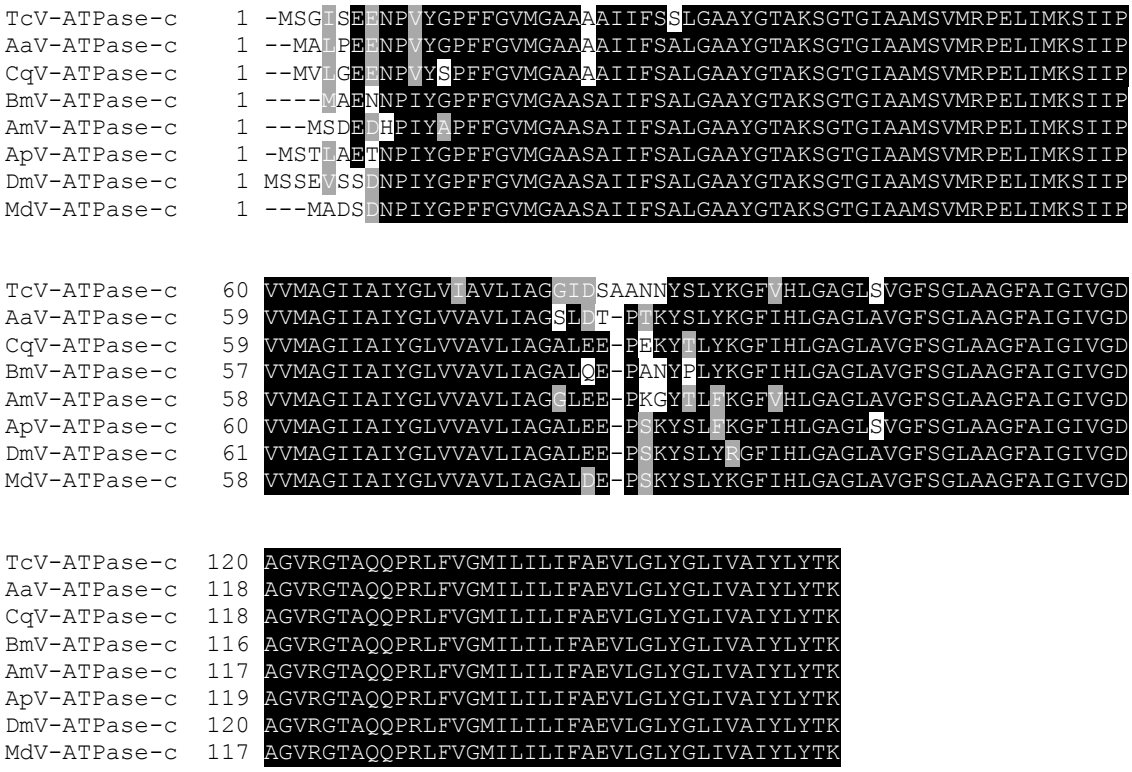

Figure A.14. Multiple alignments of amino acid sequences of V-ATPase subunit c (*Ae. aegypti, D. melanogaster, C. quinquefasciatus, M. domestica, B. mori, T. castaneum, A. mellifera, A. pisum*).

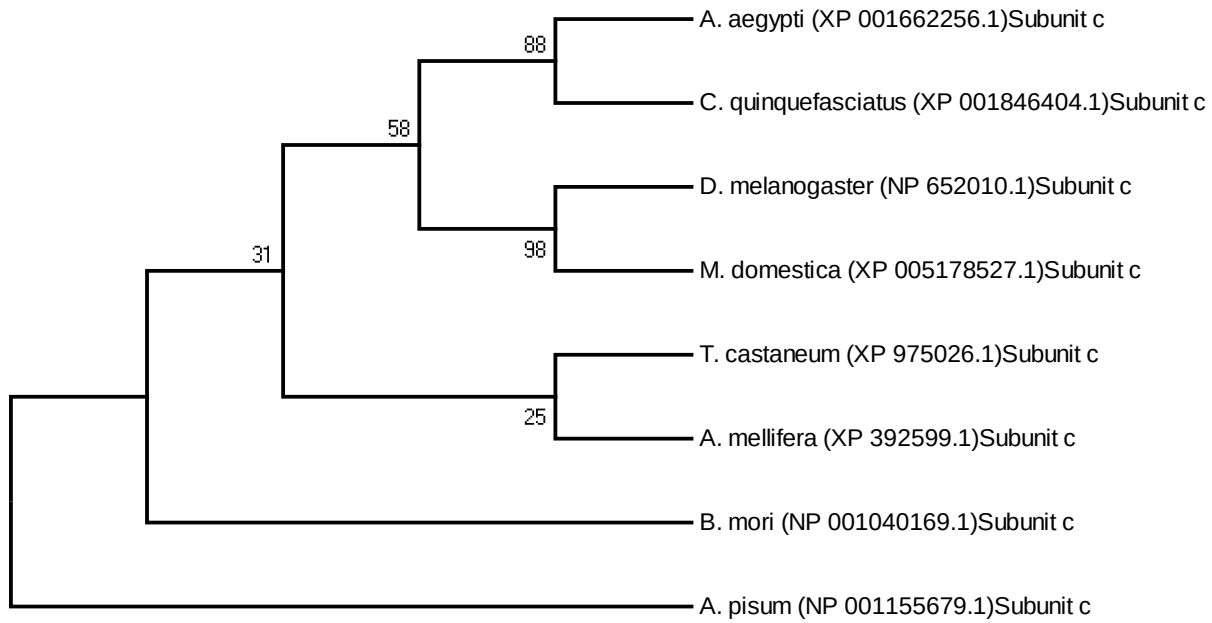

Figure A.15. Phylogenetic relationship of the deduced amino acid sequences of *V-ATPase-c”* gene.

This rooted phylogenetic tree was constructed using the maximum likelihood method. Nodes indicate bootstrap values calculated with 1000 replications.

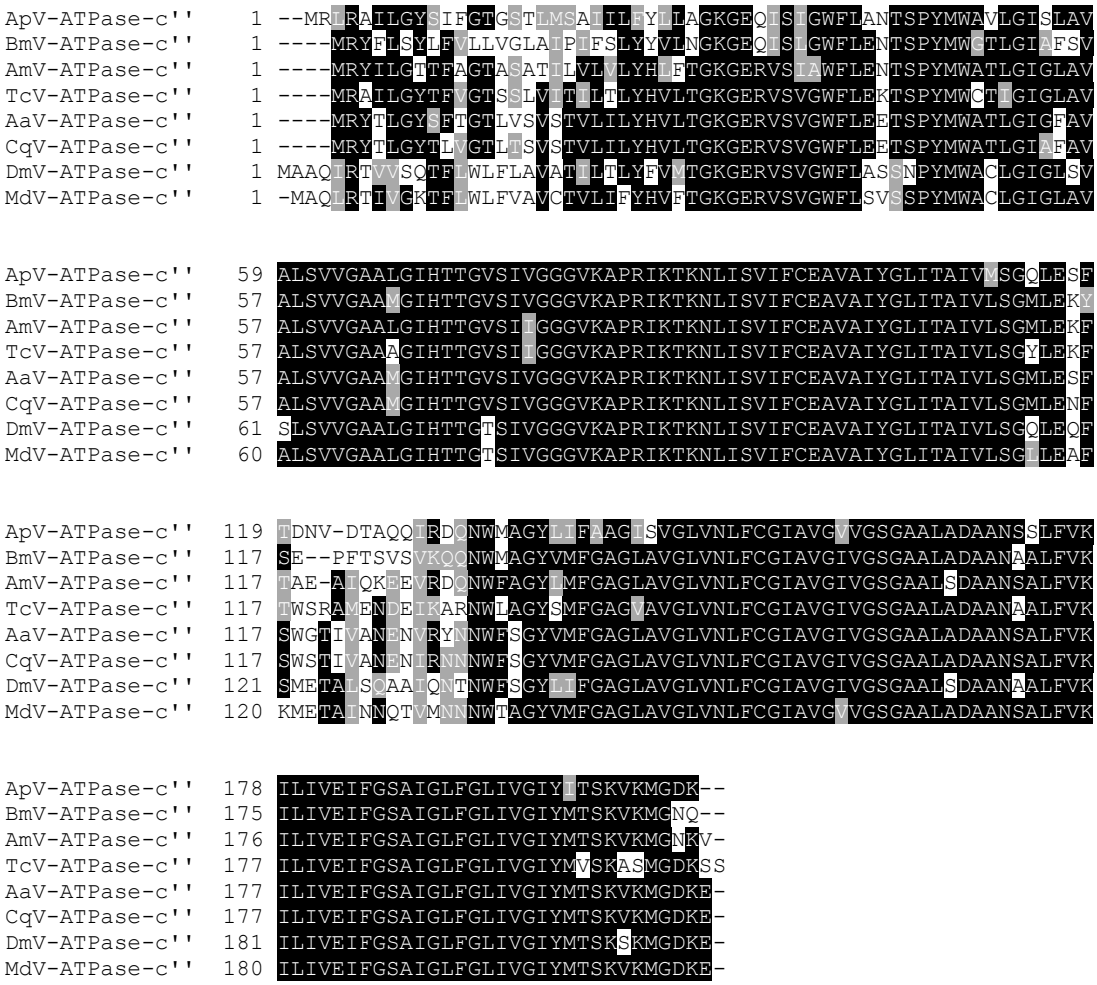

Figure A.16. Multiple alignments of amino acid sequences of V-ATPase subunit c" (*Ae. aegypti, D. melanogaster, C. quinquefasciatus, M. domestica, B. mori, T. castaneum, A. mellifera, A. pisum*).

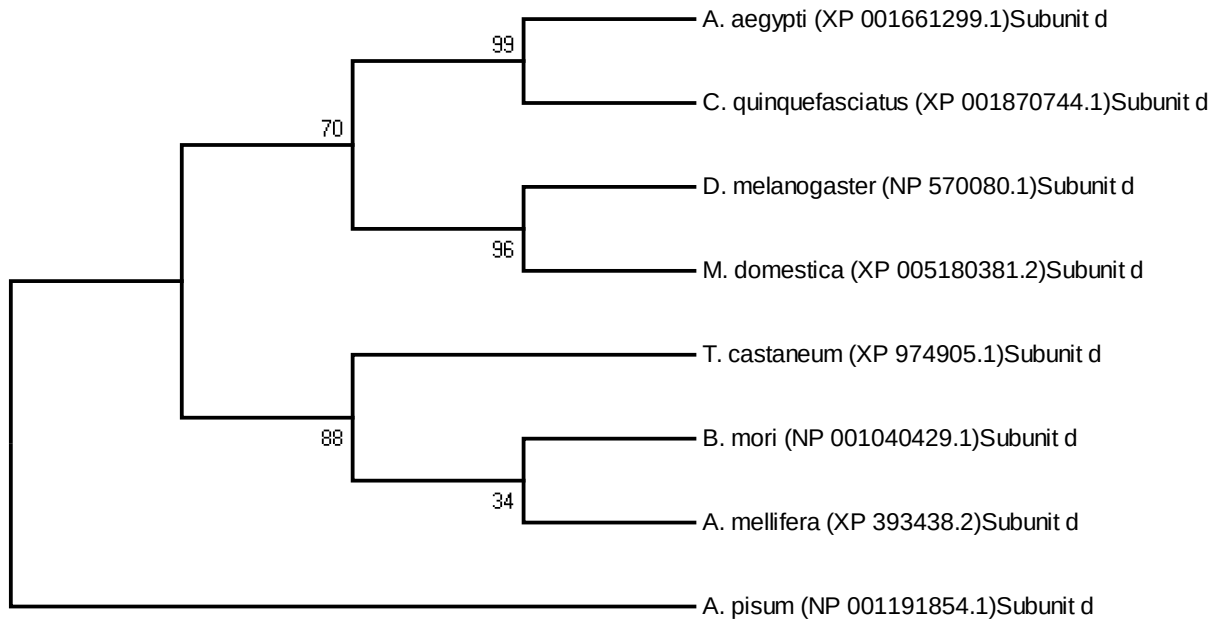

Figure A.17. Phylogenetic relationship of the deduced amino acid sequences of *V-ATPase-d* gene.

This rooted phylogenetic tree was constructed using the maximum likelihood method. Nodes indicate bootstrap values calculated with 1000 replications.

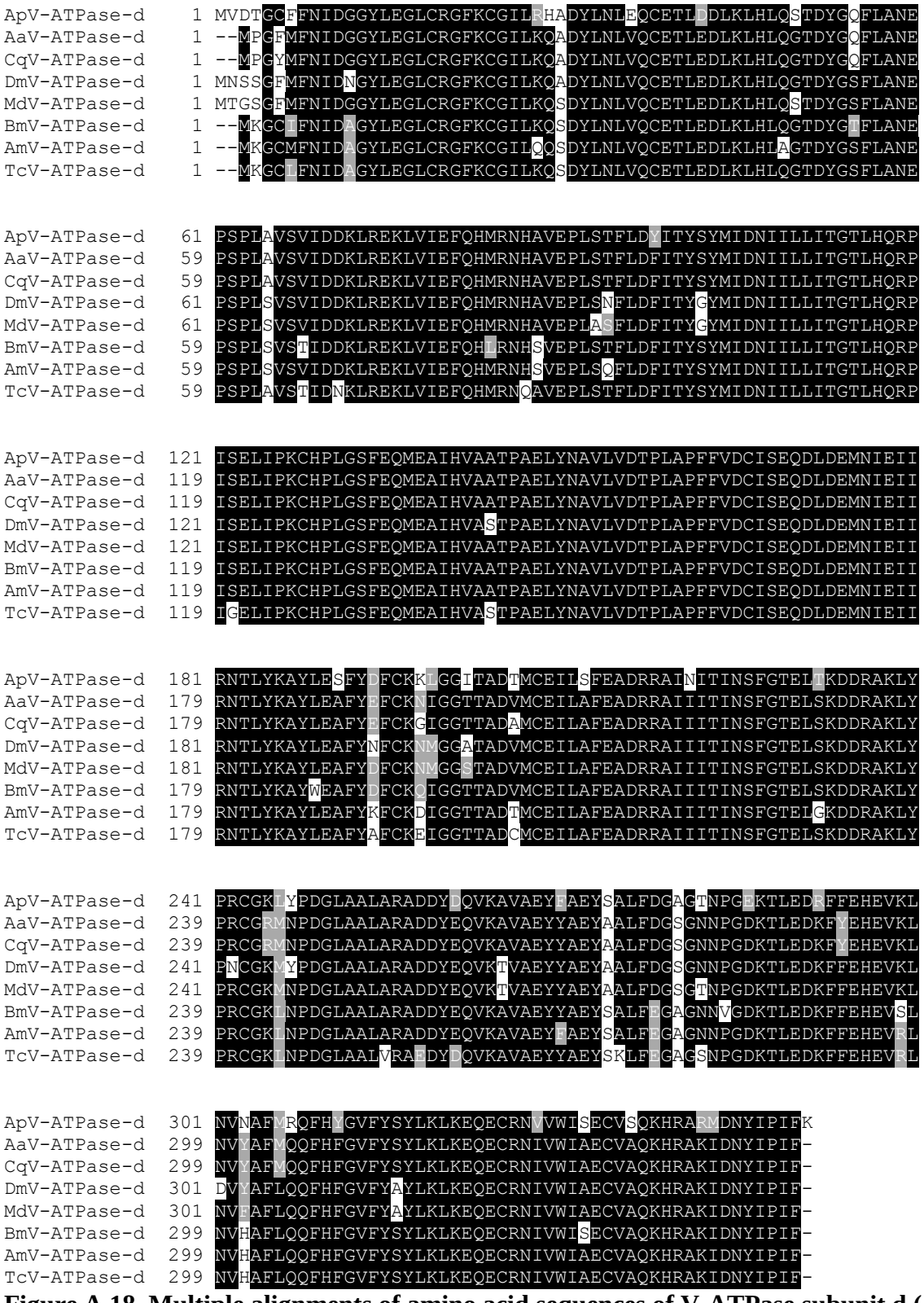

Figure A.18. Multiple alignments of amino acid sequences of V-ATPase subunit d (*Ae. aegypti, D. melanogaster, C. quinquefasciatus, M. domestica, B. mori, T. castaneum, A. mellifera, A. pisum*).

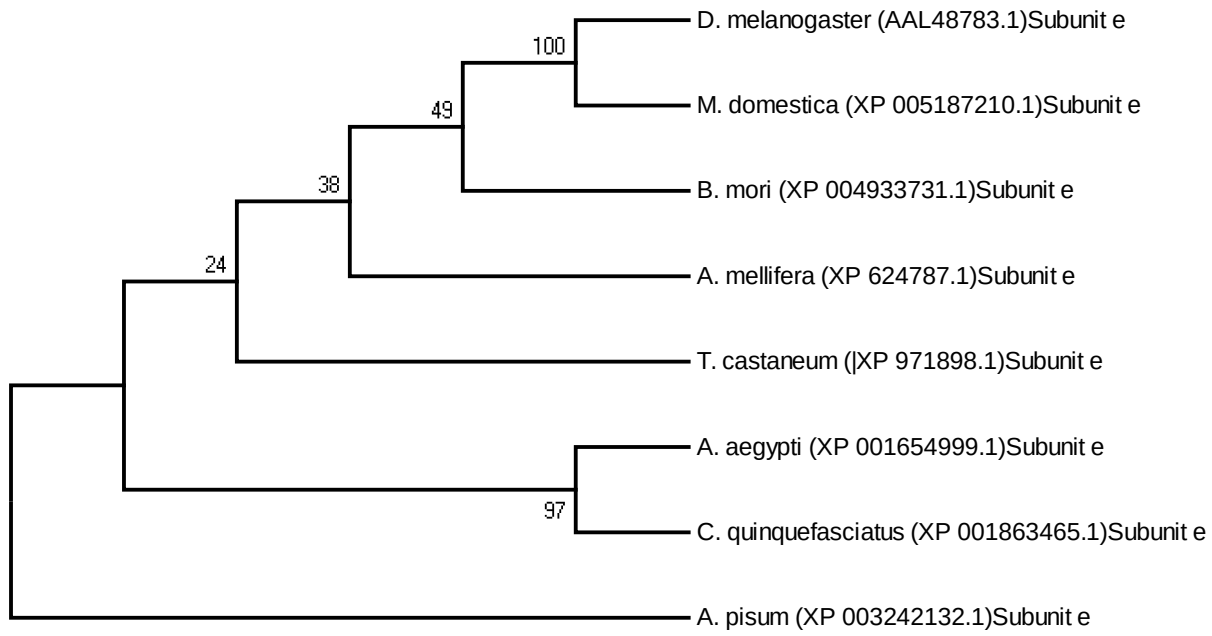

Figure A.19. Phylogenetic relationship of the deduced amino acid sequences of *V-ATPase-e* gene.

This rooted phylogenetic tree was constructed using the maximum likelihood method. Nodes indicate bootstrap values calculated with 1000 replications.

Figure A.20. Multiple alignments of amino acid sequences of V-ATPase subunit e (*Ae. aegypti, D. melanogaster, C. quinquefasciatus, M. domestica, B. mori, T. castaneum, A. mellifera, A. pisum*).